Relevance of glutathione and MRP-mediated efflux for platinum resistance

vorgelegt von

CARINA MOHN

aus

Hachenburg

Bonn 2013

1. Gutachter: Prof. Dr. U. Jaehde

2. Gutachter: Prof. Dr. M. Gütschow

Tag der Promotion: 15. Juli 2013

II

CONTENT

ABBREVIATIONS

A2780	Human ovarian carcinoma cell line
A2780cis	Cisplatin-resistant human ovarian carcinoma cell line
AAS	Atomic absorption spectroscopy
ABC	Adenosine triphosphate-binding cassette
ABCB1	ATP-binding cassette sub-family B member 1 (= P-gp, MDR1)
ABCC1	ATP-binding cassette sub-family C member 1 (= MRP1)
ABCC2	ATP-binding cassette sub-family C member 2 (= MRP2)
ABCG2	ATP-binding cassette sub-family G member 2 (= BCRP)
AP-1	Activator protein 1
APS	Ammonium persulfate
ARE	Antioxidant response element
ATP	Adenosine triphosphate
ATP7A	Copper-transporting P-type adenosine triphosphatase 7A
ATP7B	Copper-transporting P-type adenosine triphosphatase 7B
AU	Arbitrary units
Bax	Bcl-2-associated X protein
Bcl-2	B-cell lymphoma 2
Bcl-xL	B-cell lymphoma-extra large
BCA	Bicinchoninic acid
BCRP	Breast cancer resistance protein
BSA	Bovine serum albumin
BSO	Buthionine sulfoximine
Calcein AM	Acetomethoxy derivative of calcein

ABBREVIATIONS

CE	Capillary electrophoresis
cMOAT	Canalicular multispecific organic anion transporter
CTR1	Copper transporter 1
DAPI	2-(4-Amidinophenyl)-1H-indole-6-carboxamidine-dihydrochloride
DMF	Dimethylformamide
DMSO	Dimethyl sulfoxide
DNA	Deoxyribonucleic acid
DTT	Dithiothreitol
ECH	Erythroid cell-derived protein with cap'n'collar homology
EDTA	Ethylenediaminetetraacetic acid
ER	Endoplasmic reticulum
ERK	Extracellular-signal-regulated kinase
ESI	Electrospray ionization
ESCC	Esophageal squamous cell carcinoma
FCS	Fetal calf serum
γGCS	γ-Glutamylcysteine synthetase
GR	GSSG reductase
GS	Glutathione synthetase
GSH	Glutathione
GSSG	Oxidized glutathione (glutathione disulfide)
GS-R	GSH-conjugates
GST	Glutathione S-transferase
Gü83	4-[(5,6,7,8-tetrahydro-4-oxo-4H-[1]benzothieno[2,3-d][1,3]thiazin-2-yl)amino]benzoic acid
HCC	Hepatocellular carcinoma
HCT-8	Human ileocecal colorectal adenocarcinoma cell line

HCT-8ox	Oxaliplatin-resistant human ileocecal colorectal adenocarcinoma cell line
HEPES	4-(2-hydroxyethyl)-1-piperazineethanesulfonic acid
HMG	High mobility group
HPLC	High-performance liquid chromatography
HRP	Horseradish peroxidase
ICP-MS	Inductively coupled plasma mass spectrometry
IR	Infrared spectrometry
JNK	c-Jun N-terminal kinase
Keap1	Kelch-like ECH-associated protein 1
KHP	Krebs HEPES buffer
LC	Liquid chromatography resonance
MALDI	Matrix-assisted laser desorption/ionization
MAPK	Mitogen-activated protein kinase
MDCKII	Madin-Darby canine kidney cells
MDR	Multidrug resistance
MMR	Mismatch repair
MRP	Multidrug resistance-associated protein
MS	Mass spectrometry
MSD	Membrane-spanning domain
MTT	3-(4,5-Dimethylthiazol-2-yl)-2,5-diphenyltetrazolium bromide
m/z	Mass-to-charge ratio (mass spectrometry)
n	Number of measurements
n. a.	Not active
NADPH	Nicotinamide adenine dinucleotide phosphate
NBD	Nucleotide-binding domain

ABBREVIATIONS

n. d.	Not detected
NDA	Naphthalene-2,3-dicarboxaldehyde
NER	Nucleotide excision repair
NMR	Nuclear magnetic resonance
Nrf2	Nuclear factor erythroid 2-related factor 2
n. s.	Not significant
OATP1	Organic anion-transporting polypeptide 1
OCT	Organic cation transporter
PAGE	Polyacrylamide gel electrophoresis
PARP	Poly(ADP-ribose)polymerase
PBS	Phosphate buffered saline
P-gp	P-glycoprotein
PVDF	Polyvinylidene fluoride
QC	Quality control
RE	Relative error
r	Correlation coefficient
RNA	Ribonucleic acid
RNase	Ribonuclease A
ROS	Reactive oxygen species
RSD	Relative standard deviation
RSS	Residual sum of squares
S	Standard solution
SCLC	Small cell lung cancer
SD	Standard deviation
SDS	Sodium dodecyl sulfate
SDS-PAGE	Sodium dodecyl sulfate polyacrylamide gel electrophoresis

VIII

SEM	Standard error of the mean
siRNA	Small-interfering RNA
shRNA	Short hairpin RNA
Sp-1	Specificity protein 1
TBS	Tris-buffered saline
TBS-T	Tris-buffered saline with Tween®-20
TEMED	Tetramethylethylenediamine
TKI	Tyrosine kinase inhibitors
Tris	Tris(hydroxymethyl)aminomethane
WS	Working solution

1 INTRODUCTION

1.1 Cancer chemotherapy

In Germany, approximately 470,000 people are diagnosed with cancer each year [1]. After cardiovascular diseases, cancer is the second most cause of death in German population [2]. In females breast cancer followed by colon and lung cancer and in males prostate, colon and lung cancer are most frequent. Considering statistics standardized by age, cancer prevalence has been constant over the last ten years with a slight decrease in mortality rate, which is probably due to new developments in cancer treatment [1].

Treatment of cancer is based on surgery and radiation as well as on antineoplastic drugs. The term 'antineoplastic drug' traditionally comprised mainly chemotherapeutic drugs but has been expanded by new classes of drugs such as monoclonal antibodies, tyrosine kinase inhibitors and drugs modulating hormone metabolism. Recently developed drugs, which are often directed against cancer-specific targets and are thus called 'targeted drugs' are, however, frequently used as either 'add-on' therapy to long-time established drugs or drug combinations or after failure of established drugs. Hence drugs from the last century still play an important role in the current treatment of cancer and development of effective drug combinations is still the aim of research [3,4]. To optimize therapy and to find drug combinations with not only additive but synergistic effects, the understanding of the molecular way of action and mechanisms of resistance to individual drugs as well as their interaction in combination therapies are of great value.

This project focused on platinum complexes, a class of chemotherapeutics used in the treatment of solid malignancies and on mechanisms involved in cellular resistance towards these drugs.

1.2 Platinum complexes

The platinum complex first introduced in therapy was cisplatin, a square planar complex with platinum(II) as central atom, which was approved by the *Food and Drug Administration* in the United States in 1978. It is used in chemotherapy regimens for the treatment of testicular

and head and neck cancer, for example [5]. Being successful in the treatment of certain tumor types, cisplatin therapy is limited by severe adverse events, such as nephrotoxicity and neurotoxicity, and resistance of tumors, either intrinsic or acquired during therapy. Hence after the approval of cisplatin the development of further platinum complexes moved on, resulting in the approval of carboplatin in the 1980s. Carboplatin is effective in the same tumor types as cisplatin but shows a more tolerable side effect profile and has replaced cisplatin in the treatment of ovarian tumors and of non-small cell lung cancer as standard treatment. Its side effect profile differs from cisplatin as not nephrotoxicity and neurotoxicity are but myelosuppression is the major adverse event. In the 1990s a further platinum complex, oxaliplatin, was introduced. Oxaliplatin can be used in the treatment of tumors which are intrinsically resistant to cisplatin and carboplatin, such as colorectal cancer [6]. The most common toxicity associated with oxaliplatin treatment is peripheral neuropathy [7]. The chemical structure of the platinum complexes is shown in Fig. 1-1.
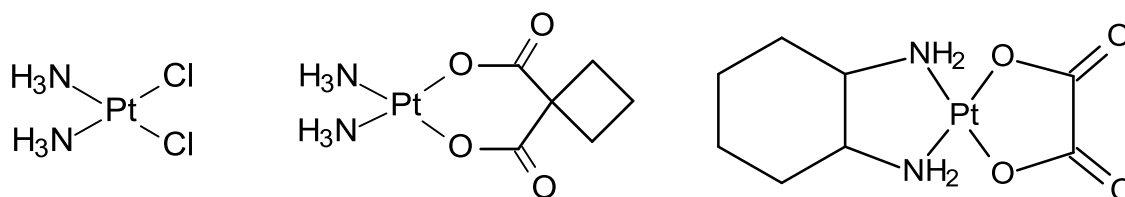
Fig. 1-1   Platinum complexes used in cancer therapy: cisplatin (cis-diamminedichloro-platinum(II)), carboplatin (cis-diammine(cyclobutane-1,1-dicarboxylate-O,O') platinum(II)) and oxaliplatin ([(1R,2R)-cyclohexane-1,2- diamine](ethanedioato-O,O') platinum(II)) (from left to right).

Further platinum complexes are only approved in individual countries (e.g. nedaplatin in Japan, lobaplatin in China, heptaplatin in the Republic of Korea) and thus were not considered in this project. Research on new platinum complexes is ongoing aiming for the development of substances with superior side effect profiles and substances overcoming resistance [8].

1.2.1   Mechanism of action

Uptake and activation

The mechanism of cellular uptake of platinum complexes has not been elucidated completely. Passive diffusion, uptake by gated channels, or active transporters such as copper

transporter 1 (CTR1) and organic cation transporters (OCT) 1 and 2 are described and a combination of diverse mechanisms is probable [9].

Inside the cell, platinum complexes undergo aquation by ligand exchange. In case of cisplatin one or both chlorido ligands are replaced by water molecules resulting in more reactive complexes [6,7,10]. In carboplatin and oxaliplatin the leaving groups, cyclobutane-1,1-dicarboxylate or oxalate, respectively, are likely to be substituted first by chlorido ligands and then by water ligands [7].

DNA platination

The reactive aquated species bind to various intracellular structures, but with respect to cytotoxicity nuclear DNA is the most important target [10]. Platinum complexes form covalent bonds with the N7 of the purine bases adenine and guanine primarily resulting in the generation of monofunctional and bifunctional adducts, the latter comprising intrastrand and interstrand crosslinks (Fig. 1-2). In case of cisplatin, intrastrand crosslinks are described to be most prevalent (involvement of two guanines: 60 to 65%, involvement of adenine and guanine: 20 to 25%, involvement of two guanines with another base in between: 2% of all adducts); interstrand crosslinks and monofunctional adducts are less frequent (each with 2% of all adducts) [6].

The platinum-DNA adducts formed by carboplatin are similar to those formed by cisplatin. The adduct formation is, however, slower and the amount of carboplatin needed to yield the same number of adducts is higher [6]. Oxaliplatin forms similar adducts, with the difference that oxaliplatin-DNA lesions contain a $[Pt(trans-R,R-diaminocyclohexane)]^{2+}$ rather than a $[Pt(NH_3)_2]^{2+}$ group. Hence the structural changes on DNA resulting from oxaliplatin binding on the one hand and cisplatin or carboplatin binding on the other hand are not the same, and therefore different cellular mechanisms are activated to cope with the platinum-DNA adducts [11]. On account of this it can be explained that DNA breaks produced by oxaliplatin are commensurate to those produced by cisplatin although the total amount of oxaliplatin-DNA adducts is significantly lower compared to cisplatin of equimolar concentrations [7,12-14].

Monofunctional adducts

Bifunctional adducts

Intrastrand crosslinks   Interstrand crosslinks
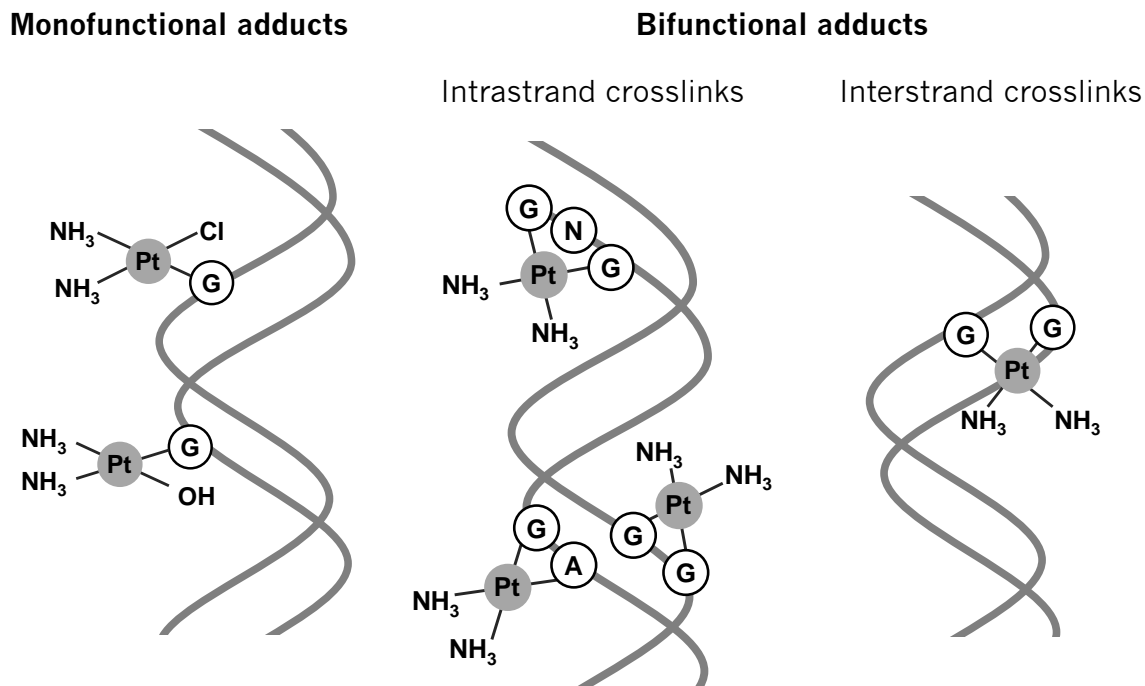
Fig. 1-2   Platinum-DNA adducts as described for cisplatin (A: adenosine, G: guanosine, N: any nucleoside) (modified from [7]).

Cellular reaction

Once platinum-DNA adducts are formed, cellular response processes are induced and result in either repair of DNA and cell survival, or apoptosis. The fate of the cell depends on the intensity of the signals generated and the crosstalk between cellular processes involved, which can be cell-type specific and either lead to sensitivity or resistance to all or single platinum complexes (for platinum resistance see chapter 1.3) [15]. There is evidence for different signaling cascades activated by cisplatin and carboplatin compared to oxaliplatin [7]. One signaling pathway involved in cytotoxicity of all platinum complexes used is the mitogen-activated protein kinase (MAPK) pathway which participates in regulating cell proliferation, differentiation, cell survival and apoptosis [10].

As described before, after damage recognition cellular survival processes can be initiated. Survival is triggered by DNA repair or increased tolerance to platinum-DNA adducts. The nucleotide excision repair (NER) is the major pathway involved in repair of platinum-DNA adducts and lesions induced by platinum complexes. Platinum-DNA adducts formed by cisplatin and carboplatin are also recognized by mismatch repair (MMR), but their repair is

not successful and results in apoptosis. Due to the different steric properties, oxaliplatin-DNA adducts are not detected by the MMR [16].

Instead of repairing platinum-DNA adducts, cells can replicate DNA bypassing the adducts without gaps in the new strand by so-called replicative bypass. Hence replicative bypass increases cellular tolerance to platinum-DNA adducts. In the context of replicative bypass high mobility group (HMG) proteins have been reported to be of importance for cytotoxic action as they bind to intrastrand crosslinks and prevent replicative bypass, but also NER and binding of transcription factors [7,17]. Oxaliplatin-DNA adducts, however, have been discussed to be poor substrates of replication enzymes involved in replicative bypass [16].

As damage recognition results in multiple cellular processes, diverse ways of apoptosis have been suggested and involvement of tumor suppressor protein p53, MAPK pathways, the Fas/Fas ligand signaling complex (activation of caspase 8 and caspase 3), mitochondrial cytochrome-c release (activation of caspase 9 and caspase 3), a caspase 3 independent apoptotic pathway or defective apoptotic pathways have been discussed [15,18]. Besides apoptosis, cells were also described to undergo necrosis when DNA is massively damaged and poly(ADP-ribose)polymerase (PARP) proteins have been induced [10,19].

In this chapter presumably the main intracellular target of platinum complexes, genomic DNA, was discussed. Since only a small proportion of intracellular platinum binds to nuclear DNA, further processes influenced by platinum complexes inside the cell need to be taken into consideration [20].

1.3 Platinum resistance

Besides toxicity, acquired or intrinsic drug resistance is the main obstacle in cancer chemotherapy using platinum complexes. Resistance to platinum complexes is not caused by a single cellular process or alteration but derives from multiple interacting factors. Considering the formation of platinum-DNA adducts as main target for the mechanism of action, resistance to platinum complexes can be structured in pre-target, on-target, post-target and off target-resistance [5].

1.3.1 Pre-target resistance

Pre-target resistance involves processes resulting in reduced cellular platinum accumulation, through reduced uptake and/or increased efflux and in increased inactivation of platinum complexes.

It is by now accepted that besides passive diffusion copper transporters and further transporters are involved in platinum uptake and efflux and hence contribute to reduced platinum accumulation found in resistant cells. The copper transporter CTR1 plays a role in the uptake of platinum complexes and CTR1-deficient cells were found to be cisplatin-resistant [18]. Regarding increased efflux, the copper-transporting P-type adenosine triphosphatases ATP7A and ATP7B seem to be involved [18,21]. Multidrug resistance-associated proteins (MRP) are also discussed to play a role in platinum resistance as they are supposed to contribute to increased efflux. More details on MRP and the relevance of MRP for platinum resistance are described in chapters 1.5 and 1.6.

Cellular thiols have also been associated with pre-target resistance. Glutathione (GSH) is likely to contribute to platinum resistance by binding and inactivating platinum complexes and reducing platinum-induced oxidative stress [18]. Besides GSH, the rate-limiting enzyme in intracellular GSH synthesis, γ-glutamylcysteine synthetase (γGCS), and the enzyme catalyzing reactions of GSH with substrates, glutathione S-transferase (GST), have been suggested to be involved in platinum resistance [5]. GSH and related enzymes and their role in platinum resistance are portrayed in chapters 1.4 and 1.6. In some studies also metallothioneins have been implicated to contribute to platinum resistance, presumably by drug binding as well. Metallothioneins are rich in thiol-containing cysteine proteins and are involved in zinc homeostasis [18].

1.3.2 On-target resistance

There is evidence that the level of cisplatin-DNA adducts correlates with the cytotoxicity of the drug [15]; on-target resistance directly relates to platinum-DNA adducts and involves increased repair of but also increased tolerance to platinum-DNA adducts.

Overexpression of components of nucleotide excision repair (NER) results in increased repair of platinum-DNA adducts and platinum resistance. Up to now, *in vitro* studies support the contribution of various DNA polymerases, topoisomerase II and homologous recombination

repair but clinical evidence proving their relevance for platinum resistance is lacking [18]. DNA mismatch repair (MMR) processing of platinum-DNA adducts and failure of repair result in apoptosis and thus contribute to platinum sensitivity. Cells with deficiency in MMR proteins show resistance against cisplatin and carboplatin due to increased tolerance to platinum-DNA adducts and reduced apoptosis [18]. The MMR system is assumed to account for differences in the mechanism of action of cisplatin/carboplatin and oxaliplatin. As oxaliplatin-DNA adducts are not detected by the MMR system, MMR deficiency does not alter cellular sensitivity to oxaliplatin [7].

1.3.3   Post-target resistance

Post-target resistance comprises cellular properties which prevent cells from undergoing apoptosis and result in survival. In platinum resistance the apoptotic response resulting from the formation of platinum-DNA adducts is reduced. In this context the role of genes regulating DNA damage, apoptosis and survival signaling are discussed [18].

Loss of p53 function and p53 downregulation have been suggested to inhibit the apoptotic signal in resistant cells as well as to suppress caspase activity and dysregulate MAPK pathways [15]. Proteins of the B-cell lymphoma 2 (Bcl-2) family, which comprises pro-apoptotic and anti-apoptotic proteins, are also discussed to play a role in post-target resistance. Overexpression of anti-apoptotic Bcl-2 family proteins, like Bcl-2 or B-cell lymphoma-extra large (Bcl-xL), and deficiency of pro-apoptotic Bcl-2 family proteins, like Bcl-2–associated X protein (Bax), are not always but often associated with platinum resistance as well [18]. In breast cancer cells, Bcl-2 overexpression was associated with an increase in cellular GSH content and in resistance to cisplatin [22].

1.3.4   Off-target resistance

Off-target resistance includes factors contributing to platinum resistance that are not directly linked to platinum-DNA adducts. Again, a variety of cellular processes have been reported and discussed in the literature and the following itemization is not necessarily exhaustive.

Autophagy, an evolutionary conserved response to multiple stress conditions, as chemotherapy, was seen in tumor cells developing resistance [5]. It involves the lysosomal degradation of cytoplasmic organelles or cytosolic components and results in survival [23].

INTRODUCTION

Several heat shock proteins have been proposed to indirectly contribute to platinum resistance as well as altered mitochondria, altered signaling pathways, upregulation of chaperones and chromosomal changes [5].

Tab. 1-1 gives an overview of some factors contributing to pre-target, on-target, post-target and off-target-resistance.

Tab. 1-1   Cellular processes and players involved in platinum resistance (modified from [5]).

Pre-target	On-target	Post-target	Off-target
Reduced uptake −CTR1	Increased repair of platinum-DNA adducts −Increased NER proficiency −HMG protein deficiency −Increased replicative bypass	Increased apoptosis inhibitors	Altered cell signaling pathways
Increased efflux −ATP7A/ATP7B −MRP2		Deficiency of apoptosis inductors	Altered mitochondria
		Suppressed activity of caspases	Upregulation of chaperones
Increased inactivation −GSH/γGCS/GST −Metallothioneins	Increased tolerance to platinum-DNA adducts −MMR deficiency	Dysregulation in MAPK pathways	Autophagy
		Reduced p53 function	Heat shock proteins

ATP7A, ATP7B: copper-transporting P-type adenosine triphosphatases A, B, CTR1: copper transporter 1; γGCS: γ-glutamylcysteine synthetase, GSH: glutathione, GST: glutathione S-transferase, HMG: high mobility group, MMR: mismatch repair, MRP2: Multidrug resistance-associated protein 2, NER: nucleotide excision repair.

1.4   Glutathione

Glutathione (γ-glutamylcysteinylglycine, GSH) is a tripeptide with an unusual gamma peptide linkage between the amine group of cysteine and the carboxyl group of the glutamate side-chain (see Fig. 1-3). The unusual bond prevents GSH from hydrolyzation by most peptidases. GSH is the most abundant cellular thiol and can be found in most mammalian and prokaryotic cells [24].
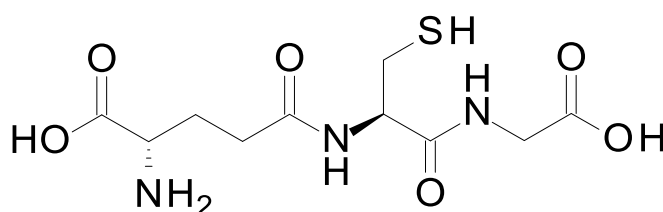
Fig. 1-3   Chemical structure of glutathione (GSH).

GSH is synthesized in the cytosol of cells from its precursor amino acids by γ-glutamylcysteine synthetase (γGCS) and GSH synthetase (GS). The amount of GSH synthesized is controlled by the expression of γGCS and cysteine available. Most of the cellular GSH exists in the reduced state, only a small amount is oxidized or conjugated (see Fig. 1-4). The oxidized form, GSSG, is a disulfide which is derived from two GSH molecules.
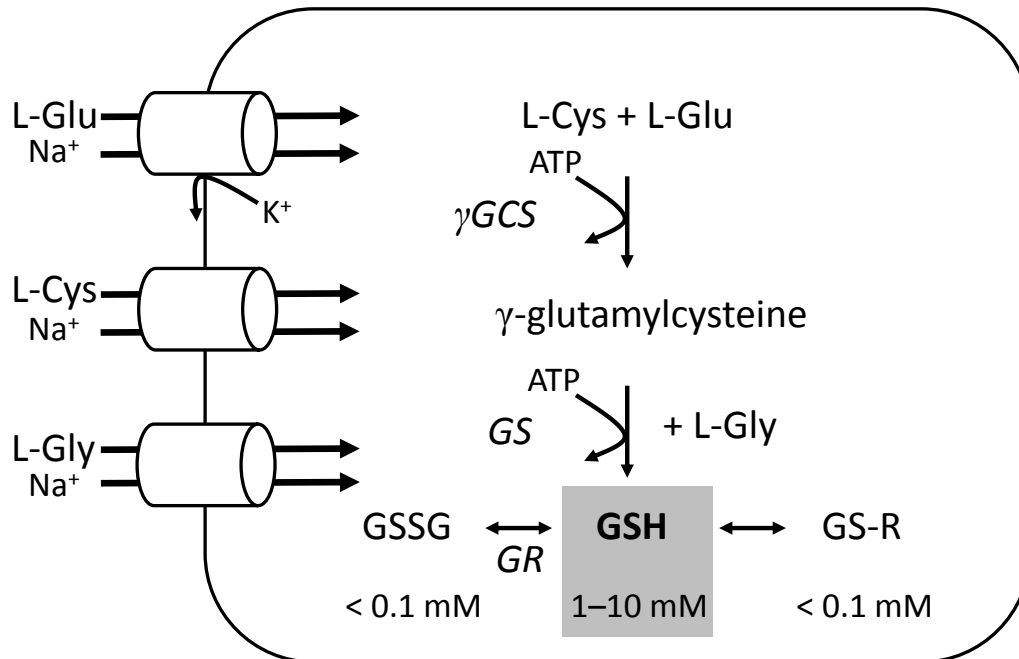
Fig. 1-4   Cellular GSH synthesis (modified from [25]).
ATP: adenosine triphosphate, L-Cys: cysteine, L-Glu: glutamine, L-Gly: glycine, GR: GSSG reductase, GS: GSH synthetase, GS-R: GSH conjugates.

GSH is degraded only in the extracellular space, mainly by the ectoenzyme γ-glutamyl transferase, which is located on the surface of cells. MRP1, MRP2 and organic anion-transporting polypeptide 1 (OATP1) have been implied to transport GSH into the extracellular space for GSH regulation (see Fig. 1-5). Besides GSH, MRP1 and MRP2 also transport GSSG and GSH conjugates (GS-R). The affinity of MRP1 and MRP2 for transport of GSH is, however, lower compared to GSSG [26,27].

After synthesis, GSH is distributed in intracellular compartments such as mitochondria, endoplasmic reticulum (ER) and nucleus and excreted into the extracellular space. GSH probably enters the nucleus by passive diffusion through nuclear pores. Dicarboxylate and oxoglutarate carriers have been discussed to transport GSH in mitochondria; the mechanism

of its transport into the ER is unclear [25]. For an overview of compartmentation and export of GSH see Fig. 1-5.
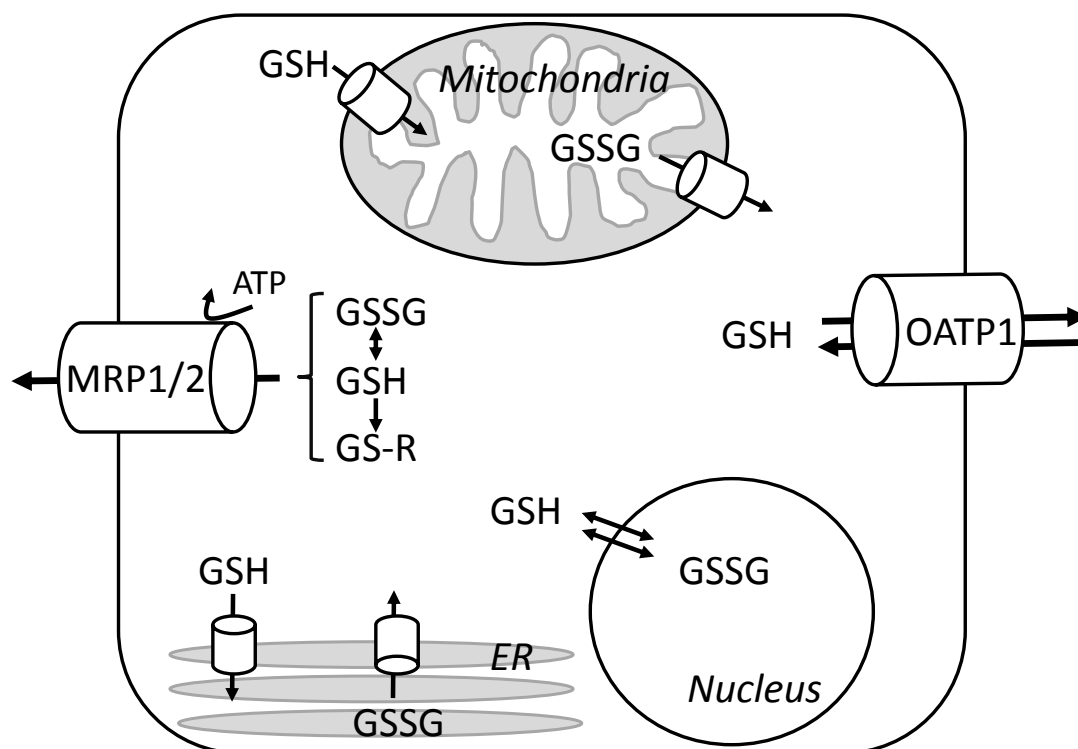
Fig. 1-5   Distribution of GSH after its synthesis (modified after [25]).
ER: endoplasmic reticulum, GS-R: GSH conjugates, MRP1/2: Multidrug resistance-associated protein 1/2, OATP1: organic anion-transporting polypeptide 1.

GSH is involved in many cellular processes of defense and metabolism, but above all, it acts as an antioxidant. The ratio of GSH to its oxidized form, GSSG, plays an important role in maintaining the cellular thiol-redox status. Changes in GSH/GSSG ratio have been associated with cell proliferation, differentiation and apoptosis. GSSG reductase (GR), a nicotinamide adenine dinucleotide phosphate (NADPH)-dependent enzyme, is responsible for keeping GSH in the reduced state [25].

Formation of GSH S-conjugates and GSH complexes has been described for endogenous and exogenous compounds like drugs or toxins, either facilitating their cellular efflux or detoxification. Formation of conjugates can be either enzymatical and catalyzed by GSH-S-transferases (GST) or non-enzymatical [24].

Additionally, diverse proteins have been described to be reversibly glutathionylated, among them transcription factors, signaling proteins and enzymes with active site thiols. Protein S-glutathionylation is increasingly recognized as cell signaling and regulatory mechanism as many apoptotic/survival signaling pathways have been shown to be regulated by reversible S-glutathionylation [25,28].

1.4.1 Glutathione in platinum resistance

GSH is a topic of interest in platinum resistance. Increased cellular GSH content and elevated activity of γGCS, the rate-limiting enzyme in GSH synthesis, have been associated with resistance to platinum complexes repeatedly [25,29,30]. Additionally, treatment of cancer cells with buthionine sulfoximine (BSO), a GSH-depleting substance which lowers GSH synthesis by inhibiting γGCS, resulted in increased sensitivity to platinum drugs *in vitro* [29,31,32]. These findings, however, are controversial as others did not find increased platinum toxicity when treating cells with BSO [33]. Up to now, it is not clear whether elevated GSH content and γGCS are causally responsible for platinum resistance or whether they are an unspecific reaction to reactive oxygen species (ROS) induced by platinum complexes [29].

It has been postulated by many authors that inside the cell the reactive aqua species of the platinum complexes form platinum-GSH adducts [5,6,34,35]. Ishikawa and Ali-Osman reported the isolation of a 1:2 cisplatin-GSH adduct from L1210 murine leukemia cells and that about 60% of cellular cisplatin reacted with GSH [35]. The kinetics of the reaction of excess GSH with platinum complexes has been investigated in experiments in buffer solutions by others, showing a relatively slow rate of adduct formation for carboplatin-GSH adducts [36]. In this setting, reaction of oxaliplatin with GSH starts quickly but stops when oxaliplatin is depleted and monofunctional adducts are formed. The reaction of cisplatin with GSH starts almost as fast but continues even when all cisplatin is bound to GSH suggesting formation of bi- or multifunctional adducts. However, information on platinum-GSH adducts is insufficient with only two research papers describing the isolation of a platinum-GSH adduct from *in vitro* experiments with cell models [35,37]. After incubation of cell lysate produced from cisplatin-resistant ovarian cancer cells, mainly macromolecular and no cisplatin-GSH adducts were identified by others [38].

INTRODUCTION

Besides resistance to platinum complexes, elevated GSH content has been associated with increased sensitivity. After transfection of small cell lung cancer derived cells with a γGCS subunit, an increased GSH content was found. In those cells formation of copper-GSH complexes and a decrease of available copper were observed. As a consequence an upregulation of copper transporter CTR1 was observed, contributing to augmented cisplatin toxicity by increased cisplatin uptake [29].

For completeness, the potential role of platinum-GSH adducts as drug reservoirs for DNA platination needs to be mentioned. Reedijk postulates that platinum-sulfur adducts, such as platinum-GSH adducts or platinum-protein adducts, may serve as a drug reservoir. Platinum could be released from sulfur and after that react with DNA or a direct nucleophilic displacement from sulfur by guanine-N might occur. The transfer, however, seems to be limited to platinum-thioether type adducts and transfer to N7 of guanines [39].

Bearing in mind also the regulation of signaling pathways by S-glutathionylation the mechanism of GSH-mediated platinum resistance is complex and is likely to be different in distinct cells and diverse mechanisms may take place simultaneously.

Glutathione S-transferases

Glutathione S-transferases (GST) are a group of multiple isoenzymes (named with Greek letters: α, μ, π, ω, θ, ζ). In general, GST catalyze a variety of reactions and accept endogenous and xenobiotic substrates. Enzymes differ widely in their amino acid sequence and different isoenzymes and polymorphic variations go along with diverse properties [40]. GST belong to the phase II detoxification enzymes. By catalyzing the reaction of GSH with electrophilic substances GST protect cellular proteins. They have been discussed to contribute to drug resistance by increasing their detoxification and hence inactivation of drugs. However, the relevance of GST in platinum resistance in terms of detoxification is probably low and their function in kinase-mediated pathways more important [41]. The GST subfamily GSTπ, encoded by the GSTP1 gene, is likely to contribute to resistance by controlling stress response, cellular proliferation and apoptosis by interaction with c-Jun N-terminal kinase (JNK). JNK is sequestered by GSTπ by formation of a JNK:GSTπ complex. Under condition of oxidative stress this complex dissociates and JNK regains functional capacity and can contribute to the induction of a stress cascade and potentially apoptosis. In this context GSTπ is understood to contribute to (platinum) drug resistance by interfering with drug-induced

apoptotic signaling. A polymorphism in GSTπ, however, was also associated with an improved response to platinum chemotherapy [40]. In clinical studies GSTπ expression inversely correlated with clinical outcome in patients with e.g. head and neck cancers or ovarian cancer treated with cisplatin [15,40,42] and polymorphisms leading to alterations in GSTπ protein primary structure were favorable for survival in patients with metastatic colorectal cancer treated with fluorouracil and oxaliplatin [43].

1.4.2 Glutathione as cytoprotective agent

As described above, GSH is discussed to be involved in resistance of tumor cells to platinum complexes. But GSH has also been administered to patients prior to platinum complexes to reduce toxicity. In patients treated with cisplatin or oxaliplatin, renal and neurological toxicity were ameliorated after intravenous administration of GSH without loss of antitumor effects although total GSH and cysteine in plasma increased significantly [44-47]. In animal experiments the protective GSH dose did not appear to influence the antitumor effects either [45]. In patients treated with fluorouracil and oxaliplatin a significant reduction of neurotoxicity was seen when patients received GSH before administration of chemotherapy. The formation of platinum-DNA adducts in leukocytes was not altered in these patients suggesting no GSH influence on platinum-DNA adduct formation in tumor cells [48].

1.5 Multidrug resistance-associated proteins

Multidrug resistance-associated proteins (MRP), as the name suggests, are established to be involved in resistance to diverse drugs and in the phenomenon of multidrug resistance (MDR) in cancer. MRP belong to the superfamily of ATP-binding cassette (ABC) transporter as they utilize energy from adenosine triphosphate (ATP) hydrolysis to transport substrates across membranes. ABC transporters are composed of two nucleotide-binding domains (NBD) and different numbers of membrane-spanning domains (MSD). Seven subfamilies of ABC transporters have been described so far (ATP-binding cassette sub-family A to G: ABCA to ABCG). Beside MRP, prominent members of ABC transporters involved in MDR are P-glycoprotein (P-gp) (ABCB1, also called MDR1) and breast cancer resistance protein (BCRP) (ABCG2). Subfamily ABCC is the biggest family comprising transporters which differ in structure, substrate specificity and cellular location, among them MRP [49]. MRP are

expressed in tissues that require protection from endogenous substances including liver, intestines and kidney. But beside transport of toxins they also transport endogenous substances [50].

In the context of platinum resistance MRP1 (ABCC1) and MRP2 (ABCC2) appear to be of importance [51,52]. These transporters, however, differ with regard to the tissues they are expressed in. MRP2 is also referred to as 'canalicular multispecific organic anion transporter 1' (cMOAT), since it is expressed in the canalicular (apical) part of hepatocytes and transports small organic anions. Localization and substrates of MRP1 and MRP2 are shown in Tab. 1-2. It has to be considered that controversial information about the transport of cisplatin by MRP1 is found in literature.

Tab. 1-2 Localization and substrates of MRP1 and MRP2, nonexhaustive enumeration [26,49,50,52,53].

Transporter	Tissues	Substrates	
		physiological	drugs (assumed)
MRP1	'Ubiquous', highest levels in lung, testis, kidney, skeletal and cardiac muscles, placenta and macrophages	Leukotriene C_4, leukotriene D_4, folate, Estrone 3-sulfate, glucuronic acid conjugates of estradiol and bilirubin, GSH conjugate of prostaglandin A_2	Doxorubicin, daunorubicin, etoposide, rhodamine, ciclosporin, GSH adducts of melphalan and chlorambucil, cisplatin
MRP2	Liver, kidney, intestine, gall bladder, placenta, peripheral nerves, placental trophoblast	Leukotriene C_4, glucuronic acid conjugates of estradiol and bilirubin, sulfate conjugate of estradiol	Doxorubicin, etoposide, methotrexate, mitoxantrone, vinblastine, sulfinpyrazone, ampicillin, pravastatin, cisplatin

Resembling each other in topology, MRP1 and MRP2 are identical in only 49% of amino acids and as mentioned above differ with regard to expression pattern (see Fig. 1-6 for topology model of MRP1 and MRP2). Despite their difference in amino acids, they show similar substrate specificity. The kinetic properties of substrate transport of MRP1 and MRP2, however, are different. For instance, MRP2 shows higher affinity for mono- and bisglucuronosyl bilirubin than MRP1 whereas MRP1 has higher affinity for leukotriene C_4 [26,49]. In case of MRP2 two distinct binding sites were discussed; one

binding site seems responsible for drug transport, the other one for regulation of transport [49,52].
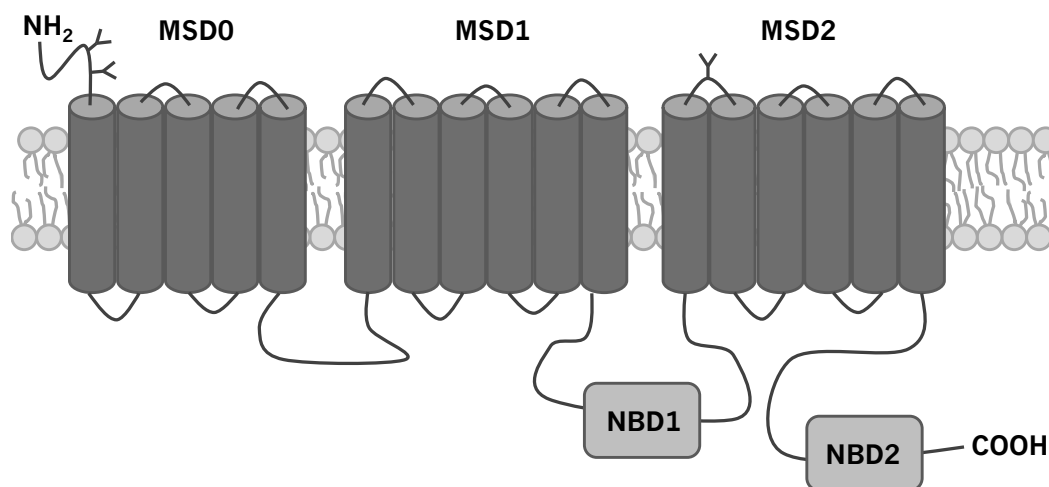
Fig. 1-6   Topology model of MRP1 and MRP2 (top: extracellular space, bottom: intracellular space). Controversial topology models of MRP2 consisting of only four transmembrane helices in MSD2 exist [49].
NBD: nucleotide-binding domain, MSD: membrane-spanning domain, Y: glycosylation.

Active substances such as verapamil and ciclosporin inhibit MRP1- and MRP2-mediated efflux, but also the efflux via P-gp. Only few specific modulators for MRP have been described to date, among them 4-aminobenzoic acid derivatives. In case of Gü83 (see Fig. 1-7) inhibition of MRP1- ($IC_{50} = 1.21\ \mu M$) and of MRP2-mediated efflux ($IC_{50} = 21.5\ \mu M$) but not of P-gp-mediated efflux has been reported by Leyers et al. using cell lines stably expressing the particular transporter [54].
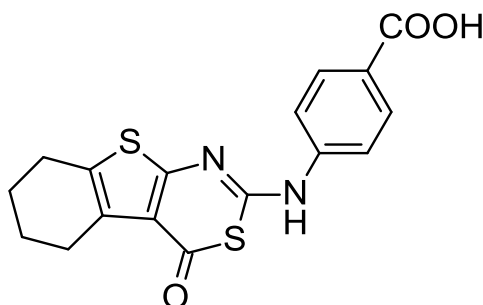
Fig. 1-7   Chemical structure of the MRP modulator Gü83 (4-[(5,6,7,8-tetrahydro-4-oxo-4H-[1] benzo-thieno[2,3-d][1,3]thiazin-2-yl)amino]benzoic acid).

1.5.1 MRP in platinum resistance

Experiments in Madin-Darby canine kidney cells (MDCKII) stably expressing either MRP1 or MRP2 have indicated that cisplatin might be transported by both MRP1 and MRP2 [53]. The results of experiments with human cancer cells, however, predominately suggest an association of MRP2 overexpression but not of MRP1 overexpression with platinum resistance [55].

MRP1 is reported to be highly expressed in leukemias, esophageal carcinomas and non-small cell lung cancer [52]. Most cancer cell experiments did not suggest a direct association of MRP1 expression with resistance to cisplatin or other platinum complexes [9]. Bracht et al. found no correlation between MRP1 expression and sensitivity to cisplatin, carboplatin or oxaliplatin in 14 human cancer cell lines [56]. In a panel of 30 unselected lung cancer cell lines, however, a correlation of MRP1 expression and cisplatin sensitivity was observed [57]. Recently published studies suggest an association of nuclear MRP1 with resistance to cisplatin [58].

MRP2 is expressed in some solid tumors originating from the kidney, colon, breast, lung and ovaries and in leukemic blasts [52] and there is evidence from *in vitro* experiments that MRP2 is involved in platinum resistance. In human pancreatic cancer cells the MRP2 but not the MRP1 expression level was associated with cisplatin resistance [59]. The level of DNA platination after incubation with cisplatin correlated inversely with the level of MRP2 expression in melanoma cells also suggesting an impact of MRP2 on cisplatin toxicity [60]. Investigating diverse human cancer cell lines overexpressing MRP2 the reversal of resistance to cisplatin was achieved by MRP2 knock out by anti-MRP2 hammer-head ribozymes [61]. In a panel of esophageal squamous cell carcinoma (ESCC) cell lines high MRP2 mRNA expression correlated with resistance to cisplatin, which could be reduced by inhibition of MRP2 expression by small-interfering RNA (siRNA) [62]. In a human ovarian cancer cell line and its cisplatin-resistant variant an increase in sensitivity to cisplatin was achieved by short hairpin RNA (shRNA) decreasing MRP2 expression [63]. An increase of MRP2 protein expression could be induced by cisplatin in a cisplatin-resistant ovarian carcinoma cell line [64].

In contrast, in colorectal adenocarcinoma cells an increased expression of MRP2 induced by fluorouracil resulted in sensitization to oxaliplatin. Authors suggested that an increased GSH efflux via MRP2 could lead to the increased sensitivity [65]. There are more data suggesting

that the contribution of MRP2 could strongly depend on cell-type. In cervical cancer cells a 20-fold lower MRP2 expression was found in cells resistant to cisplatin compared to the sensitive cells [66].

Clinical relevance of MRP-mediated efflux in platinum resistance

The assumption that rather MRP2 than MRP1 is relevant for platinum resistance is also confirmed when considering clinical data. In tumor samples of colorectal cancer patients an upregulation of MRP2 in cancerous regions compared with noncancerous regions was described and hypothesized to be associated with resistance to cisplatin [67]. In patients suffering from hepatocellular carcinoma (HCC) a negative correlation of MRP2 expression in resected specimens and tumor necrosis after cisplatin-based chemotherapy was found, suggesting that expression of MRP2 is associated with the efficacy of the chemotherapy regimen [68]. In a similar study with resected esophageal squamous cell carcinoma (ESCC) specimens the MRP2-positive patients showed poorer prognosis than MRP2-negative patients with regard to 5-year survival rate (25.6% vs. 55.7%) [62]. In tumor samples from patients with small cell lung cancer (SCLC), MRP2 expression but not MRP1 expression was associated with a worse response to cisplatin-containing chemotherapy [69]. In samples from patients suffering from ovarian cancer, MRP2 was found in the nuclear membrane. Weak expression of MRP2 in the nuclear membrane was associated with longer progression-free and overall survival. Interestingly, the correlation of MRP2 expression and survival was only found for MRP2 in the nuclear membrane and not for MRP2 in the cytoplasmic membrane [64].

1.6   Interaction between glutathione and MRP in platinum resistance

In the previous chapters the relevance of GSH (see chapter 1.4.1) and MRP-mediated efflux (see chapter 1.5.1) for platinum resistance were discussed separately but their interaction needs to be considered as well. MRP1 and MRP2 transport various endo- and exogenous substances and besides GSH and oxidized GSH (GSSG), GSH conjugates are substrates [26,27]. As formation of GSH conjugates was reported for platinum complexes and MRP have been associated with platinum resistance, an MRP mediated efflux of platinum-GSH adducts suggests itself.

However, the interaction of GSH and MRP in terms of excretion of endo- and exogenous substances is diverse and goes beyond the transport of GSH conjugates. GSH can be co-transported with substances or it can stimulate their transport without being transported itself. But also MRP1- and MRP2-mediated GSH transport has been reported to be stimulated by xenobiotics, even by substances that are not substrates [26,49,55]. GSH might even be required as a co-factor for the transport of GSH conjugates [50]. The possible scenarios of interaction of GSH, MRP and endo- or exogenous substances are summarized in Fig. 1-8.
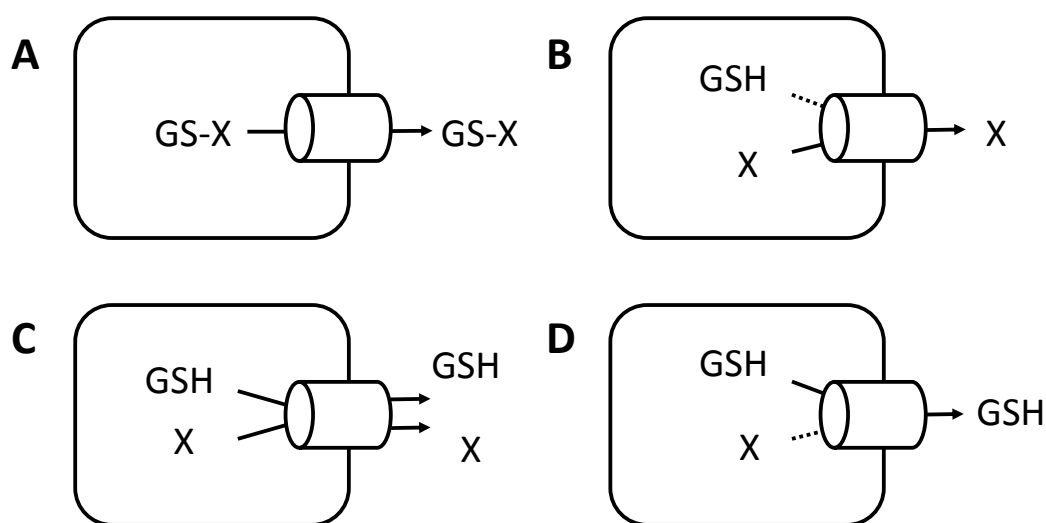
Fig. 1-8   Export of GSH and endogenous substances through MRP1 and MRP2. **A** transport of GSH conjugate, **B** transport stimulated by GSH, **C** co-transport, **D** substance stimulates GSH efflux but is not substrate (adapted from [55]).
X: endo- or exogenous substance (e.g. platinum complex), GS-X: GSH conjugate of X.

According to literature, in case of platinum complexes MRP-mediated efflux of GSH adducts is most probable and associated with platinum resistance [5,6,34,35]. Available data are, however, conflicting as results of *in vitro* experiments have also suggested that GSH does not play a role in cisplatin transport [53].

2   AIM AND OBJECTIVES

Platinum complexes are used in a variety of cancer chemotherapy regimens. However, the success of therapy is often limited as many tumor cells are intrinsically resistant or acquire resistance towards platinum complexes. By now it is known that various factors contribute to resistance. One of them is glutathione (GSH) which has been associated with platinum resistance for a long time. The mechanisms involving GSH were addressed in this project as they have not been fully elucidated yet. As the efflux of platinum complexes or platinum-GSH adducts via MRP2 is often discussed with regard to resistance, this efflux transporter has been considered in this research project as well.

Within the scope of this project the relevance of glutathione and MRP-mediated efflux for platinum resistance should be revealed in human cancer cell lines and their platinum-resistant variants. For this purpose, the following objectives were defined:

- Determination of the cellular GSH content.

- Determination of changes in cellular GSH content after exposure of the cells to platinum complexes.

- Determination of sensitivity of the cells towards platinum complexes after GSH depletion.

- Identification of changes in cellular platinum accumulation after GSH depletion.

- Identification of possible cisplatin- and oxaliplatin-GSH adducts.

- Determination of expression and localization of MRP2.

- Determination of alterations in cellular platinum accumulation and DNA platination using MRP modulators.

3   MATERIALS AND METHODS

3.1   Chemicals and reagents

Acrylamide 30% [m/V]	AppliChem GmbH, Darmstadt
Alexa Fluor® 488 goat anti-chicken IgG antibody	Invitrogen, Karlsruhe
Anti-mouse IgG horseradish peroxidase-conjugated antibody	R&D Systems GmbH, Wiesbaden-Nordenstadt
Anti-goat IgG horseradish peroxidase-conjugated antibody	R&D Systems GmbH, Wiesbaden-Nordenstadt
Argon 4.6	Air Product, Hattingen
BCA protein assay kit (Novagen®): Albumin standard ampoules (2 mg/mL bovine serum albumin) Reagent A (bicinchoninic acid) Reagent B (4% cupric sulfate)	Merck KGaA, Darmstadt
β-Actin (C4) antibody (mouse polyclonal IgG)	Santa Cruz Biotechnology, Inc., Heidelberg
Ammonium persulfate (APS)	AppliChem GmbH, Darmstadt
Boric acid	Fluka Chemie, Neu-Ulm
Bovine serum albumin (BSA)	Sigma-Aldrich, Steinheim
Bromophenol blue	AppliChem GmbH, Darmstadt
Buthionine sulfoximine (BSO)	Fluka Chemie, Neu-Ulm
Acetomethoxy derivative of Calcein (calcein AM)	Sigma-Aldrich, Steinheim
CASYton, isotonic diluting solution	Schärfe System, Reutlingen
Cisplatin	Sigma-Aldrich, Steinheim
Cobalt(II) sulfate heptahydrate	Sigma-Aldrich, Steinheim
2-(4-Amidinophenyl)-1H-indole-6-carboxamidine-dihydrochloride (DAPI)	Sigma-Aldrich, Steinheim
Dimethylsulfoxide (DMSO)	Riedel-de Haën, Seelze
3-(4,5-Dimethylthiazol-2-yl)-2,5-diphenyltetrazolium bromide (MTT)	AppliChem, Darmstadt
Disodium hydrogen phosphate dihydrate	Merck KGaA, Darmstadt

Dithiothreitol (DTT)	Applichem, Darmstadt
Elektrophoresis buffer, 10 x [25 mM Tris base, 192 mM glycin, 0.1% sodium dodecyl sulfate]	Bio-Rad Laboratories GmbH, München
Ethanol 96-100 % [V/V]	Merck KGaA, Darmstadt
Ethylenediaminetetraacetic acid (EDTA)-disodium salt dihydrate	Sigma-Aldrich, Steinheim
Fetal calf serum (FCS)	Sigma-Aldrich, Steinheim
Fluoromount™ aqueous mounting medium	Sigma-Aldrich, Steinheim
Formaldehyde 37 % [m/V]	Riedel de Haën AG, Seelze
Glucose monohydrate	Sigma-Aldrich, Steinheim
Glutathion (GSH)	Sigma-Aldrich, Steinheim
Glycerol 100% [V/V]	Applichem GmbH, Darmstadt
Glycine	Grüssing GmbH, Filsum
4-(2-hydroxyethyl)-1-piperazineethane-sulfonic acid (HEPES)	Applichem GmbH, Darmstadt
Hydrochloric acid [0.1 M and 1.0 M]	Riedel de Haën AG, Seelze
Hydrochloric acid 37% [m/V]	Merck KGaA, Darmstadt
Isopropanol 100% [V/V]	Merck KGaA, Darmstadt
Leupeptin hemisulfate	Sigma-Aldrich GmbH, Steinheim
L-Glutamin solution [200 mM]	Sigma-Aldrich, Steinheim
Methanol	Merck KGaA, Darmstadt
Milk powder	Carl Roth GmbH & Co. KG, Karlsruhe
Monosodium phosphate	Fluka Chemie, Neu-Ulm
MRP2 (H-17) antibody (goat polyclonal IgG)	Santa Cruz Biotechnology, Inc., Heidelberg
Naphthalene-2,3-dicarboxaldehyde (NDA)	Sigma-Aldrich, Steinheim
Nitric acid 65% [V/V], suprapur	Merck KGaA, Darmstadt
Oxaliplatin	Sigma-Aldrich, Steinheim
Penicillin streptomycin solution [10,000 I.E./mL, 10 mg/mL]	Sigma-Aldrich, Steinheim
Pepstatin A	Sigma-Aldrich, Steinheim
Perchloric acid 70%	Sigma-Aldrich, Steinheim
Pierce ECL Western Blotting Substrate (luminol/enhancer, peroxide buffer)	Thermo Fisher Scientific Inc., Rockford, USA
Potassium chloride	Merck KGaA, Darmstadt

Potassium dihydrogen phosphate	Fluka Chemie GmbH, Neu-Ulm

QIAmp DNA Mini Kit:
    Buffer AE (elution buffer)
    Buffer AL (lysis buffer)
    Buffer AW 1 (wash buffer)
    Buffer AW 2 (wash buffer)
	Qiagen, Hilden

RPMI-1640 medium	Sigma-Aldrich, Steinheim
Ribonuclease A (RNAse)	Sigma-Aldrich, Steinheim
Roti®-Mark (protein marker), prestained	Carl Roth GmbH & Co. KG, Karlsruhe
Sodium azide	Fluka Chemie, Neu-Ulm
Sodium bicarbonate	Fluka Chemie, Neu-Ulm
Sodium chloride	Fluka Chemie, Neu-Ulm
Sodium dihydrogen phosphate monohydrate	Sigma-Aldrich, Steinheim
Sodium dodecyl sulfate (SDS)	Applichem GmbH, Darmstadt
Sodium hydroxide [0.1 M and 1.0 M]	Riedel de Haën AG, Seelze
Sodium orthovanadate	Applichem GmbH, Darmstadt
Tetramethylethylenediamine (TEMED)	Applichem GmbH, Darmstadt
Tergitol solution	Sigma-Aldrich, Steinheim
Tris(hydroxymethyl)aminomethane (Tris base)	Applichem GmbH, Darmstadt
Triton® X-100	Sigma-Aldrich, Steinheim
Trypsin-EDTA solution [0.5 g porcine trypsin and 0.2 g EDTA in 100 ml]	Sigma-Aldrich, Steinheim
Tween®-20	Applichem GmbH, Darmstadt
Ultrapure water	Obtained by Purlab Plus™ system, Elga Labwater, Celle

3.2 Buffers and solutions

Phosphate buffered saline (PBS)

Sodium chloride	8.0 g
Potassium chloride	0.2 g
Disodium hydrogen phosphate dihydrate	1.44 g
Potassium dihydrogen phosphate	0.24 g
Ultrapure water	ad 1000.0 mL

pH adjusted to 7.4 using sodium hydroxide or hydrochloric acid

Cisplatin stock solution [5 mM]

Cisplatin	1.5 mg
Sodium chloride solution 0.9%	1.0 mL

Oxaliplatin stock solution [10 mM]

Oxaliplatin	3.97 mg
Ultrapure water	1.0 mL

3-(4,5-Dimethylthiazol-2-yl)-2,5-diphenyltetrazolium bromide (MTT) solution [5 mg/mL]

MTT	10 mg
PBS	2.0 mL

Ribonuclease A (RNase) solution [100 mg/mL]

RNase	10 mg
Buffer AL (from QIAmp DNA Mini Kit)	100.0 μL

3.2.1   Glutathione quantification

Borate buffer pH 9.2 [100 mM]

Boric acid	618.4 mg
Ultrapure water	ad 100.0 mL

pH adjusted to 9.2 using sodium hydroxide

Dithiothreitol (DTT) solution [100 mM]

DTT	30.9 mg
Borate buffer 9.2	2.0 mL

Glutathione (GSH) stock solution [10 mM]

GSH	37.2 mg
Hydrochloric acid [0.1 M] / EDTA [1 mM] (see below)	ad 100.0 mL

HCl 0.1 M / EDTA [1 mM]

$Na_2EDTA \cdot 2\ H_2O$	30.7 mg
HCl 0.1 M	ad 10.0 mL

GSH working solution 1 [100 μM]

GSH stock solution	100 μL
Perchloric acid 3.3% (see below)	ad 10.0 mL

GSH working solution 2 [10 μM]

GSH working solution 1	1000 μL
Perchloric acid 3.3% (see below)	ad 10.0 mL

Perchloric acid ($HClO_4$) 3.3%

Perchloric acid 70%	4.7 g
Ultrapure water	ad 100.0 mL

Naphthalene-2,3-dicarboxaldehyde (NDA) solution [5 mM]

NDA	9.2 mg
DMSO	ad 10.0 mL

3.2.2 SDS page and protein immunoblotting

Cell lysis

Lysis buffer

Tergitol solution	10.0 mL
Tris base	2.423 g
Sodium chloride	8.006 g
Glycerol	100.0 mL
EDTA	0.584 g
Activated sodium orthovanadate [10 mM]*	100.0 mL
Ultrapure water	ad 1000.0 mL
Leupeptin solution [5 mg/mL in ultrapure water]**	2 μL
Pepstatin A solution [2 mg/mL in DMSO]**	5 μL

* Solution of sodium orthovanadate [10 mM] in ultrapure water, pH adjusted to 10 and solution boiled yielding a clear solution. After cooling down readjusted pH to 10.

** Leupeptin and Pepstatin A solution were added shortly before usage.

SDS polyacrylamide gel electrophoresis (SDS-PAGE)

Ammonium persulfate (APS) solution [10%]

APS	100 mg
Ultrapure water	as 1000.0 μL

Dithiothreitol (DTT) solution [3.2 M]

DTT	49.4 mg
Ultrapure water	ad 1000.0 μL

Loading buffer

Stacking gel buffer	1.75 mL
Glycerol	1.5 mL
Sodium dodecyl sulfate solution (see below)	5 mL
Bromophenol blue solution*	1.25 mL

* Saturated bromphenol blue solution in ultrapure water containing 0.1% ethanol.

Sodium dodecyl sulfate (SDS) solution [10%]

SDS	1.0 g
Ultrapure water	ad 10.0 mL

Stacking gel

Acrylamide 30%	833 μL
Stacking gel buffer (see below)	625 μL
Ultrapure water	3445 μL
SDS 10%	50 μL
TEMED*	5 μL
APS 10%*	20.8 μL

   * Added last for initiation of polymerization.

Stacking gel buffer (pH 6.8)

Tris base	12.11g
Ultrapure water	ad 100.0 mL

   pH adjusted to 6.8

Separating gel

Acrylamide 30%	5000 μL
Separating gel buffer (see below)	5625 μL
Ultrapure water	4093 μL
SDS 10%	150 μL
TEMED*	27 μL
APS 10%*	105 μL

   * Added last for initiation of polymerization.

Separating gel buffer (pH 8.8)

Tris base	12.11g
Ultrapure water	ad 100.0 mL

   pH adjusted to 8.8 using hydrochloric acid

Western Blot

Tris-buffered saline (TBS)

Sodium chloride	4 g
Tris base	0.6 g
Ultrapure water	ad 500.0 mL

   pH adjusted to 7.3 using hydrochloric acid

Tris-buffered saline with Tween®-20 (TBS-T) solution

Tween®-20	1.6 mL
TBS	ad 800.0 mL

MATERIALS AND METHODS

Blocking solution

Milk powder	5 g
TBS-T solution	ad 100.0 mL

Transfer buffer

Glycine	14.4 g
Tris base	3 g
Ultrapure water	ad 800.0 mL

pH adjusted to 8.2 to 8.4 using hydrochloric acid

Antibody solutions for visualization of proteins

Primary antibody MRP2 solution [1:500]

Sodium azide	10 mg
BSA	500 mg
MRP2 (H-17) antibody (goat polyclonal IgG)	20 μL
TBS-T solution	10.0 mL

Primary antibody β-Actin solution [1:4000]

Sodium azide	10 mg
BSA	500 mg
β-Actin (C4) antibody (mouse polyclonal IgG)	2.5 μL
TBS-T solution	10.0 mL

Secondary anti-goat antibody solution [1:1000]

Milk powder	0.5 g
Anti-goat IgG horseradish peroxidase-conjugated antibody	10 μL
TBS-T solution	10.0 mL

Secondary anti-mouse antibody solution [1:1000]

Milk powder	0.5 g
Anti-mouse IgG horseradish peroxidase-conjugated antibody	10 μL
TBS-T solution	10.0 mL

3.2.3 Calcein assay

Acetomethoxy derivative of calcein (calcein AM) stock solution [1 mM]

Calcein AM	2 mg
Ultrapure water	2 mL

Calcein AM working solution [0.31 μM]

Calcein AM stock solution	5 μL
KHP (see below)	ad 4.0 mL

Krebs HEPES buffer (KHP)

Sodium chloride	3450 g
Potassium chloride	175 µg
Potassium dihydrogen phosphate	82 µg
Sodium bicarbonate	18 µg
Glucose monohydrate	1158 µg
HEPES	1192 µg
Ultrapure water	ad 500.0 mL

pH adjusted to 7.4

Cobalt(II) sulfate stock solution [10 mM]

Cobalt(II) sulfate heptahydrate	28.1 mg
Ultrapure water	10 mL

Cobalt(II) sulfate working solution [10 µM]

Cobalt(II) sulfate stock solution	10 µL
Ultrapure water	ad 10 mL

3.2.4   Immunocytochemistry

Bovine serum albumin (BSA) solution 1%

BSA	150 mg
PBS	15 mL

MRP2 antibody solution [1:20]

MRP2 (H-17) antibody (goat polyclonal IgG)	2.5 µL
1% BSA solution	47.5 µL

Alexa 488 antibody solution [1:100]

Alexa Fluor® 488 goat anti-chicken IgG antibody	6 µL
1% BSA solution	594 µL

DAPI stock solution [1 mg/mL]

DAPI	1 mg
Methanol	1000 µL

DAPI working solution [5 µg/mL]

DAPI stock solution	5 µL
Ultrapure water	ad 1000 µL

3.3 Equipment

Axiovert® 25 inverted microscope	Carl Zeiss AG, Oberkochen
Beckman Microfuge® Lite	Beckman-Coulter, Fullerton, USA
Casy®1 cell counter, Modell TT	Schärfe System, Reutlingen
Centrifuge Universal 32R	Hettich GmbH & Co. KG, Tuttlingen
Centrifuge Mikro 200R	Hettich GmbH & Co. KG, Tuttlingen
ESI-Q-qTOF QSTAR XL	Applied Biosystems, Darmstadt
Fluoroskan Ascent® microplate reader	Thermo Fisher Scientific, Langenselbold
FLUOstar™ OPTIMA microplate reader	BMG LABTECH GmbH, Ortenberg
ICP-MS Varian 820	Varian (Agilent Technologies), Darmstadt
Incubator Thermo	Thermo Electron GmbH, Dreieich
InoLab® pH level 2 pH Meter	WTW GmbH, Weilheim
Kern 770 analytical balance	Kern & Sohn GmbH, Balingen-Frommern
Kern EW analytical balance	Kern & Sohn GmbH, Balingen-Frommern
Laminar air flow work bench	Heraeus Holding GmbH, Hanau
MT Classic AB135-S analytical balance	Mettler-Toledo GmbH, Giessen
LUMIstar™ Optima microplate reader	BMG Labtech GmbH, Offenburg
Multiskan Ascent® microplate reader	Thermo Fisher Scientific, Langenselbold
Multiskan EX® microplate reader	Thermo Electron GmbH, Dreieich
Nikon A1 Eclipse Ti confocal microscope	Nikon, Kingston, UK
Purelab Plus™ system	ELGA LabWater, Celle
Shaker KS 15 control	Edmund Bühler GmbH, Hechingen
Ultrasonic bath Sonorex® Super RK 103 H	Bandelin, Berlin
UNIVAPO 100H Vacuum Concentrator Centrifuge	UniEquip GmbH, Planegg

Western blot analysis

VersaDoc™ Imaging System 5000	Bio-Rad Laboratories GmbH, München
Blotting equipment Mini-Protean® II	Bio-Rad Laboratories GmbH, München
Elektrophoresis equipment Mini-Protean® II	Bio-Rad Laboratories GmbH, München
Thermo EC Dual Mode Electrophoresis Power Supply	E-C Apparatus Corporation, Milford, USA

Atomic absorption spectrometry

Graphite tube atomizer GTA 100	Varian (Agilent Technologies), Darmstadt
Sample dispenser PSD 100	Varian (Agilent Technologies), Darmstadt
Spectrometer SpectrAA® Zeeman 220	Varian (Agilent Technologies), Darmstadt

3.3.1 Consumables

Blotting paper (cellulose), 7 x 10 cm	Sigma-Aldrich GmbH, Steinheim
Casy® tubes	Schärfe System, Reutlingen
Cell culture flasks 25, 75, 175 cm^2	Sarstedt AG & Co., Nümbrecht
Cell scraper	Sarstedt AG & Co., Nümbrecht
Conical centrifuge tubes 15, 50 mL	Sarstedt AG & Co., Nümbrecht
Cover slips (round, square)	Carl Roth GmbH & Co., Karlsruhe
Cryovials	Sarstedt AG & Co., Nümbrecht
Disposable syringe (10 mL)	B. Braun Melsungen AG, Melsungen
Glass Pipettes	Labomedic GmbH, Bonn
Graphite tubes	Varian (Agilent Technologies), Darmstadt
Microscope slides	Carl Roth GmbH & Co., Karlsruhe
Pasteur pipettes	Brand GmbH & Co., Wertheim
Petri dishes	Greiner Labortechnik, Frickenhausen
Pipette tips	Brand GmbH & Co., Wertheim
Platinum hollow cathode lamps (UltrAA® lamps)	Varian (Agilent Technologies), Darmstadt
PVDF (Polyvinylidene fluoride) membrane	Carl Roth GmbH & Co.KG, Karlsruhe
QIAamp® DNA Mini Kit	Qiagen, Hilden
Reaction tubes (0.5, 1.5, 2 mL)	Greiner Labortechnik, Frickenhausen
Sample vials (2 mL, conical)	Varian (Agilent Technologies), Darmstadt
Tissue culture plates, 96 wells	Sarstedt AG & Co., Nümbrecht
Tissue culture plates, 6 wells	Sarstedt AG & Co., Nümbrecht

3.3.2   Software

Accelrys Draw 4.0	Accelrys. Inc., San Diego, USA
Analyst® QS software	Applied Biosystems, Foster City, USA
Ascent Software (for Multiskan EX®)	Thermo Electron Inc., Dreieich
GraphPad Prism®, version 4.00	GraphPad Software, San Diego, USA
Microsoft® Excel 2007	Microsoft Corporation, Redmond, USA
MVA® 2.0	NOVIA, Frankfurt am Main
NIS-Elements software	Nikon, Kingston, UK
Quantity One® - 4.6.1	Bio-Rad Laboratories GmbH, München
SpectrAA® 220, Version 2.20	Varian, Darmstadt

3.4   Cell culture

3.4.1   Cell lines and cultivation

In this project the human ileocecal colorectal adenocarcinoma cell line HCT-8 and the oxaliplatin-resistant variant HCT-8ox (kindly provided by Dr. M. Heim, University of Essen, Germany) as well as the ovarian carcinoma cell line A2780 and the cisplatin-resistant variant A2780cis (European Collection of Cell Cultures, United Kingdom) were used. The oxaliplatin-resistant variant of HCT-8, HCT-8ox, had been obtained after incubation with increasing concentrations of oxaliplatin in turns with incubation in drug-free medium [70]. The cisplatin-resistant variant of A2780, A2780cis, had been obtained after a similar procedure using cisplatin [71].

Cells were cultivated as monolayers in RPMI-1640® medium supplemented with 10% fetal calf serum (FCS), 100 U/mL penicillin and 0.1 mg/mL streptomycin (37 °C, 5% CO_2). For A2780 and A2780cis the medium was additionally supplemented with 0.6 mM L-glutamine. Cells were cultivated to a confluence of about 90% and then sub-cultivated or used for experiments. Backups of each cell line suspended in FCS containing 10% DMSO were stored in liquid nitrogen. After using cells over a period of 12 passages at most they were discarded and a new backup was thawed. Level of resistance of the resistant variants was monitored by the MTT-based cytotoxicity assay (see chapter 3.5). If a distinct number of cells was needed for an experiment, cells in a cell suspension were counted by electronic pulse area analysis

using a Casy[®]1 cell counter. Distribution of cell volume and cell aggregation was assessed at the same time.

3.4.2 Mycoplasma test

The genus mycoplasma comprises small prokaryotes (0.22 to 2 µm) without a cell wall, which can grow on cultivated mammalian cells and are not sensitive towards common antibiotics. Contamination with mycoplasma bacteria frequently occurs in cell culture and can bias research findings. Hence cells were regularly screened for mycoplasma infections using 2-(4-Amidinophenyl)-1H-indole-6-carboxamidine-dihydrochloride (DAPI). DAPI binds cellular DNA and can be detected by fluorescence microscopy after exciting with ultraviolet light through a blue filter.

Performing the assay, cells were seeded out on microscope slides in a petri dish. After three to four days the medium was removed, the slide washed with cold PBS and 80 µL of DAPI working solution as well as 2 mL methanol were added and left for 5 min. The slide was then washed with 2 mL methanol and cover slips were fixed on the slides using mounting medium. Cells were then analyzed using a Nikon Eclipse Ti fluorescence microscope. If a blue shade surrounding cells, accounting for stained mycoplasma DNA, had been seen, a mycoplasma infection was probable. These cells were discarded.

3.5 Cytotoxicity assay

Cytotoxic properties of compounds and in consequence the sensitivity of cells towards these compounds were assessed using the MTT assay [72]. The assay is based on the reduction of 3-(4,5-dimethylthiazol-2-yl)-2,5-diphenyltetrazolium bromide (MTT), a yellow tetrazole, to a purple formazan (see Fig. 3-1). As the reduction is performed by mitochondrial dehydrogenases of living cells, the amount of purple formazan built is inversely proportional to the cytotoxicity of a compound.

The assay was performed in 96-well plates. In each well a number of $3 \cdot 10^3$ cells (HCT-8, HCT-8ox) or $10 \cdot 10^3$ cells (A2780, A2780cis) was seeded out in 90 µL cell culture medium and allowed to attach overnight (37 °C, 5% CO_2). The outer wells of the plate were not used for the experiment as evaporation might occur during the experiment. Therefore, those wells were filled with PBS only. On the next morning 10 µL of the solution of the compound

investigated was added to each well. Here, usually a control (ultrapure water or sodium chloride solution 0.9%) and nine increasing concentrations of the compound were used. Each concentration was tested in triplicate.
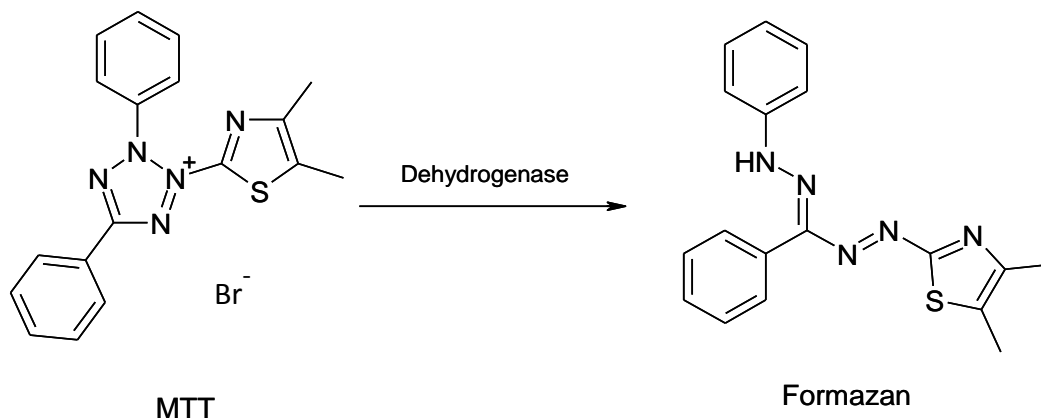
Fig. 3-1 Reaction of yellow MTT to a purple formazan.

The plates were incubated for 72 h (37 °C, 5% CO_2). Subsequently, 20 μL of MTT in PBS (5 mg/mL) was added and the plates incubated for 1 h (37 °C, 5% CO_2). The supernatant was then removed by carefully beating the plate upside down on tissue. The cells and the formazan crystals built were then lysed by addition of 100 μL of DMSO. The plates were shaken and the UV absorbance at 570 nm with background subtraction at 690 nm was measured using a Multiskan Ascent® microtiter plate reader. The procedure described was adapted from [73] but slightly modified (cell and formazan lysis with DMSO instead of 1:1 isopropanol and 1 M HCl as described by [72]). Dose-effect curves were calculated by non-linear regression using the software GraphPad Prism® (settings: no comparison, constraint: 'BOTTOM must be greater than 0.0', no weighting, consider each replicate Y value as an individual point). The regression was based on the four-parameter logistic Hill equation (see Equation 3-1 and Fig. 3-2) [74].

$$Y = \text{Bottom} + \frac{\text{Top} - \text{Bottom}}{1 + \left[\dfrac{10^{\text{LogEC}_{50}}}{10^{X}}\right]^{\text{Hill slope}}}$$

Equation 3-1

X	concentration
Y	absorption
Bottom	value for Y for the minimal curve asymptote
Top	value for Y for the maximal curve asymptote
LogEC_{50}	logarithm of drug concentration producing half maximal effect
Hillslope	steepness of concentration e response curve
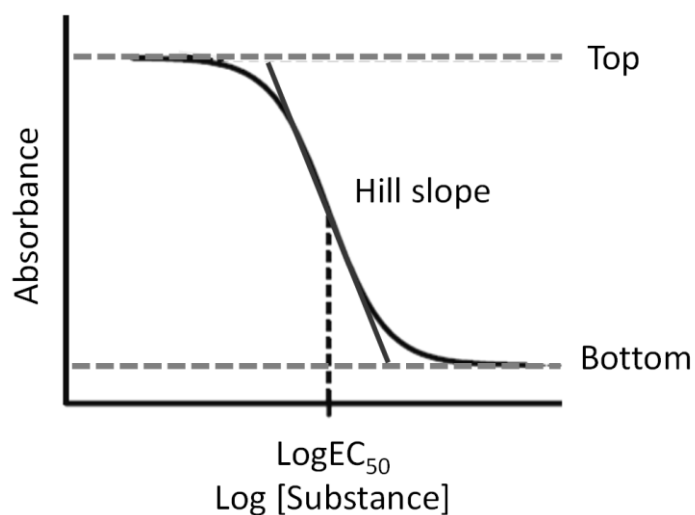
Fig. 3-2 Schematic diagram of the used Hill equation (adapted from [74]).

In this project the MTT assay was used to assess the resistance factor of resistant cell lines (HCT-8ox, A2780cis). To avoid variation between different 96-well plates the corresponding cell pair was seeded out on the same plate (see Fig. 3-3). EC_{50} values, the concentration necessary to eradicate half of the cell population, were computed as described above and the resistance factor was calculated by dividing the EC_{50} value of the resistant cells by the EC_{50} value of the respective sensitive cells.
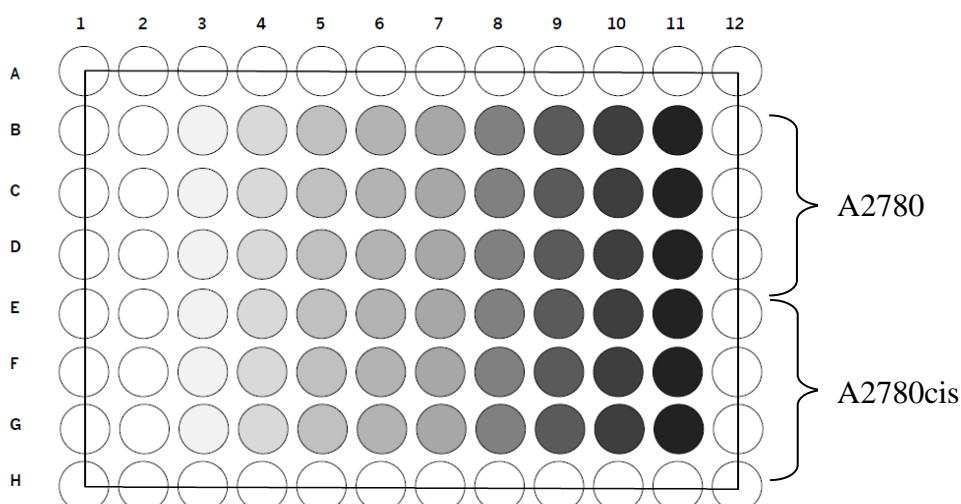
Fig. 3-3 96-well plate as prepared for assessing the resistance factor of A2780cis by the MTT assay. Darker colors symbolize higher concentrations of the platinum complex tested. Note that low concentrations of the platinum complex correspond to intense purple and high concentrations to light purple color after incubation with MTT solution and lysis with DMSO.

The assay was also used to test the influence of the MRP modulator Gü83 and the GSH depletor BSO on the cytotoxicity of platinum complexes. In this case the cells were co- and/or preincubated with the relevant compound and the platinum complex. In this case cells cultivated under control conditions (without co- or preincubation) and under experimental conditions (co- or preincubation) were seeded out on the same plate.

For Gü83 and BSO the assay was also used to assure that concentrations used in experiments were not cytotoxic. The assay was performed as described and cells were incubated with various concentrations of the respective compound either for 72 h or shorter. If the assay was performed to test the cytotoxicity after a shorter incubation time, cells were incubated with the compound for the chosen time span and subsequently incubated with cell culture medium until they were incubated 72 h altogether.

3.6 Glutathione quantification

To further investigate the role of GSH in platinum resistance an assay for determination of total cellular GSH was cross-validated based on bioanalytical guidelines [75,76]. The assay was based on the derivatization of reduced GSH with naphthalene-2,3-dicarboxaldehyde (NDA) to a fluorescent isoindole adduct (see Fig. 3-4, λ_{exc} at 472 nm and λ_{em} at 528 nm) [77].
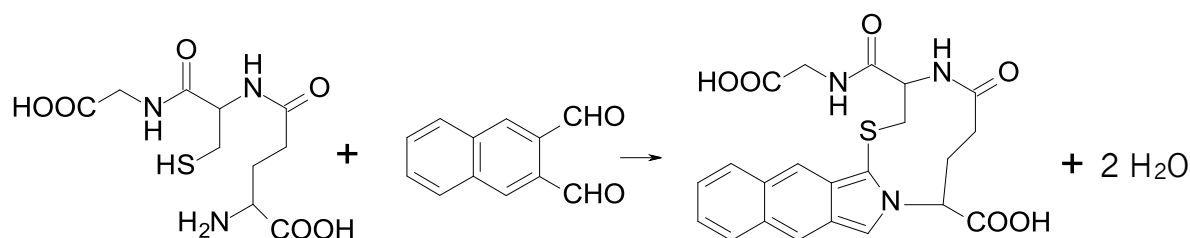
Fig. 3-4   Reaction of GSH and NDA to a fluorescent isoindole adduct.

GSH assay based on determination after sample derivatization and separation via capillary electrophoresis (CE) or high-performance liquid chromatography (HPLC) were described and validated [77-79] as well as a semi-quantitative determination without sample separation in 96-well plates [80]. Allowing higher sample throughput an assay in 96-well plates was chosen for this project.

Total cellular GSH comprises the reduced (GSH), the oxidized (GSSG) and the protein-bound (GSS-protein) form. Hence reduction of oxidized and protein-bound GSH using dithiothreitol (DTT) was necessary prior to derivatization with NDA (see Fig. 3-5). Results of the validation are presented in chapter 4.2.1.
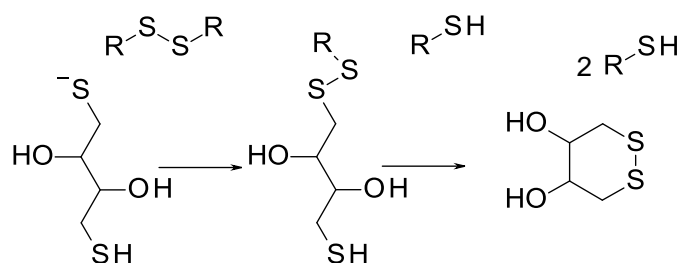
Fig. 3-5   Reduction of disulfides using DTT (pH > 7).

3.6.1   Cell lysis

Cells were seeded out in 6-well plates and allowed to attach overnight. After incubation with drugs/modulators, the cells were washed with PBS and detached using trypsin-EDTA solution. After adding cell culture medium the cells were transferred into an Eppendorf tube. Cells were centrifuged (167 g, 4 °C, 1 min) and resuspended in 1.0 mL PBS. 20 µL of the cell suspension was taken out twice for protein determination and the suspension was centrifuged again (167 g, 4 °C, 1 min). The cell pellet was washed with 1 mL of PBS again and

centrifuged (167 g, 4 °C, 1 min). The supernatant was then removed and the cell pellet lysed with 1.0 mL ice-cold perchloric acid (3.3%) followed by intensive vortexing for 10 seconds Afterwards the lysate was separated from the cell relict by centrifugation (12000 g, 4 °C, 10 min). The supernatant was transferred into a new Eppendorf tube and stored at -80 °C until GSH determination.

3.6.2 Glutathione determination

To generate a calibration curve six standard solutions and three quality control (QC) samples were freshly prepared by diluting GSH working solutions (WS) 1 and 2 with perchloric acid (3.3%) as shown in Tab. 3-1. The stock solution used for preparation of WS1 and WS2 for QC samples was different from the stock solution used for preparation of WS1 and WS2 for the calibration curve. Standards and QC samples were not prepared using the matrix of the samples, lysed cell pellet, as lysed cell pellet itself contains GSH.

Samples were carefully thawed on ice and 90 µL of each sample, standard solution and QC samples were pipetted on a 96-well plate. Standard solutions were measured in triplicate, QC samples and samples with unknown content in duplicate. For pH adjustment 50 µL of 1 M sodium hydroxide and 100 µL borate buffer pH 9.2 were added to each well. 10 µL of DTT solution was added for reduction of bound and oxidized GSH and the mixture was allowed to react for 2 min. Finally, 25 µL of NDA solution was added and the plate shaken softly for 15 min. The fluorescence signal was then measured using a Fluoroskan Ascent® microtiter plate reader (λ_{exc} 485 nm and λ_{em} 538 nm). If the fluorescence signal of a sample was above the calibration range the sample was diluted with perchloric acid (3.3%) and GSH determination was repeated.

The calibration curve was generated using a weighting factor of $1/x^2$ using MVA® 2.0 software and the concentration of the samples was calculated. When performing the assay the calibration curve was accepted when at least four out of the six calibration standards did not deviate more than 15% from their nominal values (20% for the lower limit of quantification) and when two out of three QC samples were within 15% of their nominal values (20% for lowest QC sample). The concentrations obtained were related to the protein contents of the samples to adjust for different cell volumes or sample loss during processing. The intracellular GSH content was expressed relative to the respective mean value for HCT-8.

Tab. 3-1   GSH-containing standard solutions and quality control samples for GSH determination.

	GSH content [μM]	GSH WS 1 [μL]	GSH WS 2 [μL]	Perchloric acid (3.3%) [μL]
Standard solutions				
S1	1	-	100	900
S2	2	-	200	800
S3	5	-	500	500
S4	10	-	1000	-
S5	15	150	-	850
S6	20	200	-	800
Quality control samples				
QC1	3	-	300	700
QC2	12	120	-	880
QC3	18	180	-	820

3.6.3   Effect of platinum exposure on the cellular GSH content

To investigate the effect of platinum complexes on cellular GSH content, cells were incubated with 100 nM oxaliplatin (HCT-8 and HCT-8ox) or 100 nM cisplatin (A2780 and A2780cis) for 24 h. Control cells were incubated with PBS only. Samples were taken after 0, 4, 8, 12 and 24 h, GSH and protein content were determined as described above and in chapter 3.7, respectively.

3.7   Protein quantification

In some experiments determination of protein content of samples was necessary for normalization of results to correct for different cell volumes and growth behavior as well as for sample loss during preparation. Hence the protein concentration was assessed using the bicinchoninic assay (BCA protein assay kit) according to the manufacturer's instructions. The assay is based on the reduction of Cu^{2+} to Cu^{+} by proteins. Two molecules of bicinchoninic acid react with one Cu^{+} forming a purple chelate complex. The absorbance of the purple

chelate complex at 562 nm is proportional to the concentration of this complex as well as to the concentration of proteins and was determined using a UV microtiter plate reader.

The method was validated in our working group with respect to sample preparation and with respect to the generation of the calibration curve (linearity and working range, precision and accuracy, lower limit of quantification) previously [70,81].

3.7.1 Standard solutions and quality control samples

Standard solutions and quality control (QC) samples were prepared by dilution of a 2 mg/mL solution of bovine serum albumin (BSA) provided by the manufacturer.

Tab. 3-2 Standard solutions and quality control samples for protein determination.

	Volume BSA [µM]	Volume ultrapure water [µL]	Protein concentration [µg/mL]
Standard solutions			
S1	50	1950	50
S2	75	1925	75
S3	100	1900	100
S4	200	1800	200
S5	300	1700	300
S6	400	1600	400
Quality control samples			
QC1	150	1850	150
QC2	250	1750	250
QC3	350	1650	350

3.7.2 Sample preparation

At first, 10 µL of 1 M sodium hydroxide was added to 20 µL of each sample for protein lysis. The protein samples were then sonicated at room temperature for 30 min. Afterwards samples were neutralized with 10 µL 1 M HCl. Samples were diluted with ultrapure water to be within the calibration range if necessary. Standard solutions and QC samples were treated in the same way except the dilution step.

The solutions were then transferred to a 96-well plate pipetting 20 µL of samples and QC samples in duplicate and standard solutions in triplicate. Afterwards a 50:1 mixture of BCA working reagent A (containing BCA) and BCA working reagent B (containing $CuSO_4$) was prepared, 200 µL of the mixture was added to each well and the plate was incubated for 1 h at 60 °C. UV absorbance at 570 nm was then determined using a Multiskan Ascent® microtiter plate reader.

Linear regression was performed using Microsoft® Excel 2007 and sample concentrations were calculated from the regression curve. The calibration was accepted when at least four of the standard solutions did not deviate more than 15% from the nominal value (20% at the lower limit of quantification) and two of three QC samples did not deviate more than 15% of the nominal value.

3.8 Mass spectrometry

By the use of mass spectrometry (MS) the mass-to-charge ratio (m/z) of charged molecules can be detected and chemical structures of molecules can be proposed based on characteristic isotope patterns of single ions. The technique can be used for qualitative and/or quantitative analysis. Samples are vaporized, ionized, the ions separated by the 'mass analyzer', their signals detected and the signal processed into a mass spectrum. Ionization of the samples is performed in the 'ion source' and can be achieved by 'electrospray ionization' (ESI). The basic installation used for electrospray ionization mass spectrometry (ESI-MS) is depicted in Fig. 3-6. To further elucidate chemical structures, fragmentation techniques can be applied when using tandem mass spectrometry, which involves multiple MS steps. First specific 'masses' are separated and then fragmented in a collision chamber. The fragments obtained are analyzed and can verify a molecular structure suggested.
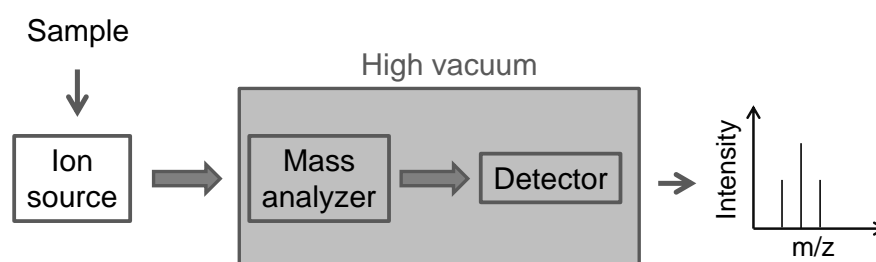
Fig. 3-6   Basic composition of an ESI-MS system (adapted from [82]).

To characterize platinum-glutathione adducts cisplatin and oxaliplatin were incubated with GSH in a ratio of 1:10 (55 µM platinum complex and 550 µM GSH) in an aqueous solution. Methanol, to permit vaporization (final concentration of 60%) and formic acid, to produce ions (final concentration of 1%), were added immediately or after a 12 h incubation time at 37 °C. Subsequently, ESI-MS measurements were performed after static sample application using an ESI-quadrupole time-of-flight mass spectrometer (ESI-Q-qTOF, type: QSTAR XL) equipped with a nanospray ion source. Spectra were collected in positive mode over m/z range of 200 to 2000. Analyst® QS software was used for analysis of spectra obtained. For these experiments the MS equipment of the working group of Dr. Sabine Metzger at the University of Düsseldorf, Germany, was used.

3.9 Platinum accumulation

To investigate the cellular platinum accumulation, 10^6 HCT-8 or HCT-8ox cells were allowed to attach in 6-well plates for 12 to 14 hours. When the effect of buthionine sulfoximine (BSO) was investigated, cells were incubated with 100 µM BSO directly after being seeded out. Cells were then incubated with oxaliplatin [100 µM] and in some experiments additionally with MRP-modulating substances. Cells were harvested using trypsin-EDTA solution after washing with ice-cold PBS and resuspended in medium. The suspension was centrifuged, the supernatant removed and the cell pellet washed with 1 mL PBS twice. The cell pellet was lysed in 65% nitric acid (1 h, 80 °C) and the platinum content was quantified using flameless atomic absorption spectrometry (SpectrAA® Zeeman 220) [83]. The platinum concentration was related to the protein content determined by the bicinchoninic acid (BCA) assay (see chapter 3.7).

3.10 Platinum efflux

The method chosen for measurement of platinum efflux was similar to the method used to assess platinum accumulation (see chapter 3.9). Cells were seeded out in 6-well plates, allowed to attach overnight and exposed for 2 h to 100 µM oxaliplatin alone or with 100 µM Gü83. Then cell culture medium was changed. At distinct time points cells were harvested after being washed with PBS twice. The samples were treated as described in chapter 3.9.

3.11 DNA platination

As described in chapter 1.2.1 binding to DNA is an important feature in view of the mechanism of action of platinum complexes. Hence the influence of the MRP modulator Gü83 on DNA platination was also investigated. Cellular DNA was isolated and quantified, afterwards lysed and the amount of platinum bound was determined. The measurements were performed adapting a method previously published [84].

For the experiments 10^6 HCT-8 or HCT-8ox cells were allowed to attach in 6-well plates for 12 to 14 hours before they were incubated with oxaliplatin (100 μM) with or without 200 μM Gü83. Cells were harvested using trypsin-EDTA solution after washing with ice-cold PBS and resuspended in medium. The suspension was centrifuged and the cell pellet was washed with 1 mL PBS twice. The samples were stored at -20 °C until further analysis.

DNA isolation was performed using a QIAmp® DNA Mini Kit for solid-phase extraction according to the manufacturer's instructions. The cell pellet was thawed, subsequently lysed by incubation with the protease solution and lysis buffer provided (10 min, 56 °C in ultrasonic bath) and finally isolated using the solid-phase extraction columns provided. Before lysis, the samples were treated with 4 μL ribonuclease A (RNase) solution [79]. Thereby ribonucleic acid (RNA) was cleaved and only DNA was isolated. DNA concentrations were measured by UV photometry [85].

The solution of isolated DNA was desiccated using a centrifugal evaporator (6 to 8 h, 39 °C) and then lysed in 2 mL 1% nitric acid (24 h, 70 °C). The platinum concentration of the samples was determined by inductively coupled plasma mass spectrometry (ICP-MS) using a Varian 820 ICP-MS at the University of Essen, Germany. In brief, for determination by ICP-MS samples are ionized by inductively coupled plasma and then the ions of interest are separated and quantified by a mass spectrometer. Each ICP-MS analysis resulted from five replicate measurements consisting of 20 scans of the relevant isotopes. For platinum quantification the most abundant platinum isotope, Pt^{195}, was chosen. Quality control samples and an internal standard were used to ensure the accuracy and precision of the measurements. The results were finally expressed as number of platinum atoms per million of nucleotides ($M_{nucleotides}$ 330 g/mol).

3.12 SDS page and protein immunoblotting

Immunoblots can be used to investigate gene expression on protein level. In this project this method was chosen for studying MRP2 protein levels using β-actin as housekeeping protein for normalization [86]. After separation of proteins by gel electrophoresis the proteins were transferred on a membrane using the western blot technique. The proteins adhering to the membrane were then detected using antibodies conjugated with horseradish peroxidase (HRP) resulting in a luminescence signal after addition of luminol [87].

3.12.1 Sample preparation

Cells were seeded out in cell culture flasks (175 cm^2) and cultivated to a confluence of about 90%. For sample preparation cell culture medium was removed and cells washed with PBS once. To release the proteins of interest cell lysis was necessary. Hence 1 mL of lysis buffer containing the protease inhibitors leupeptin and pepstatin A (see 3.2.2) to prevent proteolysis was added to the cells and evenly distributed on the cell monolayer. Cells were scratched from the bottom of the flask using a cell scraper. The lysate was transferred into a reaction tube and shaken for 30 min at 4 °C to complete cell lysis. After centrifugation (12000 g, 4 °C, 5 min) the supernatant was carried over into fresh reaction tubes for protein quantification (at 20 µL each) and for immunoblot (at 100 µL each) keeping samples on ice all the time. The tubes were stored at -20 °C (protein quantification) and -80 °C (immunoblot) respectively. The amount of sample protein obtained was quantified using the bicinchoninic assay (see chapter 3.7).

3.12.2 Gel electrophoresis and western blotting

Separation of proteins according to size was performed by sodium dodecyl sulfate polyacrylamide gel electrophoresis (SDS-PAGE). Polyacrylamide gels were prepared freshly starting with the separating gel (10% acrylamide, see chapter 3.2.2), which was filled between two glass plates clamped in an appropriate fixture and covered with a layer of 100% isopropanol. After 15 min the stacking gel (see chapter 3.2.2) was added and a comb producing wells for sample application put in place. After 30 min the comb was removed and the fixture containing the gel was placed in an electrophoresis chamber (electrophoresis

equipment Mini-Protean® II). Electrophoresis buffer was added till the gel was completely covered and the wells rinsed with buffer.

Samples were diluted with loading buffer, which was supplemented with 5% dithiothreitol (DTT) solution (see chapter 3.2.2), to a concentration of 10 µg protein per 20 µL. Loading buffer contained SDS, which binds to proteins and allows their migration in an electric field as it is charged, and DTT, which is important for denaturation of proteins. Bromphenol blue was also added to make samples visible. The proportion of DTT containing loading buffer in the mixture, however, needed to be at least 50% to effectively prepare the samples. Otherwise the amount of protein obtained was too little and the sample could not be analyzed. After leaving the samples 30 min at room temperature, samples as well as a protein marker were pipetted into the wells of the gel. Afterwards the proteins were separated applying voltage (200 V) to the gel. Voltage was removed when the sample front reached the end of the gel.

Prior to blotting proteins from the gel to a polyvinylidene fluoride (PVDF) membrane the membrane was treated with methanol for 20 seconds and shaken for 5 min in transfer buffer for equilibration. Afterwards the gel and the membrane were clamped tightly in a sandwich fixture and after that submerged in transfer buffer using the blotting equipment Mini-Protean® II. Applying electric current (100 V, 350 mA, 60 min) allowed transfer of the proteins which still were electrically charged by sodium dodecyl sulfate (SDS) and thus bound to the membrane. Afterwards the membrane was shaken in tris-buffered saline (TBS) (see chapter 3.2.2).

3.12.3 Visualization of proteins

Before the proteins bound to the membrane were tagged with a primary antibody the membrane was shaken in blocking solution containing milk powder (see chapter 3.2.2) for 1 h to minimize unspecific binding of antibodies. The membrane was shaken three times for 10 min with TBS-T solution subsequently. The solution of primary antibody against MRP2 (see chapter 3.2.2) was added and the membrane was shaken for 1 h. The membrane was left overnight at 4 °C with the antibody solution left on it. The next morning the antibody solution was removed and poured into a centrifuge tube as it was conserved by addition of sodium azide for reuse. The membrane was shaken three times for 10 min with TBS-T solution subsequently and then shaken for 1.5 h with the solution of the secondary antibody (anti-goat)

conjugated to HRP. The solution was removed and discarded. The membrane was washed three times for 10 min with TBS-T solution while shaking.

For visualization Pierce ECL Western Blotting Substrate was used. Luminol/enhancer and peroxide buffer were mixed 1:1 and 500 µL of the mixture were evenly distributed onto the membrane placed in a petri dish with the proteins upside. After 2 min the chemiluminescence signal generated by HRP and luminol was detected with the VersaDoc™ Imaging System and a digital image was produced. The digital image could be analyzed with the Quantity One® software.

After washing the membrane with TBS-T solution the procedure was repeated using the solution of primary antibody against β-actin. The membrane was incubated with the solution of the primary antibody and shaken for 1 h but the incubation at 4 °C overnight was skipped. Again, a secondary antibody (anti-mouse) conjugated to HRP was used for visualization.

3.13 Calcein assay

The calcein assay was used to investigate the influence of modulators on the cellular efflux via MRP1, MRP2 or P-gp. The acetomethoxy derivate of calcein (calcein AM) can easily enter cells as it is very lipophilic. Inside the cell the methyl ester groups are cleaved by intracellular esterases resulting in fluorescent calcein. As calcein AM is a substrate of the efflux transporters MRP1, MRP2 and P-gp, inhibition of these transporters leads to an increase of the amount of calcein formed inside the cell [88]. Calcein itself is also a weak substrate of MRP1 and MRP2 but not of P-gp. To quench extracellular fluorescence by calcein, cobalt(II) sulfate was added.

The assay was performed as described by Leyers [80]. For assessing the efflux, cells were suspended in Krebs HEPES buffer (KHP) and diluted to obtain a concentration of $3.33 \cdot 10^5$ cells/mL. 80 µL cell suspension were seeded out in each well of a 96-well plate and incubated with 10 µL of various concentrations of modulator substances for 30 min. Controls contained KHP only. Subsequently, 10 µL of cobalt(II) sulfate working solution and 33 µL of calcein AM working solution were added. The fluorescence signal was measured over 90 min using a FLUOstar™ OPTIMA microplate reader temperated at 37 °C (λ_{exc} 485 nm and λ_{em} 520 nm).

The intensity of the signal was corrected for the intensity of the signal of the controls and plotted against time. In the time span investigated the increase of fluorescence can be

assumed to be a reaction of pseudo-zero order as the ester is abundant. For each concentration the slope was determined by linear regression. The slope was then plotted against the logarithmized concentrations of the respective substance. The efficacy of modulators in inhibiting the calcein efflux was expressed by the IC_{50} (half maximal inhibitory concentration) value, which indicates the amount of inhibitor needed to yield half of the maximal inhibitory effect. IC_{50} values could be obtained by non-linear regression (four-parameter logistic equation, see Equation 3-1) using the software GraphPad Prism®.

3.14 Immunohistochemistry

Proteins can be detected by immunocytochemical staining using specific binding of antibodies to antigens. In the experiments a primary antibody mapping within an N-terminal cytoplasmic domain of human MRP2 was used. The incubation with a secondary antibody, which was labeled with a fluorophore, binding the primary antibody allowed visualization of MRP2 using confocal laser scanning microscopy.

For the experiments performed a protocol already established in the working group was used [21]. $2.5 \cdot 10^5$ cells were seeded out in 2 mL medium on round cover slips in 6-well plates and allowed to attach for 36 h (37 °C, 5.5% CO_2). Oxaliplatin stock solution was added to the medium to obtain a concentration of 100 μM and the cells were incubated for 2 h. Control samples were treated with an equivalent amount of PBS. Subsequently the medium was removed and the cover slips with the cells attached washed three times with PBS at room temperature. Cells were fixed on the cover slips by a 15 min treatment with 3.7% formaldehyde. After washing three times with PBS again cells were permeabilized by incubating with 0.02% Triton® X-100 in PBS. To block unspecific binding sites 1% bovine serum albumin (BSA) in PBS was added for 60 min. Afterwards 50 μL of the primary MRP2 antibody solution was pipetted directly on the cover slip. The cover slips were then covered with squared cover slips and the whole 6-well plate incubated for 90 min wrapped in a wet tissue and aluminum foil (37 °C, 5.5% CO_2). After addition of 1 mL PBS the squared cover slips were removed and the round cover slips with the cells attached were washed with PBS twice. The cells were then incubated with the secondary antibody (Alexa Fluor® 488 goat anti-chicken IgG) proceeding as described above for the primary antibody. The nucleus was stained using DAPI which binds DNA. Therefore 1 mL PBS and 40 μL of DAPI working solution were added and left for 5 min. Finally the cover slips were washed with 70%, 90%

and 100% ethanol subsequently and fixed with mounting medium on microscope slides. Brightfield and fluorescence microscopy were performed using a Nikon Eclipse Ti microscope and NIS-Elements software.

3.15 ^{195}Pt NMR spectroscopy

Various experiments performed investigated the influence of Gü83 on cellular oxaliplatin or cisplatin accumulation. To investigate whether Gü83 binds to either oxaliplatin or cisplatin ^{195}Pt NMR spectroscopy was applied. The platinum complexes were dissolved in a solution containing equal volumes of dimethylformamide (DMF) and PBS to obtain a concentration of 10 mM each; Gü83 was dissolved in pure DMF (10 mM). The solutions were mixed 1:1 leading to a concentration of 5 mM Gü83 and platinum complex each. The solvent of the final mixture, however, was thus composed of one quarter PBS and three quarter DMF. The platinum signal was followed over time by ^{195}Pt NMR spectroscopy (Bruker DPX 300 spectrometer). Spectra were calibrated related to K_2PtCl_4 at $\delta = -1.614$ ppm. The measurements were performed at the working group of Prof. Jan Reedijk at Leiden University by Dr. Patricia Marqués Gallego.

3.16 Statistical analysis

3.16.1 Basic statistics

Experiments were performed in triplicate and the mean was calculated from the dependent experiments. Usually the means of at least three independent experiments were calculated and the result represented as mean and standard deviation (SD) (see Equation 3-2 and Equation 3-3).

$$\text{Mean} = \frac{\sum_{i=1}^{n} x_i}{n}$$

Equation 3-2

x_i: individual measured values

n: number of measurements

$$SD = \sqrt{\frac{\sum_{i=1}^{n}(x_i - \bar{x})^2}{n-1}}$$

Equation 3-3

$\bar{x}$:   mean value of all measurements

x_i: individual measured values

n: number of measurements

Experiments were performed with a small sample size. Hence data could not be tested for normal distribution. Assuming that means are normally distributed, the significance of differences between results was tested using a two-sided Student's t-test. In case of dependent experiments the paired t-test and in case of independent experiments the unpaired t-test was used. If the significance of the influence of two independent variables on an outcome was investigated, two-way ANOVA with Bonferroni post-test was applied. In case p values were < 0.05 a difference between results was considered to be statistically significant; p values > 0.05 were considered not significant (n. s.).

EC_{50} values describing cytotoxicity (see chapter 3.5) and IC_{50} values describing inhibitory concentration (see chapter 3.13) were assumed to be log-normally distributed [74]. Thus, the negative decimal logarithms (pEC_{50} and pIC_{50}) were calculated and means were calculated from pEC_{50} and pIC_{50} values. For those experiments the standard error of the mean (SEM) was calculated to describe the accuracy of the determination of the mean (see Equation 3-4).

$$SEM = \frac{SD}{\sqrt{n}}$$

Equation 3-4

n: number of measurements

When evaluating correlation between two variables the correlation coefficient, r, was calculated using MVA® 2.0. r indicates the strength and the direction of a linear relationship between two variables and is a value between -1 and +1. The closer the value is to either +1 or -1, the stronger is the correlation. The algebraic sign indicates the direction of the correlation [89]. The statistical significance of r was calculated using a one-sided t-test.

MATERIALS AND METHODS

3.16.2 Validation of the assay for GSH determination

Accuracy

The accuracy of a method describes how a determined concentration deviates from the true concentration of an analyte and is expressed as relative error (RE). For evaluation of RE the deviation between nominal and measured concentration was related to the nominal concentration (see Equation 3-5). Accuracy was calculated for several measurements on one day (within-day accuracy) and on different days (between-day accuracy).

$$RE\,[\%] = \frac{(\overline{x} - \mu) \cdot 100}{\mu}$$ **Equation 3-5**

$\overline{x}$:   mean value of all measurements

μ: nominal value

Precision

The precision of a method specifies how individual measurements of the same sample of an analyte deviate from each other and is expressed as relative standard deviation (RSD). The RSD was calculated as shown in Equation 3-6.

$$RSD\,[\%] = \frac{SD \cdot 100}{\overline{x}}$$ **Equation 3-6**

$\overline{x}$:   mean value of all measurements

Recovery

To determine recovery the signal of the spiked matrix was assessed as well as the signal of the unspiked matrix and the percentaged recovery computed according to Equation 3-7.

$$Recovery\,[\%] = \frac{(c_s - c_u) \cdot 100}{c}$$ **Equation 3-7**

c_s: concentration measured in spiked matrix

c_u: concentration measured in unspiked matrix

c: nominal concentration of the analyte in spiked solution

4 RESULTS

4.1 Cytotoxicity and resistance factors

Within the scope of this project the relevance of glutathione (GSH) and MRP-mediated efflux for platinum resistance was investigated. Thus, knowledge of the sensitivity of cells used in experiments towards platinum complexes is crucial. The sensitivity of the cell lines towards cisplatin and oxaliplatin was determined using the MTT assay (see chapter 3.5). On the basis of the EC_{50} values the resistance factor of the resistant variants of the cell lines was calculated. Both resistant cell lines were not only resistant to the platinum complex used for acquiring resistance but were also cross-resistant to the other platinum complex tested (resistance factor HCT-8ox/HCT-8: cisplatin 2.7, oxaliplatin 12.1; resistance factor A2780cis/A2780: cisplatin 5.6, oxaliplatin 4.0; see details in Tab. 4-1 and Appendix A).

Tab. 4-1   Sensitivity of the cell lines used towards cisplatin and oxaliplatin investigated using an MTT-based cytotoxicity assay (mean $pEC_{50} \pm$ SEM, n = 3-11).

Cell line	pEC_{50} (EC_{50})	
	Cisplatin	**Oxaliplatin**
HCT-8	4.96 ± 0.10 (11.0 μM)	5.56 ± 0.06 (2.8 μM)
HCT-8ox	4.53 ± 0.12 (29.5 μM)	4.47 ± 0.05 (33.9 μM)
A2780	5.68 ± 0.08 (2.1 μM)	6.03 ± 0.26 (0.93 μM)
A2780cis	4.93 ± 0.07 (11.7 μM)	5.43 ± 0.14 (3.7 μM)

4.2   The relevance of glutathione (GSH) for platinum resistance

4.2.1   Validation of the assay for GSH determination

As the focus of this project was on the impact of GSH in platinum resistance an assay for GSH determination (see chapter 3.6) was cross-validated based on the findings of Leyers and Zisowsky [79,80] and on bioanalytical guidelines [75,76]. The assay covered a calibration range from 1 to 20 µM GSH.

Accuracy and precision

For estimation of accuracy, samples with a known GSH content (3, 12, 18 µM) were determined several times on one day (within-day accuracy) and on different days (between-day accuracy). The stock solution used for preparation of the samples was different from the stock solution used for preparation of the calibration curve. The accuracy of the individual measurements was within the acceptance level of ±15% determining various samples within a day (RE: -7.9 to 14.3%, accuracy of the means: RE: 3.2 to 6.2%, n = 6) and on different days (RE: -11.4 to 6.0%, accuracy of the means: RE: -0.7 to 1.5%, n = 5). Results can be seen in detail in Appendix B1.

The precision of a method specifies how individual measurements of the same concentration of an analyte deviate from each other and is expressed as relative standard deviation (RSD). RSD could be calculated from the results gained from the samples analyzed for determination of accuracy. The precision was within the acceptance level of ±15% analyzing samples within a day (within-day precision) (RSD: 5.9 to 8.7, n = 6) and on different days (between-day precision) (RSD: 3.0 to 6.2, n = 5). Results can be seen in detail in Appendix B1.

Recovery

In order to assess the recovery of the assay, distinct amounts of GSH were added to cell lysate as biological matrix. The signal of the spiked matrix was assessed as well as the signal of the unspiked matrix and the difference used to calculate recovery (see chapter 3.16). Mean recovery was 45.5% and ranged from 42.6% to 48.0% (0.5 µM GSH: 48.0%; 3.33 µM GSH: 42.7%; 7.5 µM GSH: 46.0%, n = 3 each).

Linearity

Correlation of the signal as a function of cell number was also tested. Mean correlation coefficient (r) was 0.9994 for HCT-8 ($p < 0.05$, t-test; values: 0.9989, 0.9999, n = 2), 0.9987 for HCT-8ox cells ($p < 0.05$, t-test; values: 0.9981, 0.9992, n = 2), 0.9604 for A2780 ($p < 0.05$, t-test; range: 0.9135 to 0.9995, n = 3) and 0.9957 for A2780cis cells ($p < 0.05$, t-test; values: 0.9920, 0.9993, n = 2), (see Fig. 4-1). Results can be seen in detail in Appendix B1.
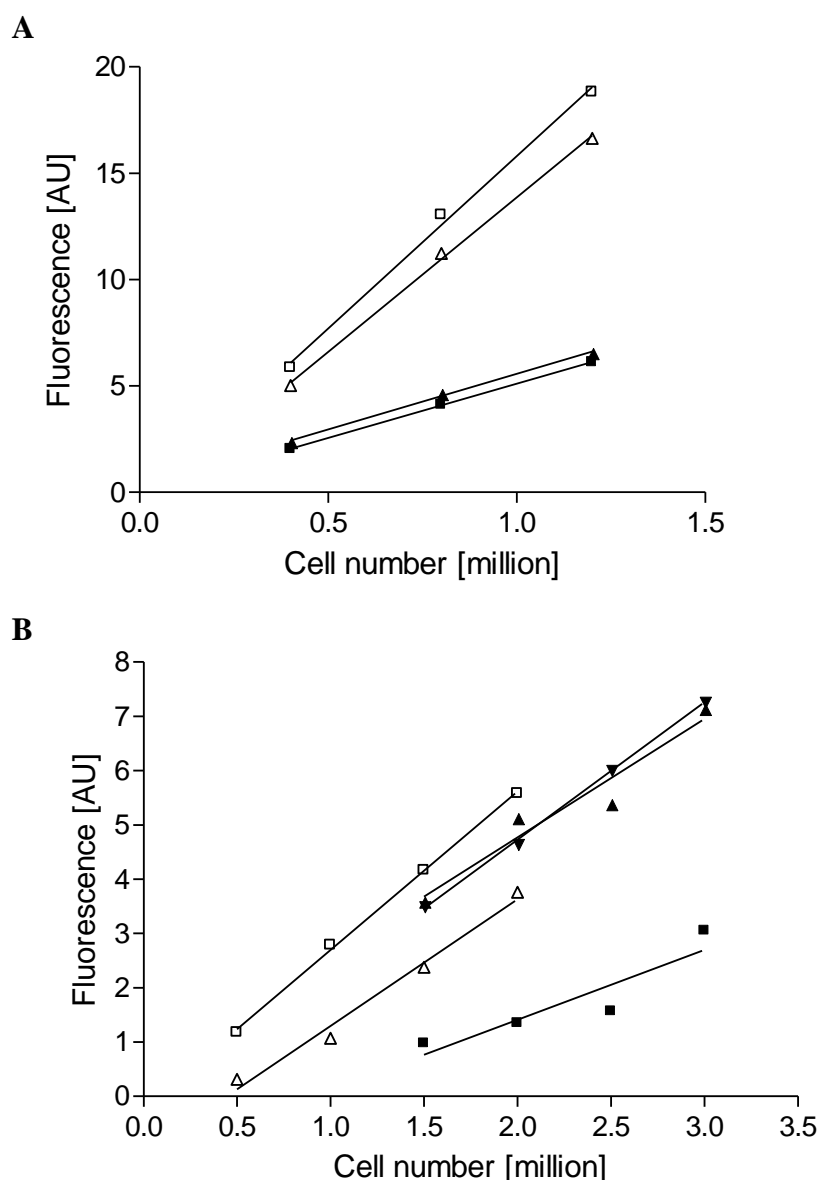

Fig. 4-1 Linearity of the fluorescence signal of the GSH-NDA adduct after lysis of different numbers of **A** HCT-8 (filled symbols) and HCT-8ox (empty symbols) cells, **B** A2780 (filled symbols) and A2780cis (empty symbols) cells (symbols represent the mean of two replicates, n = 2-3, (AU: arbitrary units)).

Calibration standard curve

For generation of a calibration curve a series of samples with known concentrations of an analyte was measured and the relationship between signal and concentration was defined by regression. The lowest standard concentration of the calibration curve was 1 μM. At this concentration the response was 5.5 times higher than the fluorescence signal of a blank sample (perchloric acid 3.3% only) (blank (mean ±SD): 0.18 ± 0.004 arbitrary units (AU), $n = 6$; 1 μM: 0.99 ± 0.03 AU, $n = 5$). For cross-validation of the GSH assay six freshly prepared non-zero standard solutionss (1, 2, 5, 10, 15 and 20 μM) were analyzed on five days. Linear regression without and with weighting (1/x, 1/x²) of results were compared using the MVA® software. The decision of the best model was based on the residual sum of squares (RSS). A small RSS is a sign of a good fit of the model to the data. As the RSS was lowest, weighting 1/x² was chosen for generation of the calibration curve for the assay (see Tab. 4-2). Results are shown in detail in Appendix B1.

Tab. 4-2 Residual sum of squares (RSS) and correlation coefficient (r) of calibration curves using different weighting ($n = 5$).

Weighting	Unweighted		1/x		1/x²	
	RSS	**r**	**RSS**	**r**	**RSS**	**r**
Mean	0.596	0.9994	0.082	0.9995	0.039	0.999
Sum	2.981	-	0.411	-	0.196	-

Accuracy and precision of the calibration standards were determined considering the results of five days. Accuracy was within the acceptance limit of ±15% (RE: -10.3 to 9.5%, accuracy of the means: RE: -3.3 to 3.5 %, $n = 5$) as well as precision (RSD: 2.3 to 4.8%, $n = 5$). Results can be seen in detail in Appendix B1.

Stability of the GSH-NDA isoindole adduct

GSH stock and working solutions as well as the NDA solution were freshly prepared when needed. As reported previously the fluorescent GSH-NDA isoindole adduct is not stable [77]. To find the optimal duration of the derivatization NDA solution was added to three solutions differing in GSH content and the fluorescence signal was detected over 50 min. As can be seen in Fig. 4-2 the signal of the adduct reached a plateau around a derivatization time of

15 min before decreasing; hence 15 min was chosen as derivatization time for the performance of the assay.
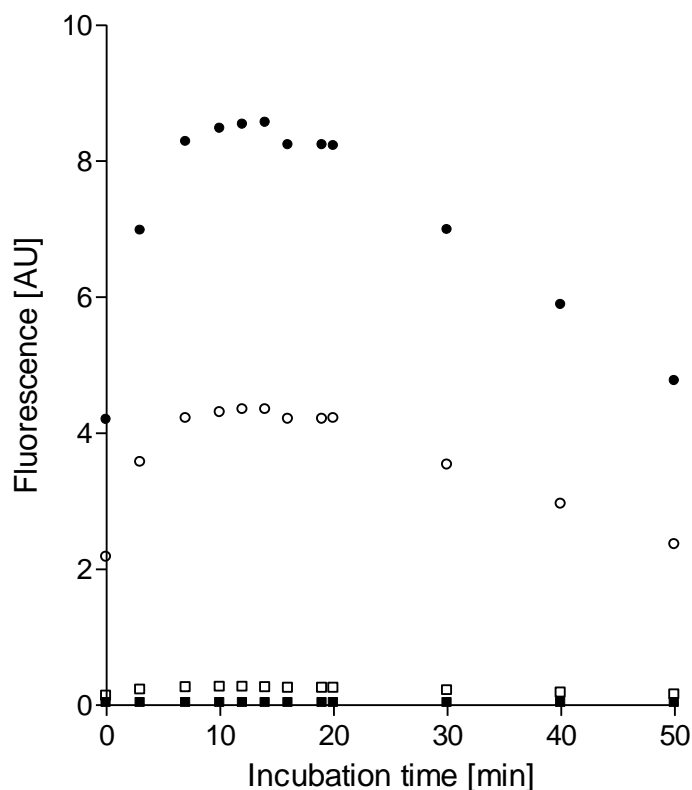
Fig. 4-2   Fluorescence signal of the fluorescent GSH-NDA isoindole adduct after adding NDA to 0 (■), 1 (□), 10 (○) and 20 (●) µM GSH (AU = arbitrary units). Figure of a representative experiment (symbols represent the mean of two replicates); (n = 3).

Sample stability

After sample production, performance of GSH determination can be delayed for days or weeks. To account for possible instability, even when samples were stored at -80 °C, stability of samples was assessed after 15 and 30 days of storage including one or two 'freeze-and-thaw' cycles, respectively. Distinct numbers of cells were lysed in perchloric acid (3.3%) and the lysate was used for determination of baseline GSH content. Aliquots of the lysate were stored at -80 °C. At least two days before day 15 and day 30 samples for testing 'freeze-and-thaw' stability were completely thawed at room temperature and refrozen afterwards.

GSH proved to be stable in both scenarios in most cases when applying a deviation from baseline level < 15% as benchmark (see Tab. 4-3). However, the sample with the lowest GSH content thawed twice and stored for 30 days showed a deviation > 15%. Thus, repeated

'freeze-and-thaw' cycles were avoided in sample handling and samples were analyzed within 30 days after generation.

Tab. 4-3 Long-term stability and freeze-and-thaw stability of GSH in samples generated from HCT-8 and HCT-8ox cells (GSH content [mM] ± relative change to baseline (day 0), n = 1).

	Day 0	Long-term stability		Freeze-and-thaw stability	
		Day 15	Day 30	Day 15	Day 30
HCT-8					
$4 \cdot 10^5$ cells	2.6	2.9 (+ 11.5%)	2.4 (- 7.7%)	2.8 (+ 7.7)	2.1 (- 19.2%)
$8 \cdot 10^5$ cells	5.5	5.9 (+ 7.3%)	5.8 (+ 5.5%)	5.3 (- 6.6%)	4.7 (- 14.5%)
HCT-8ox					
$4 \cdot 10^5$ cells	6.8	7.2 (+ 6.5%)	7.0 (+ 2.9%)	7.4 (+ 8.8%)	6.7 (- 1.5%)
$8 \cdot 10^5$ cells	16.9	17.4 (+ 3.0%)	15.8 (+ 6.5%)	15.1 (- 10.7%)	16.1 (- 4.7%)

4.2.2 Cellular GSH content

The GSH content of the two sensitive/resistant cell line pairs studied, namely HCT-8/HCT8-ox and A2780/A2780cis was determined after cell lysis and derivatization with NDA. As can be seen in Fig. 4-3 the content was the same in HCT-8 and HCT8-ox cells but was about 2.6 times higher in A2780cis compared to A2780 cells. The GSH content of the sensitive ovarian carcinoma cell line A2780 was significantly lower compared to the sensitive ileocecal colorectal adenocarcinoma cell line HCT-8 (p = 0.048) (see Appendix B2). Interestingly, the cell line with lowest GSH content (A2780) was also most sensitive towards cisplatin as well as oxaliplatin (see chapter 4.1). Despite their similar GSH content the three cell lines with higher GSH content differed in sensitivity towards the two platinum complexes investigated.
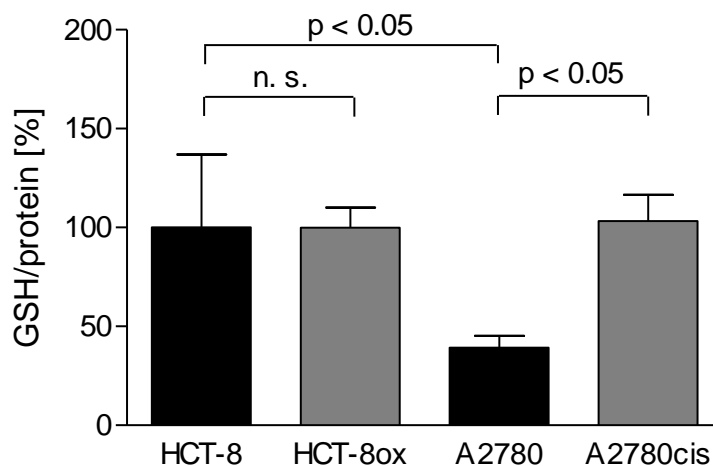
Fig. 4-3   Cellular GSH content related to the protein content in untreated cells (mean ± SD, n = 3, unpaired t-test; n. s.: not significant). The mean value in HCT-8 cells was set to 100%.

4.2.3   Effect of platinum incubation on the cellular glutathione content

To investigate the effect of platinum complexes on cellular GSH content, cells were incubated with cisplatin or oxaliplatin for 24 h and GSH content was determined. Controls were incubated with PBS only. Samples were taken after 0, 4, 8, 12 and 24 h and GSH and protein content were assessed. A small increase in cellular GSH content was seen in HCT-8 and HCT-8ox cells with a quicker onset in the resistant variant. In A2780 cells the increase in cellular GSH was of a higher magnitude than in A2780cis cells. For statistical analysis of the results describing the effect of oxaliplatin or cisplatin on GSH content over time a two-way ANOVA was performed. According to the test results, incubation of cells with the platinum complexes did not significantly influence GSH content in the investigated cell lines over time. Only in A2780cis cells the influence of time on GSH content was significant (see Fig. 4-4, Fig. 4-5 and Appendix B2).

A

B
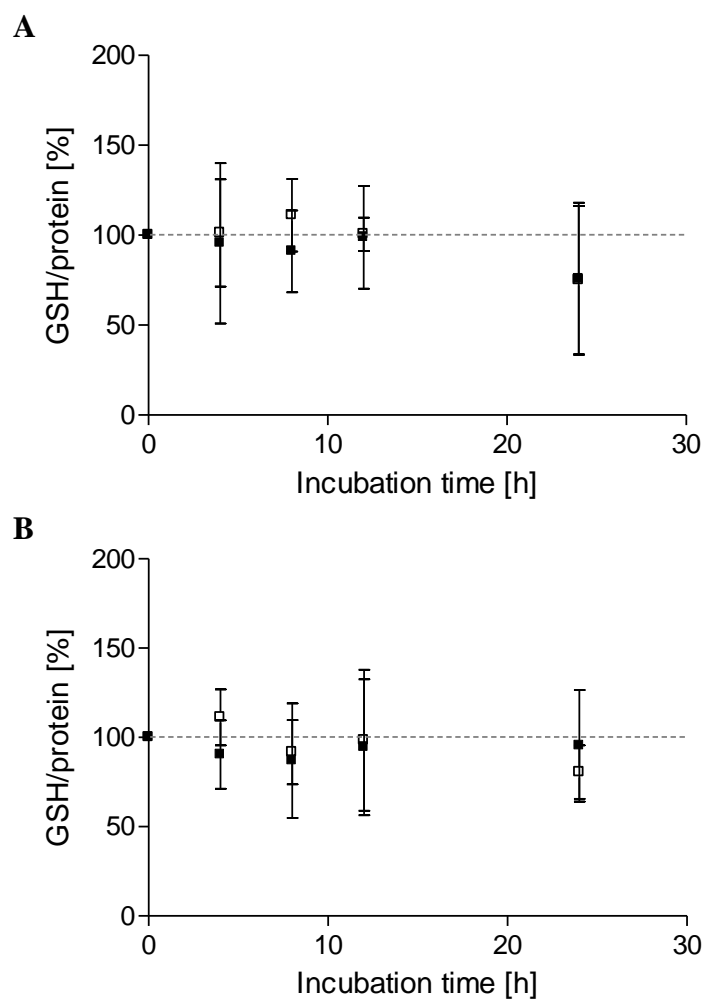
Fig. 4-4   Cellular GSH content related to the protein content (relative to baseline value) of **A** HCT-8 and **B** HCT8-ox cells during incubation with (□) or without (■) 100 nM oxaliplatin (mean ± SD, n = 3, two-way ANOVA did not show significant impact of time and oxaliplatin).

A

B
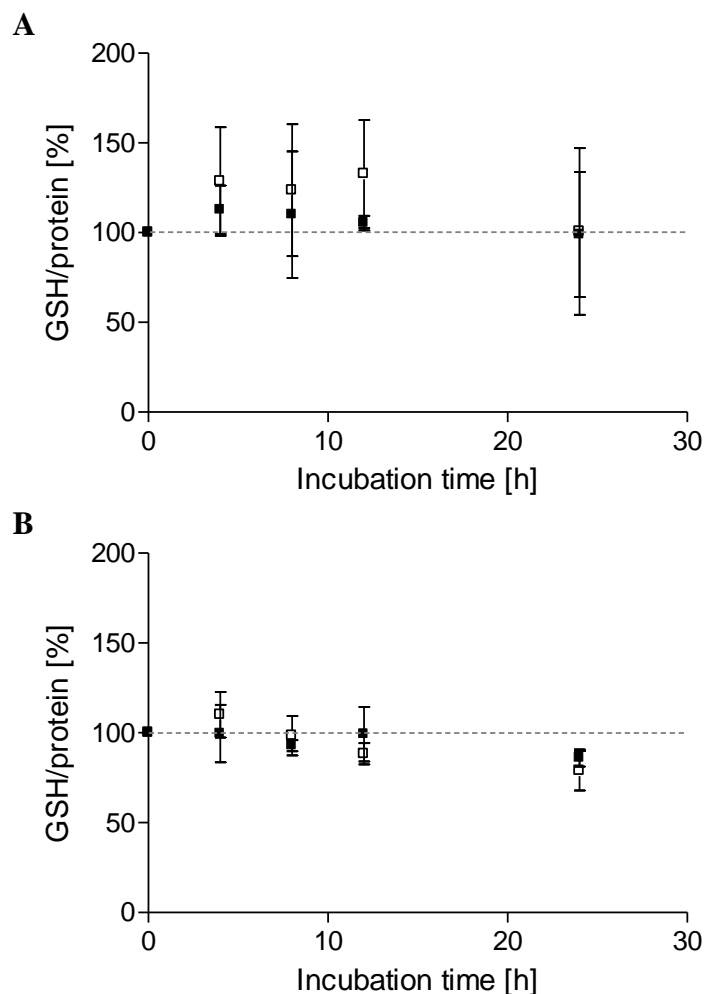
Fig. 4-5 Cellular GSH content related to the protein content (relative to baseline value) of **A** A2780 and **B** A2780cis cells during incubation with (□) or without (■) 100 nM cisplatin (mean ± SD, n = 3, two-way ANOVA performed only showed significant impact of time for A2780cis).

4.2.4 GSH depletion

To further elucidate the role of GSH with respect to platinum cytotoxicity and accumulation cellular GSH was depleted. For this purpose, buthionine sulfoximine (BSO), a GSH analogue reversibly inhibiting γ-glutamylcysteine synthetase (γGCS), the rate-limiting enzyme in GSH synthesis [24], was used. Cytotoxic effects of BSO in the concentrations used were excluded by the MTT assay. Those assays reveled that in HCT-8 and HCT-8ox cells a concentration up to 100 μM could be used for experiments (see Fig. 4-6). In preliminary experiments BSO was shown to reduce GSH levels in HCT-8 and HCT-8ox cells (Fig. 4-7).
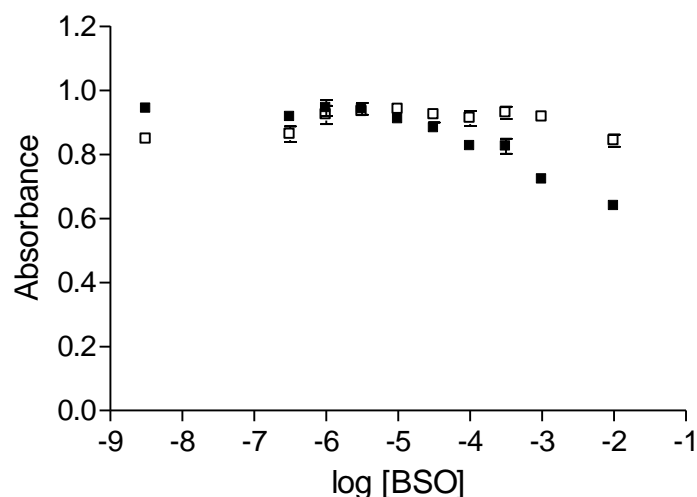
Fig. 4-6   Cytotoxicity of BSO in HCT-8 (■) and HCT-8ox (□) cells assessed using the MTT assay after incubation with various concentrations of BSO over 72 h; figure of one representative experiment performed in triplicate (mean ± SD, n = 3).

Investigating the effect of GSH depletion on oxaliplatin cytotoxicity a tendency to slightly higher pEC_{50} values of oxaliplatin (corresponding to lower EC_{50} values) could be observed but the effect was only statistically significant in HCT-8ox (Tab. 4-4). The cellular platinum accumulation was not affected by GSH depletion after 12 h incubation with 100 μM BSO as can be seen in Fig. 4-8. A difference in cellular platinum accumulation, however, was observed between the untreated controls of HCT-8 and HCT-8ox cells. Results are shown in Appendix B3 in detail.

Tab. 4-4   Impact of GSH depletion induced by incubation with 50 μM BSO on oxaliplatin cytotoxicity determined by the MTT assay (mean $pEC_{50} \pm$ SEM, n = 4-5).

Cell lines	pEC_{50} (EC_{50})		
	+ BSO	- BSO	Paired t-test
HCT-8	5.74 ± 0.17 (1.8 μM)	5.57 ± 0.19 (2.7 μM)	p = 0.0160
HCT-8ox	4.47 ± 0.05 (33.9 μM)	4.37 ± 0.10 (42.7 μM)	p = 0.2372

A

B
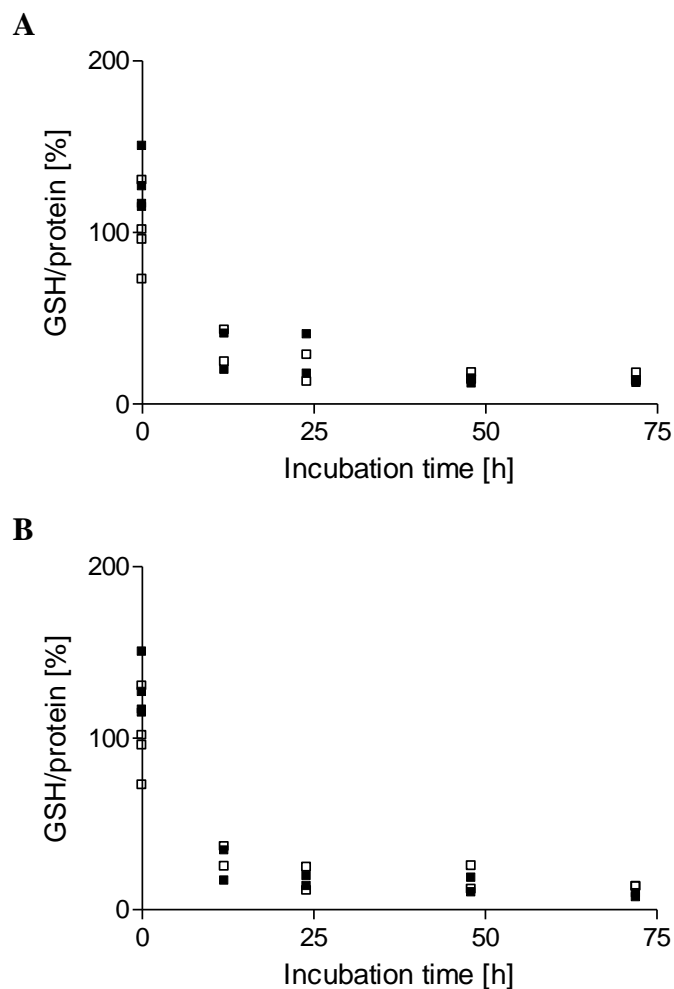
Fig. 4-7   GSH depletion over time using **A** 50 μM and **B** 100 μM BSO in HCT-8 (■) and HCT-8ox cells (□) (individual values, n = 2-4). The mean value in HCT-8 cells was set to 100%.
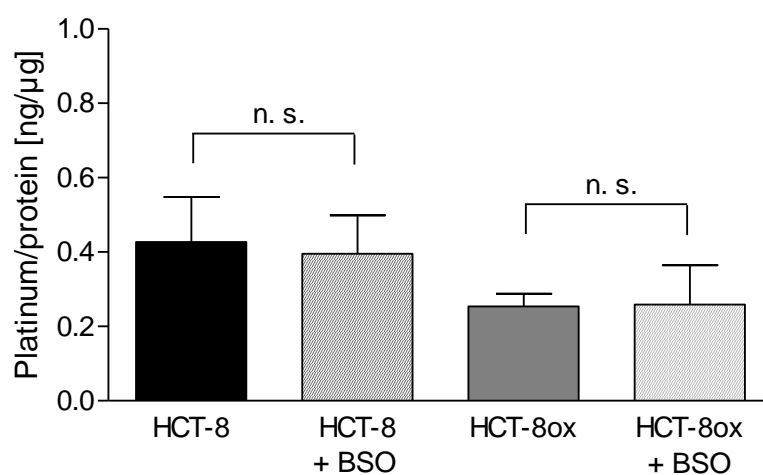
Fig. 4-8   Cellular platinum accumulation related to protein content after 2 h incubation with 100 μM oxaliplatin with or without 12 h preincubation with 100 μM BSO (mean ± SD, n = 5, paired t-test; n. s.: not significant).

4.2.5 Platinum-glutathione adducts

In literature it is widely acknowledged that intracellularly formation of platinum-GSH adducts takes place (see chapter 1.4.1). Within the scope of this project the question whether platinum complexes form platinum-glutathione (GSH) adducts was addressed. First, a literature search for previously described adducts was performed (see Appendix C1 and C2). Eight adducts were found after incubation of cisplatin and GSH solutions (adduct 1 to 8) [35,41,90-96]; one adduct, adduct 3, was also identified in L1210 leukemia cells [35]. Two adducts (adducts 9, 10) were found after incubation of oxaliplatin and GSH solutions and rat blood [97]. To facilitate the identification of adducts in mass spectrometry (MS) spectra isotope patterns of the adducts were created *in silico* with an online isotope distribution calculator (available at www.sisweb.com/mstools/isotope.htm); to give an example the isotope pattern for adduct 1 is shown in Appendix C3.

Mixtures of platinum complexes and GSH solutions were prepared and screened for platinum-GSH adducts using electrospray ionization (ESI)-MS (see chapter 3.8). The MS spectra obtained were screened for patterns characteristic for platinum-containing molecules. It was taken into account that adducts were protonated as formic acid had been added to the samples. Two cisplatin-GSH adducts were identified in this setting shortly after mixing the solutions and after 12 h incubation time at 37 °C. The MS spectrum as well as the chemical structures suggested are shown in Fig. 4-9.
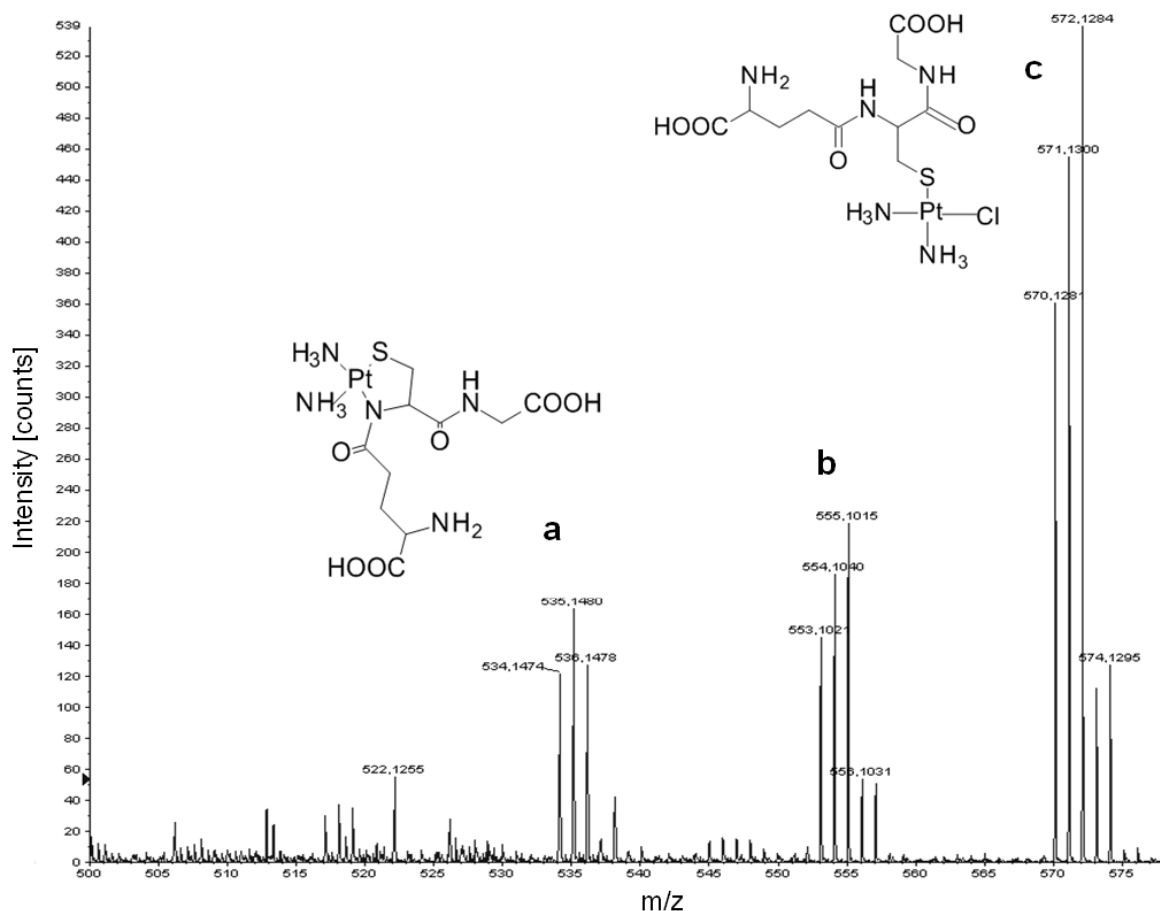
Fig. 4-9   ESI-MS spectrum of cisplatin-GSH adducts recorded shortly after aqueous solutions of GSH and cisplatin were mixed. The suggested structures for the signals **a** (adduct 2) and **c** (adduct 1) are shown. Signal **b** might be the adduct seen in **c** (adduct 1) but with an –NH₃ group (mass difference 17) missing.

An oxaliplatin-GSH adduct was not found directly. However, when a signal showing a typical platinum pattern at m/z 704 was fragmented, adduct 9 (see Appendix C2) could be identified among the fragments at m/z 614. The signal at m/z 704 was probably produced by adduct 9 with one molecule oxalic acid bound to it as the mass difference 90 corresponds to one molecule of oxalic acid. Before binding to the adduct oxalic acid was presumably separated from oxaliplatin while mixing the substances or during the process of ESI. The spectrum is shown in Fig. 4-10 B. The adduct was found shortly after mixing the solutions as well as after 12 h incubation time at 37 °C.
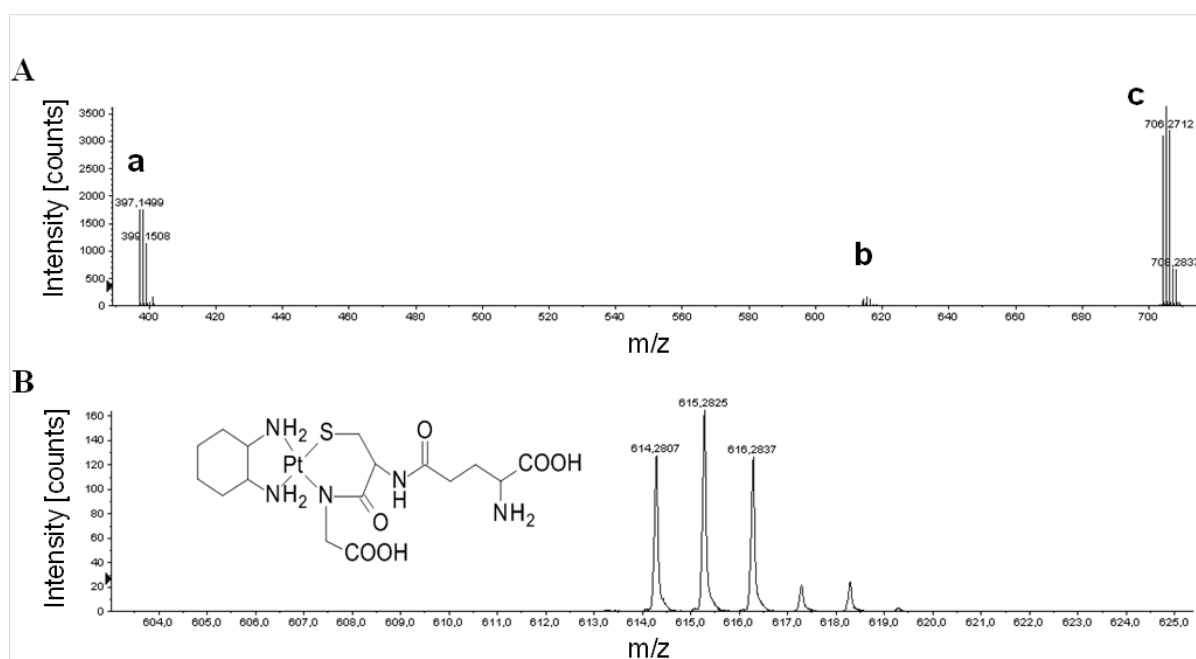
Fig. 4-10 ESI-MS spectrum recorded shortly after aqueous solutions of GSH and oxaliplatin were mixed showing the spectrum obtained after fragmentation of the signal at m/z 704 (signal c). **A** shows m/z from 300 to 800; in **B** the m/z area around signal b is enlarged and a possible structure of an adduct is presented. Signal **a** results from unbound oxaliplatin.

4.3 The relevance of MRP2 for platinum resistance

The transport of endo- and exogenous substances as GSH adducts via MRP transporters has been frequently suggested. It is widely acknowledged that these efflux transporters are of importance in platinum resistance as well. This project focused on MRP2, as there is most evidence for its involvement among all MRP (see chapter 1.5.1).

4.3.1 Protein expression

At first the expression of MRP2 on the protein level was investigated in the cell lines used using SDS page and immunoblot (see chapter 3.12). A representative immunoblot is shown in Fig. 4-11. β-Actin expression was also assessed as it was selected as housekeeping marker for normalization. As shown in Fig. 4-12 the MRP2 expression was in the same range in HCT-8 and HCT-8ox cells. MRP2 was not detected in A2780 but was expressed on a low level in A2780cis cells. In HCT-8 and HCT-8ox cells the experiments were also performed after 12 h incubation with 10 µM oxaliplatin. In these experiments the expression was increased in HCT-8 (not significantly) but not in HCT-8ox cells. Results are shown in detail in Appendix D1.

MRP2 (190-200 kDa)

β-actin (42 kDa)

A   B   C   D   E   F
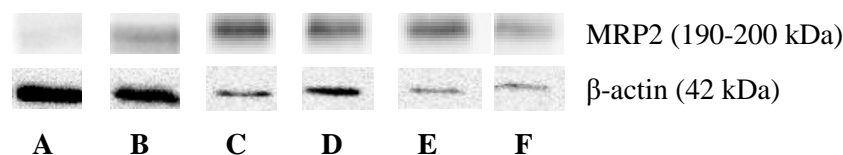
Fig. 4-11   Immunoblot analysis of MRP2 and β-actin expression in **A** A2780, **B** A2780cis **C** HCT-8 and **D** HCT-8ox, Expression was also assessed in HCT-8 and HCT-8ox cells treated with 10 µM oxaliplatin for 12 h (**E**, **F**). Figure of a representative immunoblot, n = 2-6).
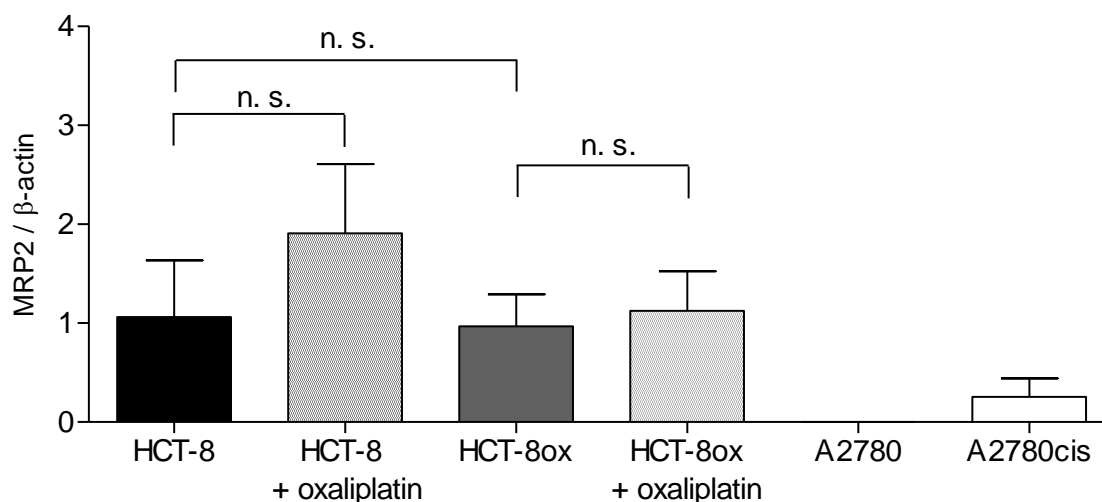
Fig. 4-12 Expression of MRP2 normalized to β-actin in untreated cells and after treatment with 10 μM oxaliplatin for 12 h (mean ± SD, n = 2-6 (n = 2 only for A2780), unpaired t-test; n. s.: not significant).

Relationship between MRP2 expression and cytotoxicity of platinum complexes

As described in chapter 1.5.1, MRP2 overexpression is associated with decreased sensitivity to platinum complexes. To check if this relationship can also be found in the cell lines used within this project expression data obtained (see chapter 4.3.1) was related to EC_{50} values of cisplatin and oxaliplatin, representing sensitivity to the platinum complexes (see chapter 4.1). As can be seen in Fig. 4-13 an association between MRP2 expression and sensitivity is apparent when considering A2780, A2780cis and HCT-8ox cells. HCT-8 cells, however, have EC_{50} values similar to A2780cis while showing highest MRP2 expression.
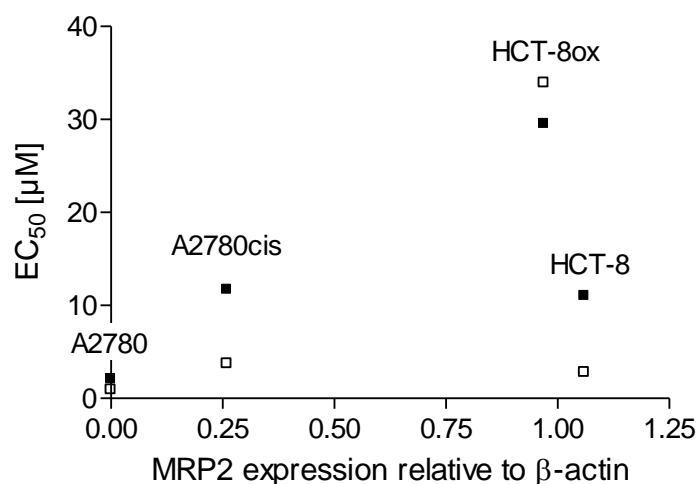
Fig. 4-13 Relationship between MRP2 expression relative to β-actin and EC_{50} values of cisplatin (■) and oxaliplatin (□) in A2780, A2780cis, HCT-8ox and HCT-8 cells (from left to right).

4.3.2 Fluorescence microscopy

Localization of MRP2 was assessed in HCT-8 and HCT-8ox cells by use of immunofluorescence microscopy (see chapter 3.14). To compare the localization in the sensitive and resistant cells after immunohistochemical staining cells were viewed in brightfield and with confocal laser scanning microscopy. As shown in Fig. 4-14 A to C immunofluorescence localization of MRP2 (green) was similar in both cell lines and distributed equally around the nuclei (blue). As already described by Buss HCT-8ox cells have a greater diameter than HCT-8 [70]. The localization of MRP2 was not altered after 2 h treatment with 100 μM oxaliplatin.
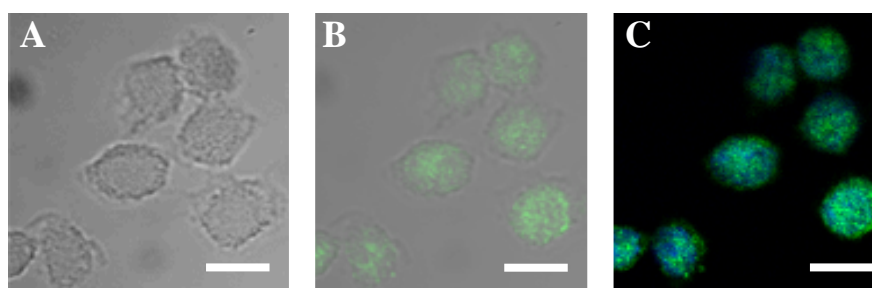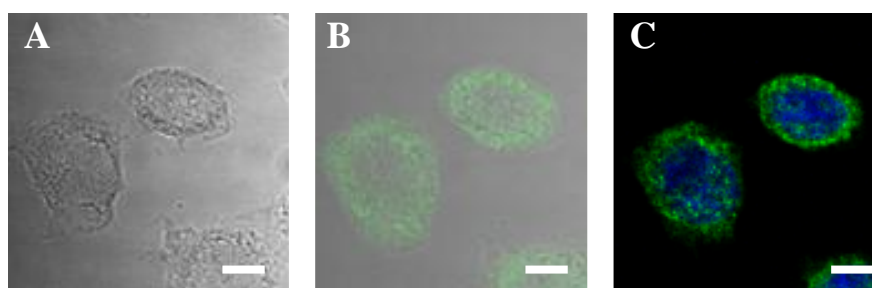
HCT-8

HCT-8ox

Fig. 4-14 Microscopic images of HCT-8 and HCT-8ox cells after immunostaining of MRP2 and staining of the nuclei using DAPI: **A** brightfield, **B** immunofluorescence localization of MRP2 (green) overlay with brightfield and **C** immunofluorescence localization of MRP2 (green) with stained nuclei (blue). Scale bars represent 10 μM.

4.3.3 MRP modulation by Gü83

The efflux of platinum complexes or their GSH adducts, respectively, has been described in literature but is still under debate (see chapter 1.6). To further clarify this issue, the effect of Gü83, a 4-aminobenzoic acid derivative modulating the efflux via MRP1 and MRP2, was studied (see chapter 1.5).

To assure that Gü83 is not toxic in the concentration used in further experiments cell viability was tested using the MTT assay. No difference in cell viability expressed as absorbance was seen comparing untreated cells and cells treated with Gü83 (see Fig. 4-15).
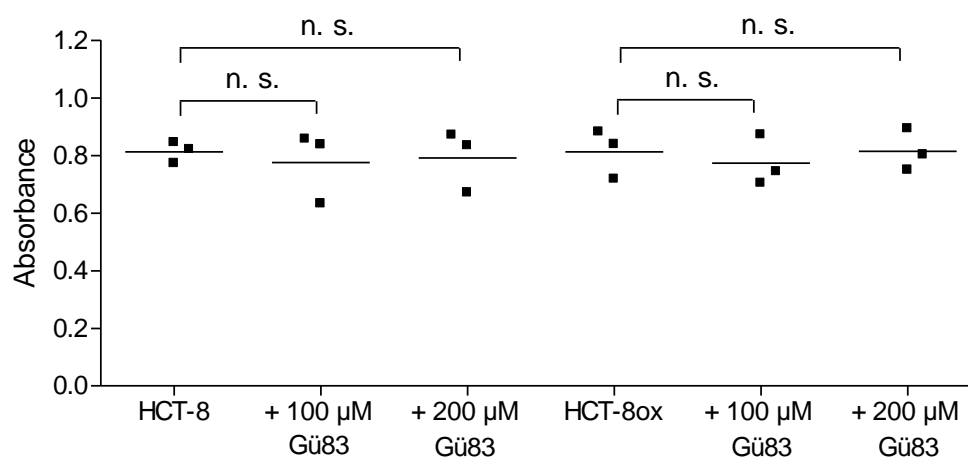
Fig. 4-15　Viability of cells after 4 h incubation with or without two different concentrations of Gü83 assessed using the MTT assay (mean and individual values, n = 3, unpaired t-test; n. s.: not significant).

4.3.3.1 Chemical reaction of Gü83 with platinum complexes

Platinum complexes are potential binding partners for molecules used in experiments for modulation of cellular platinum accumulation [98]. The following experiments were conducted to exclude binding of Gü83 to oxaliplatin or cisplatin. Therefore solutions of the respective complexes were mixed and the platinum signal followed over time by ^{195}Pt NMR spectroscopy (see chapter 3.15). ^{195}Pt shift strongly depends on surrounding ligands and thus any reaction of the respective platinum compound with Gü83 would result in an altered signal. As shown in Fig. 4-16, the platinum signal was not altered after addition of Gü83. Hence a chemical reaction of Gü83 with oxaliplatin as well as cisplatin could be excluded.

A

B
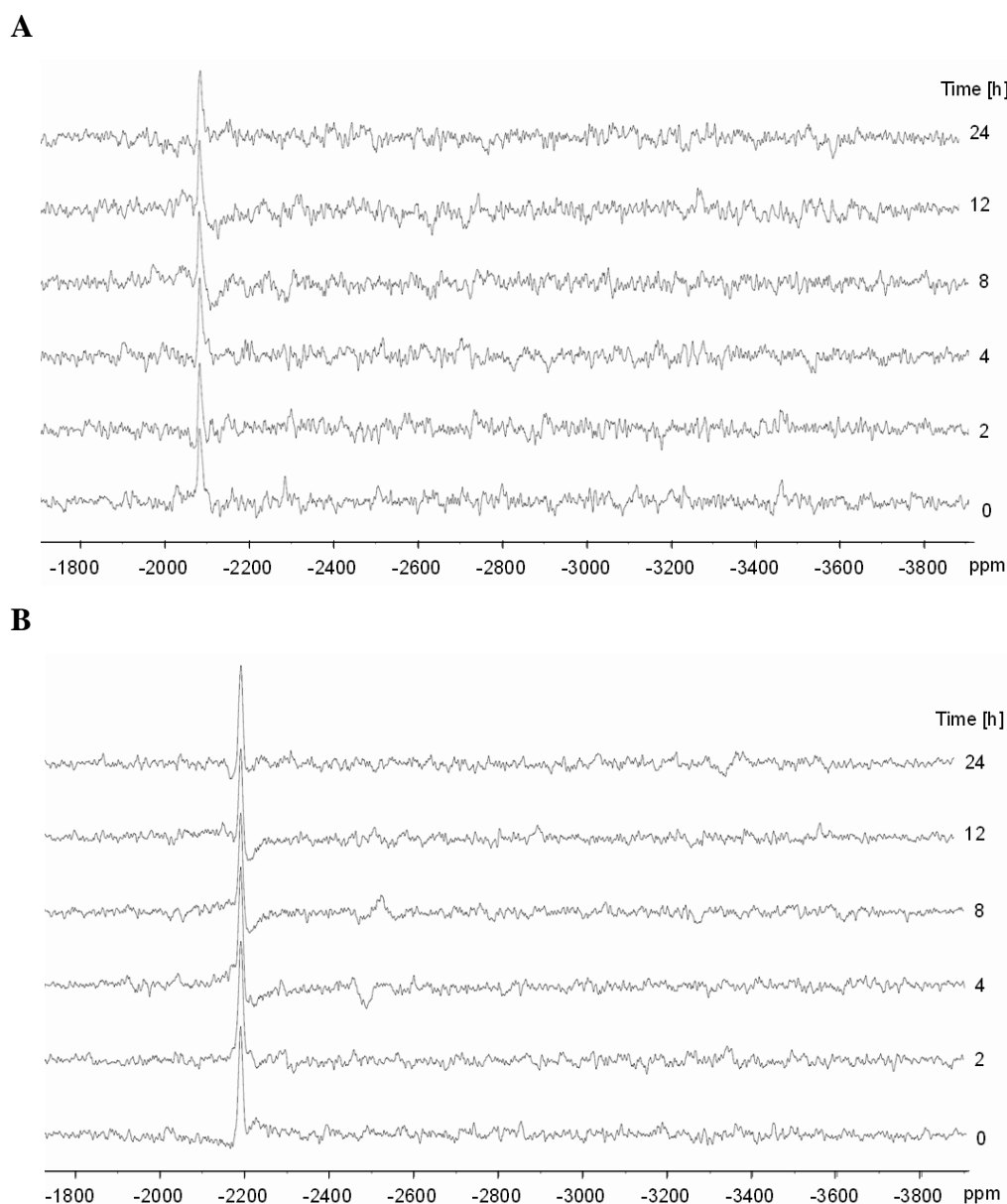
Fig. 4-16 ^{195}Pt NMR spectrum monitoring the reaction of Gü83 [5 mM] with **A** oxaliplatin [5 mM] and **B** cisplatin [5 mM] in a DMF solution containing 25% PBS.

4.3.3.2 Platinum accumulation upon oxaliplatin exposure

To further address the question whether platinum complexes are excreted via MRP the impact of MRP inhibition by Gü83 on cellular platinum accumulation was assessed. The experiments were primarily performed using HCT-8 and HCT-8ox cells as MRP2 expression was confirmed in those cells. In the experiments performed, platinum accumulation increased as a consequence of MRP1 and MRP2 inhibition with Gü83 in a concentration-dependent manner upon incubation with oxaliplatin (see Fig. 4-17). It should be noted that Gü83 might be

cytotoxic in the two highest concentrations used as alterations in cell viability were only assessed up to 200 μM ($10^{-3.7}$M) (see Fig. 4-15). As the solubility of Gü83 was limited higher concentrations could not be investigated. The effect was also seen when monitoring the influence of Gü83 [100 μM] on cellular platinum accumulation over 3 h (Fig. 4-18). For statistical analysis of the effect of Gü83 over time a two-way ANOVA was performed. According to the test results, time as well as incubation with Gü83 significantly influenced platinum accumulation in HCT-8 and HCT-8ox cells. Results are shown in detail in Appendix D2.
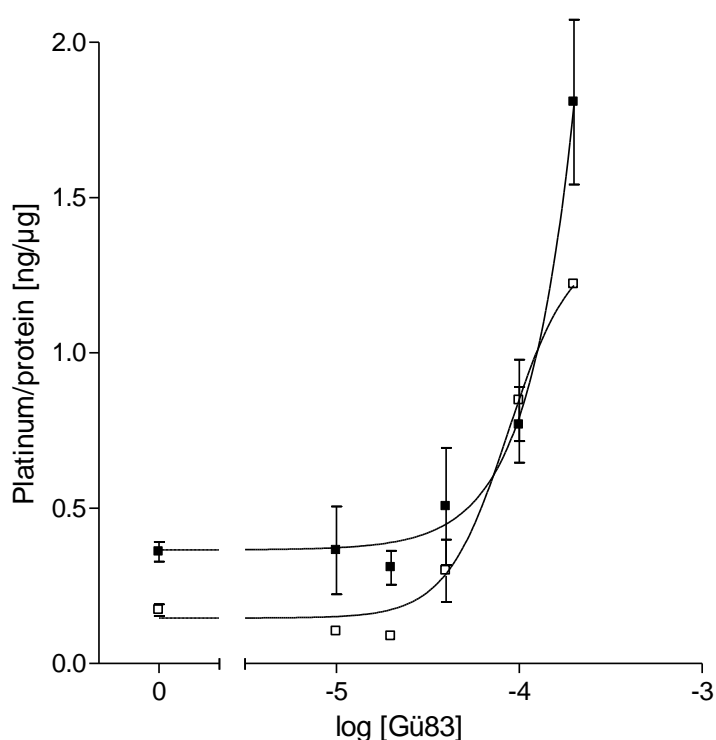
Fig. 4-17 Cellular platinum accumulation related to protein content after 2 h incubation with different concentrations of Gü83 and 100 μM oxaliplatin in HCT-8 (■) and HCT-8ox (□) cells (mean ± SD if applicable; n = 1-5).

A

B
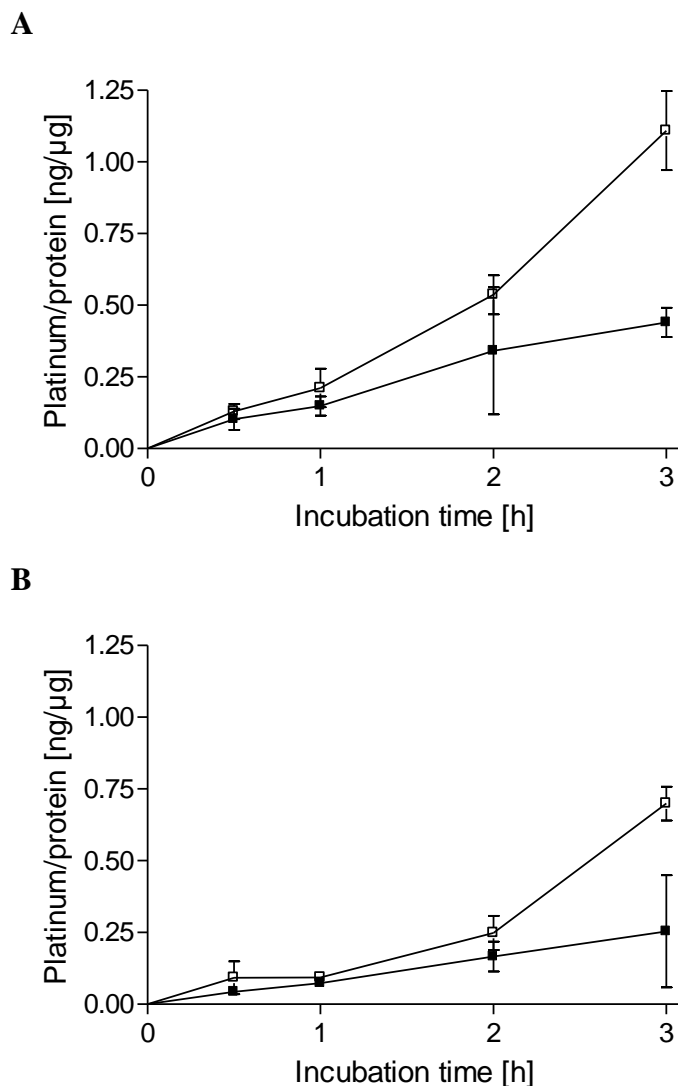
Fig. 4-18 Cellular platinum accumulation related to protein content after incubation with DMSO (■) or 100 µM Gü83 in DMSO (□) and 100 µM oxaliplatin in **A** HCT-8 and **B** HCT-8ox cells (mean ± SD, n = 3, two-way ANOVA showed significant impact of time and Gü83 on platinum accumulation).

4.3.3.3 Platinum accumulation upon cisplatin exposure

Similar experiments were also performed using cisplatin in the same concentration as oxaliplatin before. The concentration of Gü83 [100 µM] and the duration of incubation (2 h), however, were not varied. Again a higher platinum accumulation was found in the cells coincubated with the MRP modulator (Fig. 4-19). The difference was statistically significant in HCT-8 cells ($p < 0.05$, paired t-test). For details see Appendix D2.
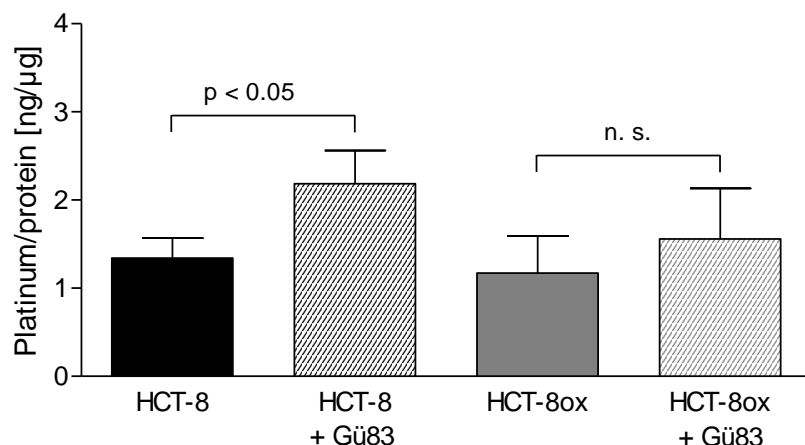
Fig. 4-19 Cellular platinum accumulation related to protein content after 2 h incubation with 100 μM Gü83 and 100 μM cisplatin (mean ± SD, n = 4-5, paired t-test; n. s.: not significant).

In Tab. 4-5 the changes in platinum accumulation induced by Gü83 are summarized and are expressed as a factor for illustration. The amount of platinum accumulated was generally higher in the case of cisplatin compared to oxaliplatin. The increase was in the same range for all cells but seems to be higher in the sensitive cells. Comparing the uptake in sensitive and resistant cells the difference is more obvious after oxaliplatin incubation than after cisplatin incubation.

Tab. 4-5 Cellular platinum accumulation after 2 h incubation with 100 μM platinum complex and 100 μM Gü83. For clarification only means are shown, variablility is illustrated in Fig. 4-18 and Fig. 4-19.

	Platinum accumulation (platinum/protein [ng/μg], mean)					
	Oxaliplatin	Oxaliplatin + Gü83	*Factor of increase*	Cisplatin	Cisplatin + Gü83	*Factor of increase*
HCT-8	0.34	0.54	*1.6*	1.34	2.18	*1.6*
HCT8-ox	0.17	0.25	*1.5*	1.12	1.56	*1.4*
HCT-8/ HCT-8ox	*2*	*2.2*		*1.2*	*1.4*	

The impact of Gü83 on cellular platinum accumulation after incubation with cisplatin was also investigated in A2780 and A2780cis cells. As described by Zisowsky et al. the platinum accumulation was significantly lower in the cisplatin-resistant cells in the control experiments (see Fig. 4-20) [99]. In the resistant cells a small but not significant increase was observed when Gü83 was added ($p > 0.05$, paired t-test). In the sensitive cells even a small but not statistically significant decrease was observed ($p > 0.05$, paired t-test). Data are shown in Appendix D2.
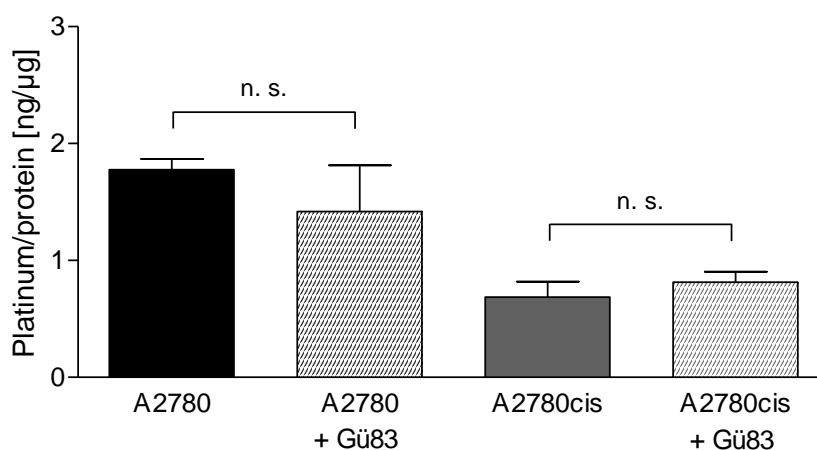
Fig. 4-20 Cellular platinum accumulation related to protein content after 2 h incubation with 100 μM Gü83 and 100 μM cisplatin (mean ± SD, n = 3, paired t-test).

4.3.3.4 Platinum efflux

Platinum accumulation comprises platinum uptake and platinum efflux. The latter was also addressed experimentally. Platinum efflux was assessed similar to platinum accumulation. After a certain time of incubation with oxaliplatin with or without Gü83 the cell culture medium was replaced with a platinum-free medium. Samples were taken at certain time points (for details see chapter 3.10). In Fig. 4-21 the platinum accumulation at these time points is illustrated. Platinum decrease over time demonstrates the efflux. No impact of Gü83 on efflux was observed in HCT-8 cells over the time period studied. For statistical analysis of the results describing the effect of Gü83 over time a two-way ANOVA was performed. According to the results incubation with Gü83 did not significantly influence platinum efflux in HCT-8 and HCT-8ox cells. Time had only an effect in HCT-8 cells. Results are shown in detail in Appendix D2.
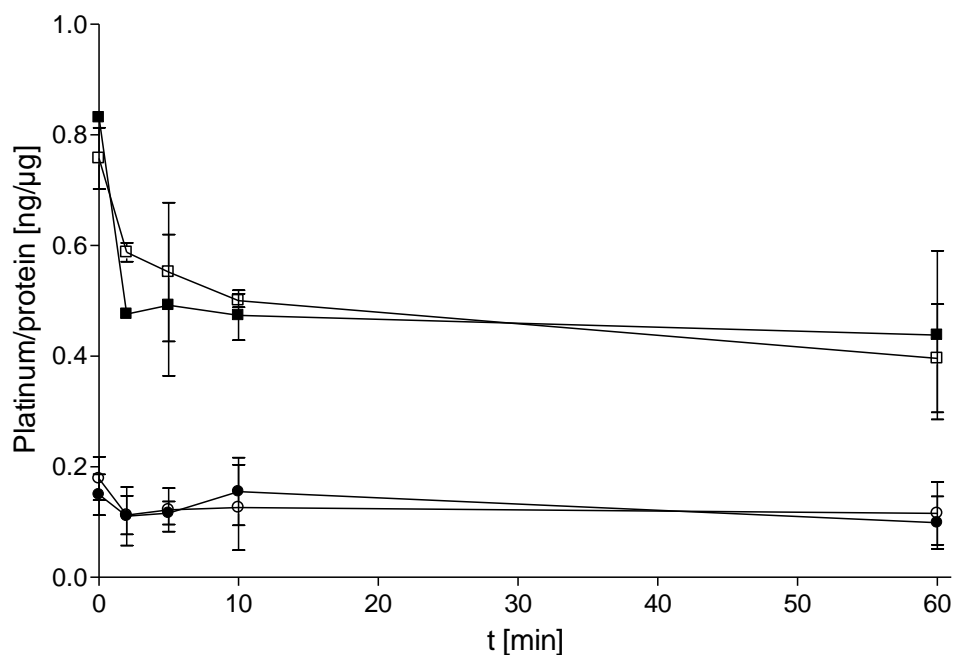
Fig. 4-21   Platinum efflux illustrated as cellular platinum content in HCT-8 (■/□) and HCT-8ox (●/○) after 2 h incubation with 100 µM oxaliplatin without (filled symbols) or with 100 µM Gü83 (empty symbols) over time after replacing cell culture medium (mean ± SD, n = 3, two-way ANOVA showed significant impact only for time in HCT-8 cells).

4.3.3.5   DNA platination

As described above, an effect of Gü83 on platinum accumulation could be shown. DNA platination is important for the mode of action of platinum complexes. Hence the influence of Gü83 on this intracellular target was investigated as well. The results shown in Fig. 4-22 illustrate that coincubation of Gü83 led to an increase in DNA platination. The increase was statistically significant only in the sensitive cells (unpaired t-test).

In Fig. 4-23 the association between DNA platination and cellular platinum accumulation is depicted considering all values without differentiation of cell-type and treatment. It seems that lower cellular platinum content effects DNA platination stronger compared to higher cellular platinum content. Data are shown in Appendix D2.
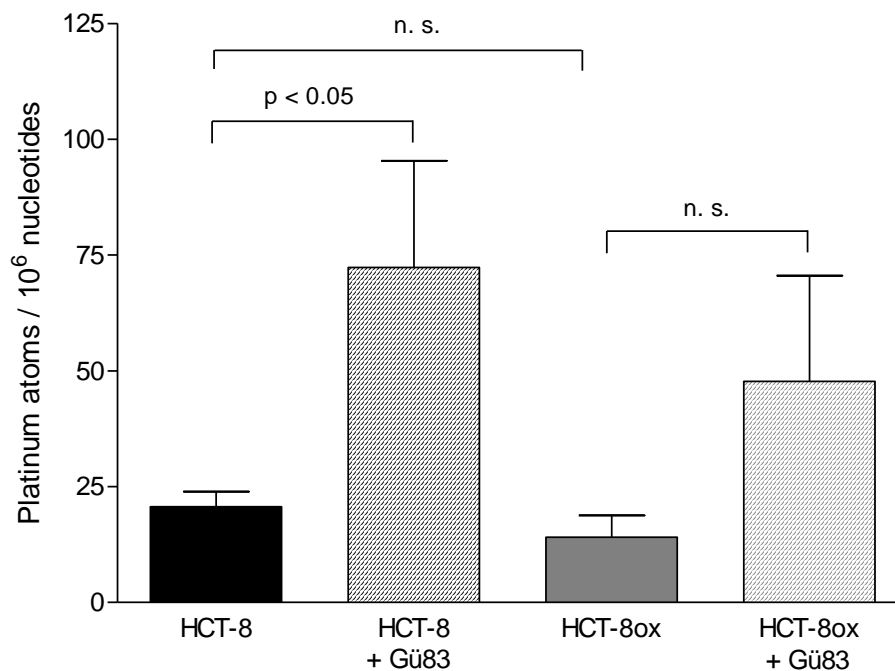
Fig. 4-22   DNA platination after 3 h incubation with 200 μM Gü83 and 100 μM oxaliplatin (mean ± SD, n = 3, unpaired t-test).
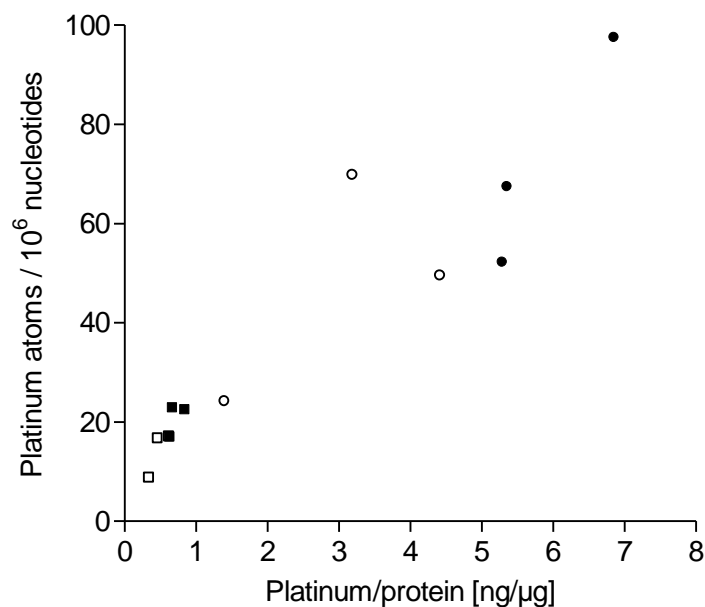
Fig. 4-23   Association of DNA platination and cellular platinum accumulation after 3 h incubation and 100 μM oxaliplatin in HCT-8 (■) and HCT-8ox cells (□) and after coincubation with 200 μM Gü83 (HCT-8 ((●) and HCT-8ox cells (○); n = 3.

4.3.3.6 Effects of indometacin and ciclosporin on platinum accumulation

So far an effect on cellular platinum accumulation was studied using the MRP modulator Gü83. To exclude that this effect is not due to specific properties of Gü83 the influence of further MRP modulators on platinum accumulation was investigated. Substances used were the non-steroidal anti-inflammatory drug indometacin and the immunosuppressant ciclosporin. Both substances led to an increase in cellular platinum accumulation, which was only statistically significant for ciclosporin in HCT-8 cells (Fig. 4-24 and Fig. 4-25). Ciclosporin showed only a marginal effect in HCT-8ox cells. For detailed results see Appendix D2.

For indometacin a higher concentration was chosen [200 µM] than for Gü83 and ciclosporin [100 µM each] as IC_{50} values for MRP1 and MRP2 inhibition are higher in case of indometacin [54].
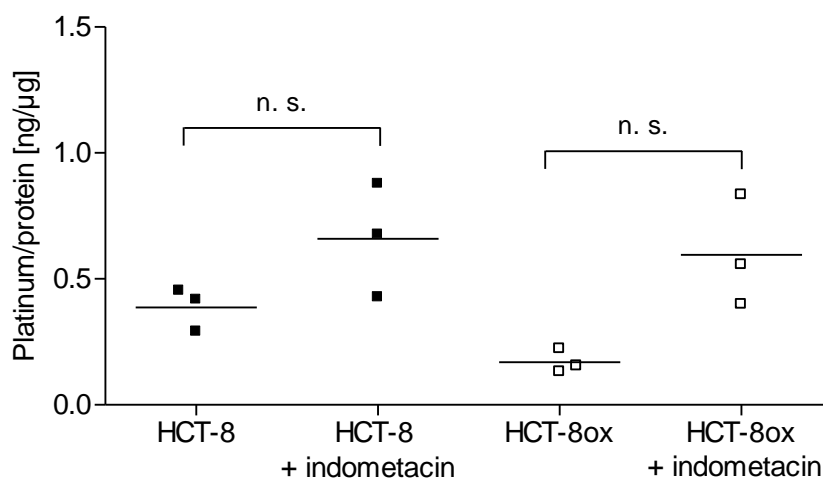
Fig. 4-24   Cellular platinum accumulation related to protein content after 2 h incubation with 200 µM indometacin and 100 µM oxaliplatin (scatter blot of individual values and mean, n = 3, paired t-test; n. s.: not significant).
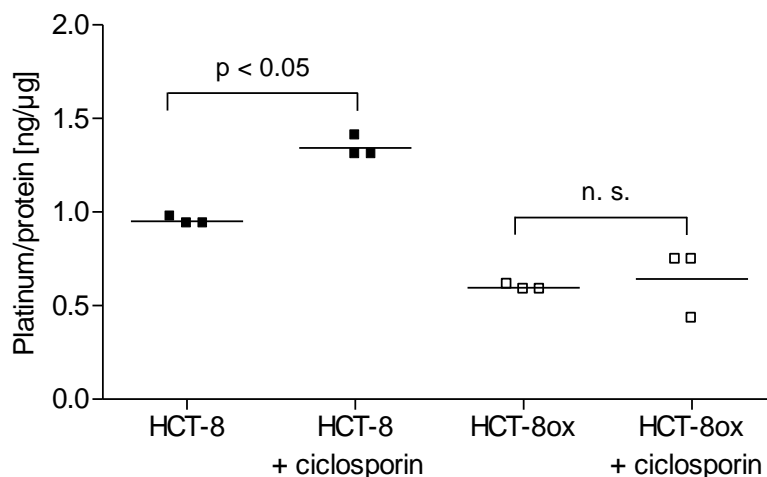
Fig. 4-25   Cellular platinum accumulation related to protein content after 2 h incubation with 100 µM ciclosporin and 100 µM oxaliplatin (scatter blot of individual values and mean, n = 3, paired t-test; n. s.: not significant).

4.3.3.7   Comparative potency of MRP modulators

As an influence of MRP inhibition on cellular platinum accumulation was observed, it was interesting to reveal if HCT-8 and HCT-8ox cells can functionally excrete substances via MRP and/or P-gp and if the effect on platinum accumulation shown was indeed due to MRP inhibition. For this purpose, the calcein assay was performed (see chapter 3.13). The calcein assay can be used to investigate the efflux via MRP1, MRP2 and P-gp and the influence of modulators on cellular efflux. The assay is not specific for any of the three transporters and the results summarize the effect of the three transporters together. In Fig. 4-26 and Fig. 4-27 the results of the calcein assay using various concentrations of the modulators are shown. The term 'response' represents the slope of the increasing calcein fluorescence signal that was determined by linear regression. For the MRP modulator Gü83 (Fig. 4-26) a sigmoidal dose-response curve was obtained. Hypothesizing that oxaliplatin might be a substrate of MRP and as such compete with the substrate calcein, the assay was also performed using oxaliplatin. The platinum complex, however, did not have an effect on the slope of the calcein fluorescence signal (Fig. 4-26).
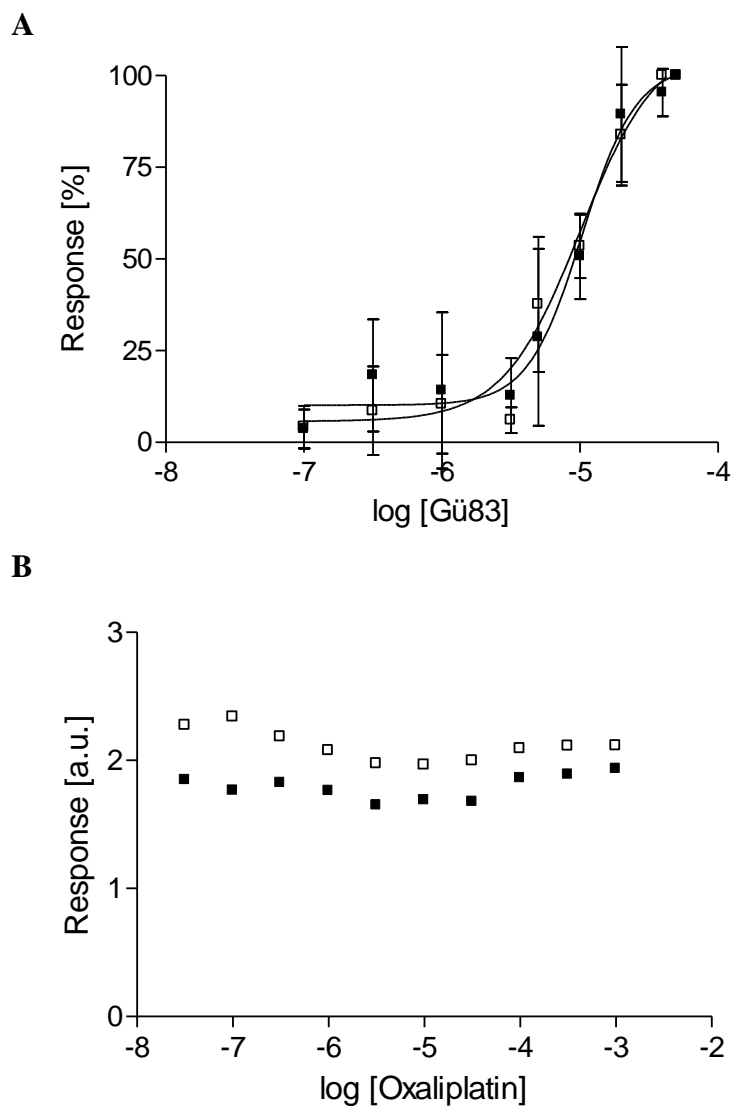
Fig. 4-26   Calcein efflux after incubation of HCT-8 (■) and HCT-8ox (□) cells with 0.3 μM calcein AM and different concentrations of **A** Gü83 and **B** oxaliplatin (response = slope; **A:** mean ± SD, n = 3 **B:** absolute values, representative graph, n = 3).

The previous experiments implied an effect of the MRP modulators indometacin and ciclosporin on platinum accumulation after incubation with oxaliplatin. The influence of these substances on calcein efflux was also investigated using various concentrations of the modulators (Fig. 4-27).

A

B
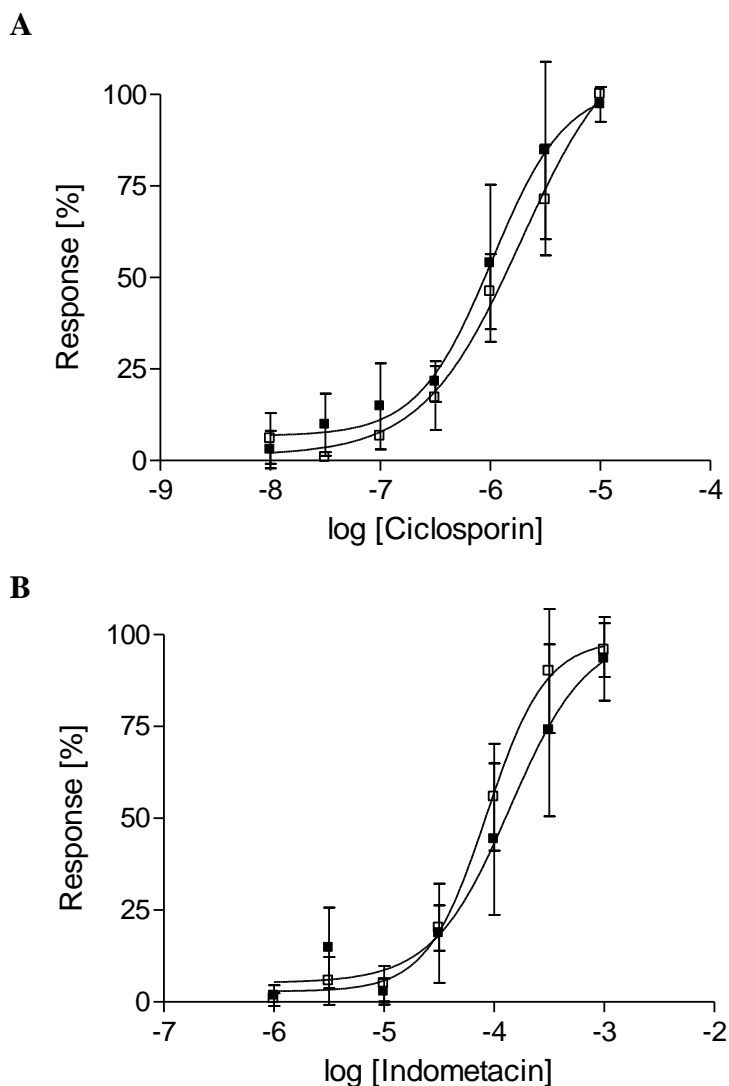
Fig. 4-27 Calcein efflux after incubation of HCT-8 (■) and HCT-8ox (□) cells with 0.3 µM calcein-AM and different concentrations of **A** ciclosporin and **B** indometacin (response = slope, mean ± SD, n = 3).

From the concentration-response curves the IC_{50} values were estimated with four-parameter logistic non-linear regression using the software GraphPad Prism® (see Tab. 4-6). The values give an idea about the concentration which is effective in inhibiting MRP1, MRP2 and P-gp in HCT-8 and HCT-8ox cells. Ciclosporin was most and indometacin least effective in inhibiting calcein efflux in HCT-8 and HCT-8ox cells. Results of individual testing days are shown in Appendix D3.

Tab. 4-6 pIC$_{50}$ values of MRP modulators derived from calcein efflux experiments (mean pIC$_{50}$ ± SEM, n = 3).

	pIC$_{50}$ (IC$_{50}$)	
	HCT-8	HCT-8ox
Gü83	5.21 ± 0.34 (6.2 µM)	4.76 ± 0.20 (17.4 µM)
Indometacin	3.68 ± 0.36 (208.9 µM)	4.00 ± 0.16 (100.0 µM)
Ciclosporin	5.78 ± 0.27 (1.7 µM)	5.75 ± 0.15 (1.8 µM)

4.3.3.8 Effect of Gü83 on cytotoxicity

As MRP modulators have an effect on cellular platinum accumulation and DNA platination they could as well alter the sensitivity of cells towards platinum complexes. To test this hypothesis the MTT assay (see chapter 3.5) was performed with oxaliplatin in the presence and absence of Gü83. It was found that EC$_{50}$ values increased when cells were coincubated with 100 µM Gü83 as can be seen in Tab. 4-7. The effect was found to be significant in HCT-8 cells. For results in detail see Appendix D4.

Tab. 4-7 pEC$_{50}$ of oxaliplatin with or without coincubation with 100 µM Gü83 (mean pEC$_{50}$ ± SEM, n = 4, paired t-test).

Cell lines	pEC$_{50}$ (EC$_{50}$)		
	+ Gü83	- Gü83	p value
HCT-8	5.35 ± 0.09 (4.5 µM)	5.45 ± 0.08 (3.5 µM)	0.027
HCT-8ox	4.62 ± 0.22 (24.0 µM)	4.84 ± 0.11 (14.4 µM)	0.146

5   DISCUSSION

In chapters 5.1 and 5.2 the investigations with regard to GSH and MRP-mediated efflux are reviewed. The implications of the results with regard to the interaction between GSH and MRP in platinum resistance are discussed in chapter 5.3. As a final point the clinical relevance of the findings is highlighted in chapter 5.4.

5.1   Glutathione and platinum resistance

5.1.1   Assay for GSH determination

This project aimed at further elucidating the impact of GSH on platinum resistance. To address the investigations on GSH, an assay for GSH determination was established and validated. Most assays for GSH determination previously described were performed by high-performance liquid chromatography (HPLC) or capillary electrophoresis (CE) which are characterized by low detection levels and selectivity [78,100-103]. In this project a semi-quantitative 96-well plate-based assay was chosen to allow high sample throughput.

The assay was adapted from a naphthalene-2,3-dicarboxaldehyde (NDA)-based assay validated for GSH determination using yeast cells [77], which has also been applied in other cell models [80]. As originally yeast cells were used and a different calibration range was chosen (0.3 to 6.5 µM by Lewicki et al. vs. 1 to 20 µM in this project) the assay was adapted and extensively validated. Validating the assay, accuracy and precision were according to the requirements [75,76]. For generation of the calibration standard curve a weighted calibration $(1/x^2)$ was shown to go along with smallest residues and was chosen for the assay. The GSH content was related to the protein content of the sample to account for sample loss during performance of the assay, different cell growth over time and different cell sizes [104].

The relatively low recovery found (around 45%) could be due to the matrix effect of the cell pellet as higher amounts of perchloric acid in cell lysis were reported to correlate with higher recovery [77]. The volume of perchloric acid was not increased as a fast sample processing was more feasible using 1 mL only. The cell number was either not reduced as otherwise the GSH content would have been too low in the lysate generated especially from A2780 cells.

DISCUSSION

However, as the volume of perchloric acid was reported to be decisive, strictly 1.0 mL of perchloric acid was used and the linearity of the fluorescence signal for GSH extracted from different cell numbers was tested and verified. Hence effects of the cell mass/perchloric acid-ratio on the amount of GSH determined can be excluded. To account for the low recovery, the results of the determination of GSH content were expressed as relative values either related to baseline value or related to the respective mean value for HCT-8.

Selectivity has not been investigated in this project. Lewicki et al. tested the assay on different thiols (GSH, GSSG, γ-glutamylcysteine, cysteinylglycine, cysteine, homocysteine, thioglycolic acid, DTT, dithionite) and found significant fluorescence signals only for GSH and its precursor γ-glutamylcysteine. The latter is the precursor of GSH in its *de novo* synthesis exhibiting low levels in eukaryotic cells. Thus, this finding has only little impact on GSH determination [77].

5.1.2   Cellular GSH content

The cellular GSH content of the four human cancer cell lines investigated in this project was determined. In A2780cis cells, the variant resistant to cisplatin, the cellular GSH content is increased compared to A2780 cells, as has been described for cisplatin-resistant and oxaliplatin-resistant cells repeatedly [25,29,30,105,106]. On the contrary, there was no difference in GSH content related to the protein content in HCT-8 cells and the oxaliplatin-resistant variant HCT-8ox cells. Considering the results of all cell lines, it is obvious that the cellular GSH content is similar in HCT-8, HCT-8ox and A2780cis but is lower in A2780 cells. Considering all cell lines there is no relationship between GSH content and the sensitivity to cisplatin and oxaliplatin. The findings are in agreement with previous studies as no correlation between total GSH content and sensitivity to cisplatin, carboplatin and oxaliplatin was found investigating a variety of diverse human cancer cell lines [56,107,108]. It is, however, noteworthy that the cell line with the lowest GSH content, A2780, was most sensitive to cisplatin and oxaliplatin.

Elevated GSH levels have been found in various types of cancer cells. The differences in basal GSH content among different cancer cells found in this and other projects [56,107] could be due to varying activities of intracellular pathways leading to increased GSH synthesis. Extracellular-signal-regulated kinase (ERK) and c-Jun N-terminal kinase (JNK)-mediated activation of activator protein 1 (AP-1) was found to increase cellular GSH content.

The change was described to be caused by altered expression of γ-glutamylcysteine synthetase (γGCS), the rate-limiting enzyme in GSH synthesis, as the region of DNA that initiates transcription of the γGCS gene, the γGCS promoter, contains recognition sites for AP-1 [109].

Moreover, the activation of the antioxidant response element (ARE) by the transcription factor 'nuclear factor erythroid 2-related factor 2' (Nrf2) might account for increased GSH content. Nrf2 is negatively regulated by Kelch-like ECH-associated protein 1 (Keap1) but in case of oxidative or electrophilic stress Nrf2 translocates to the nucleus and activates ARE. ARE is located in the promoter region of diverse genes encoding for enzymes involved in phase I/phase II detoxification and GSH homeostasis like γGCS, GSH reductase and GSH peroxidase [110]. However, Nrf2 might also cause higher GSH synthesis by stimulating the pro-oxidative action of Bcl-2 family anti-apoptotic proteins. Bcl-2 activation can be followed by an increase of ROS produced by mitochondria. In consequence, the resulting oxidative stress environment could lead to an increased cellular GSH content. The mechanism, however, is not clear [25]. Over-expression of Bcl-2 has amongst others been reported to result in higher GSH content and to recruit GSH to the nucleus and thus to prevent apoptosis as nuclear GSH is important for glutathionylation of proteins and in consequence for the regulation of protein functions during the cell cycle [111]. As described in chapter 1.3.3 Bcl-2 overexpression was associated with resistance to cisplatin in breast cancer cells [22] and also stable overexpression of Nrf2 was shown to result in resistance to cisplatin and downregulation of this factor in sensitization [112]. However, as increased GSH content was only associated with resistance in A2780/A2780cis cells a contribution of Nrf2 and Bcl-2 to resistance via GSH can only be assumed in this cell model.

To further investigate if and how GSH is involved in detoxification of platinum complexes cellular GSH content was also determined after addition of oxaliplatin or cisplatin to the cells. Here only a tendency towards a small increase in cellular GSH content was seen in HCT-8, HCT-8ox and A2780cis cells. The increase in A2780 cells was more obvious but was not significant either. Interestingly, the response to a platinum complex with respect to GSH content was most evident in the cell line with lowest baseline GSH content, suggesting that the other cell lines already exhibit a high GSH content which cannot be increased any further. In human melanoma cells a change in reduced GSH content after addition of cisplatin (2 and 5 µM for 3 and 6 h) was not seen either [113]. In contrast, in HCT-8 variants resistant to cisplatin a 6-fold increase in GSH was reported after cisplatin incubation [37]. These results

reflect the heterogeneity in data on GSH response to platinum complexes. The effect is probably dependent on cell type and baseline GSH content but could also differ among individual platinum complexes, as GSH content was not assessed after cisplatin incubation in HCT-8 and HCT-8ox cells but only after oxaliplatin treatment. Moreover, it has to be taken into consideration that non-toxic concentrations of the platinum complexes were used which could have been too low to observe a distinct effect on GSH content.

5.1.3   Effects of GSH depletion

The GSH-depleting agent buthionine sulfoximine (BSO) was used to further clarify the role of GSH in platinum resistance in HCT-8/HCT-8ox cells. BSO was reported to effectively reduce cellular GSH which was shown in HCT-8 and HCT-8ox cells in this project as well [113]. In different cell models accumulation of cisplatin was not altered after GSH depletion, corresponding to the findings of unchanged platinum accumulation after incubation with oxaliplatin in HCT8 and HCT-8ox cells [80,114]. In consequence, the cellular GSH content does not seem to be relevant for platinum accumulation upon oxaliplatin exposure in the cells investigated.

Assuming that GSH is an important cytoprotectant in cancer cells, an augmented toxicity of platinum complexes would be the logical consequence of GSH depletion and has been observed in cell culture experiments [31,113,114]. In this study HCT-8 cells were sensitized by GSH depletion. The same tendency was also observed in the oxaliplatin-resistant cell line HCT-8ox but the effect was smaller and not significant. Hence results suggest that GSH depletion does not overcome oxaliplatin resistance.

As GSH depletion was not associated with an altered platinum accumulation there must be other reasons for the sensitization towards oxaliplatin. The effect achieved could be due to the fact that less intracellular platinum is detoxified by GSH or to an inhibition of DNA repair in consequence of GSH depletion [115]. However, also disturbance of regulation of cell signaling involving protein S-glutathionylation and dysfunction of the cellular redox system are possible explanations for an increased sensitivity towards oxaliplatin [25,109].

5.1.4 Platinum-glutathione adducts

Formation of platinum-GSH adducts and transport out of the cell by transporters such as MRP is a widely recognized mechanism of platinum resistance [5,6,34,35]. In this project two platinum-GSH adducts for cisplatin und one for oxaliplatin were identified after incubation of the platinum complexes with GSH. The adducts, however, were not obtained from experiments with cells as the detection method was sensitive towards salts and the investigation of cell extracts would have required extensive extraction and purification steps. Thus, the structures identified can only serve as indicators for further studies with cells or cellular extracts. A separation step, like high-performance-liquid chromatography (HPLC), has not been performed prior to ESI and should be considered in future experiments as ESI-MS, also coupled with liquid chromatography (LC), has been successfully used for detection of platinum complexes [116,117] and for identification of formation of aqua complexes of cisplatin [118]. Moreover, polynuclear platinum adducts were detected by using ESI-MS investigating the reaction of [Pt(L-methionine-S,N)Cl$_2$] with GSH [119].

Research on putative intracellular GSH adducts is still ongoing and the state of knowledge is conflicting. Recently published results raise doubt about GSH as main intracellular binding partner of platinum complexes. When reviewing literature it appears that the identification of intracellularly formed platinum-GSH adducts from cell culture experiments has been reported only twice, with both research groups choosing similar analytical methods [35,37]. Ishikawa and Ali-Osman have isolated a putative platinum-GSH adduct from a mixture of cisplatin and GSH which they could identify in cell extract from cells incubated with cisplatin as well. They postulated that 60% of cisplatin were bound to GSH [35]. Goto et al. repeated the experiments using inside out vesicles prepared from A2780 and HCT-8 cells and cisplatin-resistant variants. They identified the same platinum-GSH adduct described by Ishikawa and Ali-Osman finding higher excretion from resistant variants [37]. The experiments were performed in the early/mid 1990s and the MS applied did not give a spectrum in high resolution as it could be obtained nowadays. The authors assumed to have found a distinct adduct rather by mass than by isotope pattern or fragmentation. However, they confirmed the findings with NMR [35].

Investigating the incubation of aqueous extracts of cancer cells with cisplatin with the aid of 2D nuclear magnetic resonance (NMR) spectroscopy Kasherman el al. observed that only up to 20% of cisplatin formed platinum-GSH adducts and that most of the platinum was found in

the high molecular mass fraction (> 3 kDa) indicating binding of platinum or platinum-GSH adducts to proteins [38]. In Escherichia coli, cisplatin was found to bind to carboxylato and hydroxyl as well as to methionyl-S atom binding sites of ribosomal proteins, DNA binding proteins and other proteins [120]. These data show that further research should not focus only on sulfhydryl groups but also on other nucleophilic binding sites of cellular structures such as proteins when investigating intracellular binding partners of platinum complexes.

5.2 MRP-mediated efflux and platinum resistance

5.2.1 Expression and localization of MRP2

In *in vitro* experiments with human cancer cells MRP2 expression level was found to be associated with platinum resistance and also *in vivo* studies reflect a relationship between MRP2 expression and clinical outcome after platinum-containing chemotherapy [59-61,63,68,69]. Hence experiments on MRP2 expression in the cell models investigated were performed. By SDS PAGE and protein immunoblotting MRP2 expression was detected in HCT-8 and HCT-8ox cells with a tendency towards a higher expression after oxaliplatin incubation in HCT-8 cells (not significant). MRP2 expression on protein level was negligible in A2780 cells and was low in A2780cis cells. It has to be noted that MRP2 levels detected were divergent from those reported by others, as expression of MRP2 was reported in A2780 and A2780cis cells on mRNA and protein level [63,64]. Nevertheless, in the work of Hector et al. also low MRP2 protein levels were reported for A2780 cells and even lower for a variant resistant to oxaliplatin [106]. This divergence might be due to different cultivation conditions (cultivation duration, cell culture medium) and differences in the methods used for generating the resistant variants.

In this project MRP2 expression was not determined on mRNA level but only on protein level. Generating data on mRNA expression would have further elucidated the role of MRP2 and allowed comparison with results of others investigating mRNA levels. A posttranscriptional control of protein expression of MRP2 has been described and thus could be important for the understanding of MRP2 as MRP2 expression is regulated at several steps (translation, transcription, membrane removal and membrane reinsertion) [49,121].

Surowiak et al. postulated that MRP2 expression in the nuclear membrane correlated with cellular resistance to cisplatin [64]. Using fluorescence microscopy, expression of MRP2 was illustrated but a nuclear expression was not shown in HCT-8 and HCT-8ox cells. Research findings suggest that MRP2 can be rapidly removed from the nuclear membrane or be inserted into canalicular membranes [121]. As no significant change in MRP2 protein expression was seen after addition of platinum complexes, MRP2 may have been inserted into membranes to a greater extent as response to addition of platinum complexes instead of being increasingly expressed. This effect, however, could not be confirmed in fluorescence microscopy experiments either.

5.2.2 Effects of MRP modulators

Platinum accumulation

MRP modulators led to an increase in platinum accumulation in the cell lines with higher MRP2 expression (HCT-8 and HCT-8ox cells) but not in those with negligible or low MRP2 expression (A2780 and A2780cis cells). Hence MRP-mediated efflux is likely to take place. Regarding platinum accumulation in HCT-8 and HCT-8ox cells upon oxaliplatin exposure, the effect of MRP modulators was significant with Gü83 [100 µM] but when ciclosporin [100 µM] and indometacin [200 µM] were applied it was only significant for ciclosporin in HCT-8 cells. Nevertheless, the tendency towards an increase in platinum accumulation was also seen for indometacin in HCT-8 and HCT-8ox cells. Considering the IC_{50} values described by Leyers et al. the chosen concentrations were far above the reported IC_{50} values of Gü83 and ciclosporin. The chosen concentration of indometacin was below the IC_{50} value for MRP2 and hence a higher concentration might have led to a significant effect [54]. The effect of indometacin and ciclosporin was not assessed over time, which probably would have provided more information than the investigation at only one time point.

The effect of Gü83 on platinum accumulation was similar for cisplatin and oxaliplatin, supporting the findings of Wortelboer et al. suggesting that both platinum complexes are substrates of MRP1 and MRP2 [53]. As the modulator substances used modulate MRP1 and MRP2, it is not possible to distinguish between both transporters. The increase in platinum accumulation was comparable in the sensitive and resistant variant and thus MRP-mediated efflux does not necessarily contribute to resistance in HCT-8ox.

DISCUSSION

Regarding the platinum accumulation without any modulator, the acknowledged hypothesis that reduced cellular platinum accumulation is associated with resistance was confirmed, as higher platinum accumulation was found in the sensitive cells (A2780, HCT-8) compared to cells of the resistance variants (A2780cis, HCT-8ox) [5]. This difference was not seen when the platinum accumulation upon cisplatin exposure was investigated in HCT-8 and HCT-8ox cells although HCT-8ox cells were cross-resistant to cisplatin, suggesting that platinum accumulation can be but is not necessarily a predicting factor of resistance which also was reported by others [108].

The effect of MRP modulator Gü83 on platinum efflux was also addressed experimentally. According to the results, incubation with Gü83 did not significantly influence platinum efflux in HCT-8 and HCT-8ox cells. As platinum accumulation, which comprises platinum uptake and platinum efflux, was significantly increased by Gü83 and the substance was described to modulate platinum efflux, a difference in efflux is probable but the method used for assessing the efflux was possibly not sensitive enough to prove it. A longer incubation time and consequently a higher level of platinum accumulation might have generated a more distinct effect. In HCT-8 cells, however, results indicate a reduced efflux when Gü83 is co-administered at least in the first 10 min.

DNA platination

The observed increase in platinum accumulation after addition of Gü83 to oxaliplatin treatment of HCT-8 and HCT-8ox cells was accompanied by an increase in DNA platination. DNA platination was higher in HCT-8 compared to HCT-8ox cells and hence the results reproduce the lower DNA platination in oxaliplatin-resistant cells described by others [122]. The difference was not significant after 3 h but in the same cell models a significant difference was shown incubating cells with oxaliplatin over 4 h [70].

When DNA platination was related to platinum accumulation it appeared that the increase of platinum accumulation achieved by Gü83was not associated with a proportional increase in DNA platination, indicating that DNA was not damaged as efficiently by a higher amount of intracellular oxaliplatin. This could have been due to increased detoxification or DNA repair. However, scatter was too high and the sample size too small to establish generalizations.

Comparative potency of MRP modulators

Using the calcein assay the effect of modulator substances on calcein efflux and hence on efflux via MRP1, MRP2 and P-gp can be investigated. However, when performing the assay the effect of MRP1, MRP2 and P-gp cannot be distinguished [88]. In HCT-8 and HCT-8ox cells MRP2 expression was determined. MRP1 and P-gp expression was described for HCT-8 in literature [123,124].

Investigating the inhibitory effect of substances on calcein efflux, ciclosporin was associated with lowest IC_{50} values in HCT-8 and HCT-8ox cells. This finding is probably due to the fact that it is active in modulation of MRP1, MRP2 and P-gp. Gü83 as well as indometacin modulate MRP1 and MRP2 but not P-gp. Their respective IC_{50} values were different in HCT-8 compared with HCT-8ox cells, which cannot be explained in this place apart from inaccuracy as reflected by high experimental variation. IC_{50} values of indometacin were higher compared with Gü83 as already reported [54].

Coincubation with MRP modulators affected cellular platinum accumulation of cisplatin and oxaliplatin and hence it can be assumed that transport of cisplatin and oxaliplatin by MRP1 and/or MRP2 takes place. As no effect on calcein efflux was seen in the calcein assay with various concentrations of oxaliplatin a modulation of MRP1-, MRP2- or P-gp-mediated efflux by oxaliplatin is not likely.

Cytotoxicity

As described above, Gü83 led to an increase of platinum accumulation and DNA platination after 3 h coincubation with oxaliplatin. Hence an increase in oxaliplatin cytotoxicity was expected when the impact of Gü83 on oxaliplatin cytotoxicity was investigated. But the opposite effect, as demonstrated by higher EC_{50} values for oxaliplatin in HCT-8 and HCT-8ox cells, was observed. Results indicate that the achieved increase in platinum accumulation and DNA platination by Gü83 is not helpful in overcoming oxaliplatin resistance or in sensitizing cells towards oxaliplatin. This paradox result suggests that an increased MRP-mediated efflux is a first defensive mechanism but is not decisive for long-term cytotoxicity.

To understand why increased DNA platination does not necessarily lead to sensitization it has to be considered that the mechanism of action of platinum complexes involves more than the processes started by DNA platination. For cisplatin, involvement of ER and for oxaliplatin, involvement of mitochondria in apoptosis was shown in enucleated cells [125,126]. The

consequences of Gü83 co-incubationon on the effect of oxaliplatin on cellular structures apart from DNA were not assessed. But as Gü83 was not supportive in sensitizing cells, further cellular targets involved in oxaliplatin cytotoxicity were probably not affected. Another possible explanation for the unexpected result may be that MRP1 and MRP2 inhibition leads to increased cellular accumulation of oxaliplatin metabolites, such as mono-GSH adducts, which still bind to DNA but are not capable anymore to form inter- or intrastrand crosslinks and thus do not result in increased cytotoxicity.

A limitation of the results is that the conditions of the MTT assay differed from the conditions used for measuring platinum accumulation and DNA platination. Whereas platinum accumulation and DNA platination were assessed up to 3 h of oxaliplatin incubation, the protocol of the MTT assay included an incubation period of 72 h. Thus, it is possible that the MRP inhibition is only effective during a relatively short incubation period. Modifications in the protocol of the MTT assay or further methods should be applied for confirming that MRP inhibition does not affect oxaliplatin cytotoxicity in the cells investigated. As a second assay for determination of cytotoxicity the adenosine triphosphate (ATP) assay could be used. By assessing the ATP content and thus cellular energy exchange, the ATP assay can detect cytotoxic effects already after short incubation periods [73].

5.3   Interaction between glutathione and MRP in platinum resistance

An association of MRP-mediated efflux of oxaliplatin and GSH was not found in HCT-8 and HCT-8ox cells. MRP-mediated efflux of oxaliplatin was confirmed (see chapter 5.2.2) but as GSH depletion did not affect platinum accumulation (see chapter 5.1.3), GSH does not seem to play a role in MRP-mediated efflux of oxaliplatin. Whether the oxaliplatin-GSH adduct identified (see chapter 5.1.4) is intracellularly formed in HCT-8 and HCT-8ox cells cannot be answered by the results of this project. However, in view of the finding that GSH does not have a function in MRP-mediated efflux it is not likely that a large proportion of oxaliplatin is excreted in the form of oxaliplatin-GSH adducts. In summary, none of the potential ways of interaction of GSH, MRP and endo- or exogenous substances described in chapter 1.6 seems to be relevant in case of oxaliplatin.

Nevertheless, a relationship between MRP and GSH is probable as genes coding for MRP and for proteins involved in GSH homeostasis are partially regulated by the same transcription

factors. AP-1 and Nrf2 are involved in GSH regulation (see chapter 5.1.2) but were also associated with MRP2 expression [110,112,121,127]. Hence both cellular mechanisms of defense can be activated by the same cellular signals. This connection, however, does not seem to be relevant for MRP-mediated efflux of oxaliplatin in HCT-8/HCT-8ox cells.

5.4 Clinical relevance

The results of the conducted *in vitro* experiments do not emphasize certain resistance mechanisms towards platinum complexes which could be therapeutically targeted. The effects of GSH depletion by BSO have been addressed in this project and an increase of oxaliplatin cytotoxicity was found. GSH depletion by BSO has also been and is currently investigated in clinical trials to improve the efficacy of melphalan, an alkylating chemotherapeutic agent, but there does not seem to be clinical research on co-administration of BSO and platinum complexes [128,129]. As described in chapter 1.4.2, instead of GSH depletion administration of GSH in addition to platinum-containing chemotherapy has been tested in clinical trials aiming to ameliorate toxicity. The results of this research project do not support the use of GSH as cytoprotectant as depletion of GSH was associated with sensitization towards oxaliplatin and thus an increase of GSH might be associated with decreased sensitivity. However, it has to be considered that intravenous administration of GSH does not necessarily cause increased GSH concentrations in patients' tumor tissue.

MRP modulation using Gü83 did not result in sensitization of HCT-8 or the oxaliplatin-resistant variant HCT-8ox towards oxaliplatin. This finding is consistence with results from clinical trials aiming to overcome multidrug resistance (MDR) to cancer chemotherapy by co-administration of modulator substances. To date, the trials involving a greater subset of patients ($\geq$ phase II) have not proven sufficient benefit in the treatment of solid tumors and addition of modulator substances to chemotherapy was often associated with severe adverse effects. Hence the respective drugs have not received marketing authorisation so far and are currently not therapeutically used. It has to be considered that trials were performed in heavily pre-treated patients with recurrent disease and that a clinical benefit is difficult to prove in this kind of study population. In Tab. 5-1 MDR modulators tested in clinical trials and their target protein are listed.

DISCUSSION

Tab. 5-1   MDR modulators added to cancer chemotherapy in clinical trials.

Modulator	Target protein	Tumor	Study types	Reference
Biricodar (VX-710)	P-gp, MRP1, BCRP	Small cell lung cancer, ovarian cancer	Phase I, II	[130,131]
Valspodar (PSC 833)	P-gp	Breast cancer, ovarian cancer, multiple myeloma, peritoneal cancer	Phase I to III	[132-136]
Dofequidar fumarate (MS-209)	P-gp, MRP1	Breast cancer	Phase I to III	[137]
Tariquidar (XR 9576)	P-gp, BCRP	Various solid tumors, among them are breast cancer, non-small cell lung cancer, ovarian cancer	Phase I to III	[129,138]

As the use of modulator substances and GSH depletion do not seem to be succesful strategies in overcoming platinum resistance, another approach related to GSH and MRP-mediated efflux may be more promising. Recently, a clinical trial with navitoclax (ABT-263), an agent which mimics cellular Bcl-2 antagonists and inhibits anti-apoptotic activity of Bcl-2 and Bcl-xL, was conducted in patients suffering from solid tumors [139]. For navitoclax monotherapy there was no benefit in patients with relapsed small cell lung cancer [139]. However, as Bcl-2 overexpression might account for elevated GSH content in tumor cells (see 5.1.2) and as it was associated with platinum resistance, the co-administration of navitoclax and platinum-containing chemotherapy might be a beneficial perspective in the light of the results of this project [22]. In addition to approaches targeting single proteins biochemical modulation strategies, i.e. drugs that interfere with pathways mediating resistance, should be further explored to circumvent platinum resistance in *in vitro* experiments as well as in clinical trials [20].

6 CONCLUSIONS AND OUTLOOK

This study provides a systematic approach to investigate the relevance of GSH and MRP-mediated efflux on platinum cytotoxicity and platinum resistance. In conclusion, the results suggest that intracellular GSH content is associated with oxaliplatin cytotoxicity but not with oxaliplatin resistance. Oxaliplatin or its metabolites were transported by MRP1 and/or MRP2 but inhibition of MRP-mediated efflux did not result in an increase of sensitivity to oxaliplatin suggesting that MRP-mediated efflux does not influence cytotoxic activity of oxaliplatin.

When investigating cellular GSH, total cellular GSH was determined in this study. Future research should focus on differentiation between unbound and protein-bound GSH, the ratio of GSH to its oxidized form, GSSG and of the distribution of GSH in cellular compartments as GSH might be an important factor regulating nuclear protein function in cell proliferation.

Intracellular formation of platinum-GSH adducts is likely but the extent to which platinum complexes react with GSH, whether adducts are transported by MRP and the implications for cellular platinum resistance need to be further questioned. To address these issues sophisticated analytical methodology is required as cellular extracts or biologic samples should be analyzed directly to monitor the formation of adducts over time.

The findings suggest that alterations in platinum accumulation and DNA platination assessed after only a few hours of incubation do not necessarily result in changes in sensitivity to platinum complexes determined after longer time intervals. Platinum resistance is not based on simple mechanisms and for its elucidation intracellular signal cascades need to be taken into consideration rather than single proteins. Future research needs to investigate the complex interactions between cellular signal cascades resulting in apoptosis or cell proliferation after incubation with platinum complexes in sensitive and platinum-resistant tumour cells. Here, the systematic analysis of changes in gene expression, gene transcription and protein expression after exposure of cells to platinum complexes would be valuable. For a comprehensive approach whole cells or even their interaction in a united cell structure/organism need to be considered.

7 SUMMARY

Therapeutic resistance towards platinum complexes is a multicausal interaction of diverse mechanisms. This project aimed to reveal the role of GSH and MRP-mediated efflux. Elevated GSH content, formation of platinum-GSH adducts and their efflux via MRP2 has been suggested to be associated with platinum resistance in many cases. In this project the impact of GSH and MRP-mediated efflux was investigated in two human cancer cell lines and their cisplatin- or oxaliplatin-resistant variant. The experiments focused on the platinum complex oxaliplatin as there is only limited research on the contribution of GSH and MRP-mediated efflux to oxaliplatin resistance so far.

The results of this project indicate that GSH is associated with oxaliplatin cytotoxicity but not with oxaliplatin resistance. Depletion of GSH resulted in an increase of sensitivity towards oxaliplatin but did not affect platinum accumulation in human tumor cells. However, GSH depletion did not overcome oxaliplatin resistance and also incubating cells with oxaliplatin did not result in alterations of GSH content. ESI-MS was applied as a method for detection and structural analysis of platinum-GSH adducts. Furthermore, chemical structures of one oxaliplatin-GSH and two cisplatin-GSH adducts could be identified. The formation of intracellular platinum-GSH adducts is probable but still has to be confirmed in human cancer cells.

Platinum accumulation was found to be increased after combined incubation of oxaliplatin or cisplatin with MRP modulators in cells expressing detectable levels of MRP2. Thus an efflux of cisplatin and oxaliplatin via MRP in the cells investigated is likely. But as GSH depletion did not affect platinum accumulation, the efflux does not seem to depend on GSH. In the case of oxaliplatin, DNA platination was also assessed and augmented accumulation was associated with an increase of platinated DNA. Despite these findings, MRP modulator co-incubation did not result in sensitization towards oxaliplatin and hence a direct association of MRP-mediated efflux and platinum resistance could not be shown. Moreover, oxaliplatin itself did not modulate MRP1- and/or MRP2-mediated efflux.

In summary, this project contributes to the knowledge of the relevance of GSH and MRP-mediated efflux in platinum resistance. Based on the results cellular GSH content is associated with oxaliplatin cytotoxicity but not with oxaliplatin resistance. Results also

suggest that oxaliplatin as well as cisplatin are likely to be transported by MRP1 and/or MRP2. However, MRP-mediated efflux does not seem to play a role in oxaliplatin resistance.

8 REFERENCES

[1] Robert Koch-Institut und die Gesellschaft der epidemiologischen Krebsregister in Deutschland e.V.. Krebs in Deutschland 2007/2008. 8. Ausgabe, 2012. Available at www.rki.de. Last retrieved on January 10, 2013.

[2] Statistisches Bundesamt. Gesundheit − Todesursachen in Deutschland 2010. 2011. Available at www.destatis.de. Last retrieved on January 10, 2013.

[3] Arzneimittel-Atlas 2011 – der Arzneimittelverbrauch der GKV. München: Urban & Vogel; 2011.

[4] Glaeske G, Schicktanz C. BARMER GEK Arzneimittelreport 2011. Available at www.barmer-gek.de. Last retrieved on January 10, 2013.

[5] Galluzzi L, Senovilla L, Vitale I, Michels J, Martins I, Kepp O et al. Molecular mechanisms of cisplatin resistance. Oncogene 2012; 31: 1869-83.

[6] Kelland L. The resurgence of platinum-based cancer chemotherapy. Nat Rev Cancer 2007; 7: 573-84.

[7] Rabik CA, Dolan ME. Molecular mechanisms of resistance and toxicity associated with platinating agents. Cancer Treat Rev 2007; 33: 9-23.

[8] Wheate NJ, Walker S, Craig GE, Oun R. The status of platinum anticancer drugs in the clinic and in clinical trials. Dalton Trans 2010; 39: 8113-27.

[9] Burger H, Loos WJ, Eechoute K, Verweij J, Mathijssen RH, Wiemer EA. Drug transporters of platinum-based anticancer agents and their clinical significance. Drug Resist Updat 2011; 14: 22-34.

[10] Wang D, Lippard SJ. Cellular processing of platinum anticancer drugs. Nat Rev Drug Discov 2005; 4: 307-20.

[11] Todd RC, Lippard SJ. Inhibition of transcription by platinum antitumor compounds. Metallomics 2009; 1: 280-91.

[12] Woynarowski JM, Chapman WG, Napier C, Herzig MC, Juniewicz P. Sequence- and region-specificity of oxaliplatin adducts in naked and cellular DNA. Mol Pharmacol 1998; 54: 770-7.

[13] Goodisman J, Hagrman D, Tacka KA, Souid AK. Analysis of cytotoxicities of platinum compounds. Cancer Chemother Pharmacol 2006; 57: 257-67.

[14] Chaney SG, Campbell SL, Bassett E, Wu Y. Recognition and processing of cisplatin- and oxaliplatin-DNA adducts. Crit Rev Oncol Hematol 2005; 53: 3-11.

[15] Siddik ZH. Cisplatin: mode of cytotoxic action and molecular basis of resistance. Oncogene 2003; 22: 7265-79.

[16]   Di Francesco AM, Ruggiero A, Riccardi R. Cellular and molecular aspects of drugs of the future: oxaliplatin. Cell Mol Life Sci 2002; 59: 1914-27.

[17]   Sharma A, Ramanjaneyulu A, Ray R, Rajeswari MR. Involvement of high mobility group B proteins in cisplatin-induced cytotoxicity in squamous cell carcinoma of skin. DNA Cell Biol 2009; 28: 311-8.

[18]   Stewart DJ. Mechanisms of resistance to cisplatin and carboplatin. Crit Rev Oncol Hematol 2007; 63: 12-31.

[19]   Ahmad S. Platinum-DNA interactions and subsequent cellular processes controlling sensitivity to anticancer platinum complexes. Chem Biodivers 2010; 7: 543-66.

[20]   Cepeda V, Fuertes MA, Castilla J, Alonso C, Quevedo C, Perez JM. Biochemical mechanisms of cisplatin cytotoxicity. Anticancer Agents Med Chem 2007; 7: 3-18.

[21]   Kalayda GV, Wagner CH, Buss I, Reedijk J, Jaehde U. Altered localisation of the copper efflux transporters ATP7A and ATP7B associated with cisplatin resistance in human ovarian carcinoma cells. BMC Cancer 2008; 8: 175.

[22]   Rudin CM, Yang Z, Schumaker LM, VanderWeele DJ, Newkirk K, Egorin MJ et al. Inhibition of glutathione synthesis reverses Bcl-2-mediated cisplatin resistance. Cancer Res 2003; 63: 312-8.

[23]   Kroemer G, Marino G, Levine B. Autophagy and the integrated stress response. Mol Cell 2010; 40: 280-93.

[24]   Anderson ME. Glutathione: an overview of biosynthesis and modulation. Chem Biol Interact 1998; 111-112: 1-14.

[25]   Ballatori N, Krance SM, Notenboom S, Shi S, Tieu K, Hammond CL. Glutathione dysregulation and the etiology and progression of human diseases. Biol Chem 2009; 390: 191-214.

[26]   Keppler D. Multidrug resistance proteins (MRPs, ABCCs): importance for pathophysiology and drug therapy. Handb Exp Pharmacol 2011; 201: 299-323.

[27]   Leier I, Jedlitschky G, Buchholz U, Center M, Cole SP, Deeley RG et al. ATP-dependent glutathione disulphide transport mediated by the MRP gene-encoded conjugate export pump. Biochem J 1996; 314: 433-7.

[28]   Mieyal JJ, Gallogly MM, Qanungo S, Sabens EA, Shelton MD. Molecular mechanisms and clinical implications of reversible protein S-glutathionylation. Antioxid Redox Signal 2008; 10: 1941-88.

[29]   Chen HH, Kuo MT. Role of glutathione in the regulation of Cisplatin resistance in cancer chemotherapy. Met Based Drugs 2010; 2010: 430939.

[30]   Chen G, Hutter KJ, Zeller WJ. Positive correlation between cellular glutathione and acquired cisplatin resistance in human ovarian cancer cells. Cell Biol Toxicol 1995; 11: 273-81.

REFERENCES

[31] Meijer C, Mulder NH, Timmer-Bosscha H, Sluiter WJ, Meersma GJ, de Vries EG. Relationship of cellular glutathione to the cytotoxicity and resistance of seven platinum compounds. Cancer Res 1992; 52: 6885-9.

[32] Zhang K, Chew M, Yang EB, Wong KP, Mack P. Modulation of cisplatin cytotoxicity and cisplatin-induced DNA cross-links in HepG2 cells by regulation of glutathione-related mechanisms. Mol Pharmacol 2001; 59: 837-43.

[33] Andrews PA, Murphy MP, Howell SB. Differential sensitization of human ovarian carcinoma and mouse L1210 cells to cisplatin and melphalan by glutathione depletion. Mol Pharmacol 1986; 30: 643-50.

[34] Hall MD, Okabe M, Shen DW, Liang XJ, Gottesman MM. The role of cellular accumulation in determining sensitivity to platinum-based chemotherapy. Annu Rev Pharmacol Toxicol 2007; 48: 18.1-18.41.

[35] Ishikawa T, Ali-Osman F. Glutathione-associated cis-diamminedichloroplatinum(II) metabolism and ATP-dependent efflux from leukemia cells. J Biol Chem 1993; 268: 20116-25.

[36] Hagrman D, Goodisman J, Souid AK. Kinetic study on the reactions of platinum drugs with glutathione. J Pharmacol Exp Ther 2004; 308: 658-66.

[37] Goto S, Yoshida K, Morikawa T, Urata Y, Suzuki K, Kondo T. Augmentation of transport for cisplatin-glutathione adduct in cisplatin-resistant cancer cells. Cancer Res 1995; 55: 4297-301.

[38] Kasherman Y, Sturup S, Gibson D. Is glutathione the major cellular target of cisplatin? A study of the interactions of cisplatin with cancer cell extracts. J Med Chem 2009; 52: 4319-28.

[39] Reedijk J. Why does Cisplatin reach Guanine-N7 with competing S-donor ligands available in the cell? Chem Rev 1999; 99: 2499-510.

[40] Townsend DM, Findlay VL, Tew KD. Glutathione S-transferases as regulators of kinase pathways and anticancer drug targets. Methods Enzymol 2005; 401: 287-307.

[41] Peklak-Scott C, Smitherman PK, Townsend AJ, Morrow CS. Role of glutathione S-transferase P1-1 in the cellular detoxification of cisplatin. Mol Cancer Ther 2008; 7: 3247-55.

[42] Surowiak P, Materna V, Kaplenko I, Spaczynski M, Dietel M, Lage H et al. Augmented expression of metallothionein and glutathione S-transferase pi as unfavourable prognostic factors in cisplatin-treated ovarian cancer patients. Virchows Arch 2005; 447: 626-33.

[43] Stoehlmacher J, Park DJ, Zhang W, Groshen S, Tsao-Wei DD, Yu MC et al. Association between glutathione S-transferase P1, T1, and M1 genetic polymorphism and survival of patients with metastatic colorectal cancer. J Natl Cancer Inst 2002; 94: 936-42.

[44] Aebi S, Assereto R, Lauterburg BH. High-dose intravenous glutathione in man. Pharmacokinetics and effects on cyst(e)ine in plasma and urine. Eur J Clin Invest 1991; 21: 103-10.

[45] Wang X, Guo Z. The role of sulfur in platinum anticancer chemotherapy. Anticancer Agents Med Chem 2007; 7: 19-34.

[46] Cascinu S, Catalano V, Cordella L, Labianca R, Giordani P, Baldelli AM et al. Neuroprotective effect of reduced glutathione on oxaliplatin-based chemotherapy in advanced colorectal cancer: a randomized, double-blind, placebo-controlled trial. J Clin Oncol 2002; 20: 3478-83.

[47] Colombo N, Bini S, Miceli D, Bogliun G, Marzorati L, Cavaletti G et al. Weekly cisplatin +/- glutathione in relapsed ovarian carcinoma. Int J Gynecol Cancer 1995; 5: 81-6.

[48] Milla P, Airoldi M, Weber G, Drescher A, Jaehde U, Cattel L. Administration of reduced glutathione in FOLFOX4 adjuvant treatment for colorectal cancer: effect on oxaliplatin pharmacokinetics, Pt-DNA adduct formation, and neurotoxicity. Anticancer Drugs 2009; 20: 396-402.

[49] Jedlitschky G, Hoffmann U, Kroemer HK. Structure and function of the MRP2 (ABCC2) protein and its role in drug disposition. Expert Opin Drug Metab Toxicol 2006; 2: 351-66.

[50] Leitner HM, Kachadourian R, Day BJ. Harnessing drug resistance: using ABC transporter proteins to target cancer cells. Biochem Pharmacol 2007; 74: 1677-85.

[51] Cole SP, Deeley RG. Transport of glutathione and glutathione conjugates by MRP1. Trends Pharmacol Sci 2006; 27: 438-46.

[52] Chen ZS, Tiwari AK. Multidrug Resistance Proteins (MRPs/ABCCs) in Cancer Chemotherapy and Genetic Diseases. FEBS J 2011; 278: 3226-45.

[53] Wortelboer HM, Balvers MG, Usta M, van Bladeren PJ, Cnubben NH. Glutathione-dependent interaction of heavy metal compounds with multidrug resistance proteins MRP1 and MRP2. Environ Toxicol Pharmacol 2008; 26: 102-8.

[54] Leyers S, Häcker H-G, Wiendlocha J, Gütschow M, Wiese M. A 4-aminobenzoic acid derivative as novel lead for selective inhibitors of multidrug resistance-associated proteins. Bioorg Med Chem Lett 2008; 18: 4761-3.

[55] Cnubben NH, Wortelboer HM, van Zanden JJ, Rietjens IM, van Bladeren PJ. Metabolism of ATP-binding cassette drug transporter inhibitors: complicating factor for multidrug resistance. Expert Opin Drug Metab Toxicol 2005; 1: 219-32.

[56] Bracht K, Liebeke M, Ritter CA, Grunert R, Bednarski PJ. Correlations between the activities of 19 standard anticancer agents, antioxidative enzyme activities and the expression of ATP-binding cassette transporters: comparison with the National Cancer Institute data. Anticancer Drugs 2007; 18: 389-404.

REFERENCES

[57] Young LC, Campling BG, Cole SP, Deeley RG, Gerlach JH. Multidrug resistance proteins MRP3, MRP1, and MRP2 in lung cancer: correlation of protein levels with drug response and messenger RNA levels. Clin Cancer Res 2001; 7: 1798-804.

[58] Cai BL, Xu XF, Fu SM, Shen LL, Zhang J, Guan SM et al. Nuclear translocation of MRP1 contributes to multidrug resistance of mucoepidermoid carcinoma. Oral Oncol 2011; 47: 1134-40.

[59] Noma B, Sasaki T, Fujimoto Y, Serikawa M, Kobayashi K, Inoue M et al. Expression of multidrug resistance-associated protein 2 is involved in chemotherapy resistance in human pancreatic cancer. Int J Oncol 2008; 33: 1187-94.

[60] Liedert B, Materna V, Schadendorf D, Thomale J, Lage H. Overexpression of cMOAT (MRP2/ABCC2) is associated with decreased formation of platinum-DNA adducts and decreased G2-arrest in melanoma cells resistant to cisplatin. J Invest Dermatol 2003; 121: 172-6.

[61] Materna V, Liedert B, Thomale J, Lage H. Protection of platinum-DNA adduct formation and reversal of cisplatin resistance by anti-MRP2 hammerhead ribozymes in human cancer cells. Int J Cancer 2005; 115: 393-402.

[62] Yamasaki M, Makino T, Masuzawa T, Kurokawa Y, Miyata H, Takiguchi S. Role of multidrug resistance protein 2 (MRP2) in chemoresistance and clinical outcome in oesophageal squamous cell carcinoma. Br J Cancer 2011; 104: 707-13.

[63] Ma JJ, Chen BL, Xin XY. Inhibition of multi-drug resistance of ovarian carcinoma by small interfering RNA targeting to MRP2 gene. Arch Gynecol Obstet 2009; 279: 149-57.

[64] Surowiak P, Materna V, Kaplenko I, Spaczynski M, Dolinska-Krajewska B, Gebarowska E et al. ABCC2 (MRP2, cMOAT) can be localized in the nuclear membrane of ovarian carcinomas and correlates with resistance to cisplatin and clinical outcome. Clin Cancer Res 2006; 12: 7149-58.

[65] Theile D, Grebhardt S, Haefeli WE, Weiss J. Involvement of drug transporters in the synergistic action of FOLFOX combination chemotherapy. Biochem Pharmacol 2009; 78: 1366-73.

[66] Li Q, Peng X, Yang H, Rodriguez JA, Shu Y. Contribution of organic cation transporter 3 to cisplatin cytotoxicity in human cervical cancer cells. J Pharm Sci 2012; 101: 394-404.

[67] Hinoshita E, Uchiumi T, Taguchi K, Kinukawa N, Tsuneyoshi M, Maehara Y et al. Increased expression of an ATP-binding cassette superfamily transporter, multidrug resistance protein 2, in human colorectal carcinomas. Clin Cancer Res 2000; 6: 2401-7.

[68] Korita PV, Wakai T, Shirai Y, Matsuda Y, Sakata J, Takamura M et al. Multidrug resistance-associated protein 2 determines the efficacy of cisplatin in patients with hepatocellular carcinoma. Oncol Rep 2010; 23: 965-72.

[69]   Ushijima R, Takayama K, Izumi M, Harada T, Horiuchi Y, Uchino J et al. Immunohistochemical expression of MRP2 and clinical resistance to platinum-based chemotherapy in small cell lung cancer. Anticancer Res 2007; 27: 4351-8.

[70]   Buss I. Cellular influx and toxicity of oxaliplatin analogues. Universität Bonn: Dissertation; 2010.

[71]   Behrens BC, Hamilton TC, Masuda H, Grotzinger KR, Whang-Peng J, Louie KG et al. Characterization of a cis-diamminedichloroplatinum(II)-resistant human ovarian cancer cell line and its use in evaluation of platinum analogues. Cancer Res 1987; 47: 414-8.

[72]   Alley MC, Scudiero DA, Monks A, Hursey ML, Czerwinski MJ, Fine DL et al. Feasibility of drug screening with panels of human tumor cell lines using a microculture tetrazolium assay. Cancer Res 1988; 48: 589-601.

[73]   Müller H, Kassack MU, Wiese M. Comparison of the usefulness of the MTT, ATP, and calcein assays to predict the potency of cytotoxic agents in various human cancer cell lines. J Biomol Screen 2004; 9: 506-15.

[74]   Motulsky H, Christopoulos A. Fitting models to biological data using linear and non-linear regression. New York: Oxford University Press; 2004.

[75]   Food and Drug Administration. Guidance for Industry – Bioanalytical method validation. 2001. Available at www.fda.gov. Last retrieved on January 10, 2013.

[76]   European Medicines Agency. Guideline on bioanalytical method validation. 2012. Available at www.ema.europa.eu. Last retrieved on January 10, 2013.

[77]   Lewicki K, Marchand S, Matoub L, Lulek J, Coulon J, Leroy P. Development of a fluorescence-based microtiter plate method for the measurement of glutathione in yeast. Talanta 2006; 70: 876-82.

[78]   Parmentier C, Wellman M, Nicolas A, Siest G, Leroy P. Simultaneous measurement of reactive oxygen species and reduced glutathione using capillary electrophoresis and laser-induced fluorescence detection in cultured cell lines. Electrophoresis 1999; 20: 2938-44.

[79]   Zisowsky J. Charakterisierung der Platinsensitivität von cisplatinsensitiven und -resistenten Tumorzellen. Universität Bonn: Dissertation; 2004.

[80]   Leyers S. Funktionelle Untersuchungen der Multidrug-Resistance-Associated Proteins (MRP) 1 und 2. Universität Bonn: Dissertation; 2009.

[81]   Garmann D. Reaktivität und zelluläre Aufnahme albuminbindender Platinkomplexe und neuer Oxaliplatin-Analoga. Universität Bonn: Dissertation; 2007.

[82]   Banerjee S, Mazumdar S. Electrospray ionization mass spectrometry: a technique to access the information beyond the molecular weight of the analyte. Int J Anal Chem 2012; 2012: 282574.

REFERENCES

[83]   Kloft C, Appelius H, Siegert W, Schunack W, Jaehde U. Determination of platinum complexes in clinical samples by a rapid flameless atomic absorption spectrometry assay. Ther Drug Monit 1999; 21: 631-7.

[84]   Kloft C, Eickhoff C, Schulze-Forster K, Maurer HR, Schunack W, Jaehde U. Development and application of a simple assay to quantify cellular adducts of platinum complexes with DNA. Pharm Res 1999; 16: 470-3.

[85]   Pieck AC. Pharmakokinetik und Platin-DNA-Adduktbildung von Oxaliplatin. Universität Bonn: Dissertation; 2004.

[86]   Ferguson RE, Carroll HP, Harris A, Maher ER, Selby PJ, Banks RE. Housekeeping proteins: a preliminary study illustrating some limitations as useful references in protein expression studies. Proteomics 2005; 5: 566-71.

[87]   Rehm H, Letzel T. Der Experimentator − Proteinbiochemie/Proteomics. Heidelberg: Spektrum Akademischer Verlag, 2010.

[88]   Essodaigui M, Broxterman HJ, Garnier-Suillerot A. Kinetic analysis of calcein and calcein-acetoxymethylester efflux mediated by the multidrug resistance protein and P-glycoprotein. Biochemistry 1998; 37: 2243-50.

[89]   Kirkwood RB, Sterne JAC. Medical statistics. Oxford: Blackwell Publishers Ltd; 2003.

[90]   Appleton TG, Connor JW, Hall JR, Prenzler PD. NMR study of the reactions of the cis-diamminediaquaplatinum(II) cation with glutathione and amino acids containing a thiol group. Inorg Chem 1998; 28: 2030-7.

[91]   Bernareggi A, Torti L, Facino RM, Carini M, Depta G, Casetta B et al. Characterization of cisplatin-glutathione adducts by liquid chromatography-mass spectrometry. Evidence for their formation in vitro but not in vivo after concomitant administration of cisplatin and glutathione to rats and cancer patients. J Chromatogr B Biomed Appl 1995; 669: 247-63.

[92]   Berners-Price SJ, Kuchel PW. Reaction of cis- and trans-$[PtCl_2(NH_3)_2]$ with reduced glutathione inside human red blood cells, studied by ^{1}H and ^{15}N-$[^1$H]DEPT NMR. J Inorg Biochem 1990; 38: 327-45.

[93]   Dedon PC, Borch RF. Characterization of the reactions of platinum antitumor agents with biologic and nonbiologic sulfur-containing nucleophiles. Biochem Pharmacol 1987; 36: 1955-64.

[94]   Heudi O, Brisset H, Cailleux A, Allain P. Chemical instability and methods for measurement of cisplatin adducts formed by interactions with cysteine and glutathione. Int J Clin Pharmacol Ther 2001; 39: 344-9.

[95]   Odenheimer B, Wolf W. Reactions of cisplatin with sulfur-containing amino-acids and peptides − cysteine and glutathione. Inorganica Chim Acta 1982; 66: 41-3.

[96] Townsend DM, Marto JA, Deng M, Macdonald TJ, Hanigan MH. High pressure liquid chromatography and mass spectrometry characterization of the nephrotoxic biotransformation products of Cisplatin. Drug Metab Dispos 2003; 31: 705-13.

[97] Luo FR, Wyrick SD, Chaney SG. Biotransformations of oxaliplatin in rat blood in vitro. J Biochem Mol Toxicol 1999; 13: 159-69.

[98] Buss I, Kalayda GV, Marques-Gallego P, Reedijk J, Jaehde U. Influence of the hOCT2 inhibitor cimetidine on the cellular accumulation and cytotoxicity of oxaliplatin. Int J Clin Pharmacol Ther 2009; 47: 51-4.

[99] Zisowsky J, Kögel S, Leyers S, Devarakonda K, Kassack MU, Osmak M et al. Relevance of drug uptake and efflux for cisplatin sensitivity of tumor cells. Biochem Pharmacol 2007; 73: 298-307.

[100] Bayle C, Causse E, Couderc F. Determination of aminothiols in body fluids, cells, and tissues by capillary electrophoresis. Electrophoresis 2004; 25: 1457-72.

[101] Carru C, Zinellu A, Pes GM, Marongiu G, Tadolini B, Deiana L. Ultrarapid capillary electrophoresis method for the determination of reduced and oxidized glutathione in red blood cells. Electrophoresis 2002; 23: 1716-21.

[102] Lakritz J, Plopper CG, Buckpitt AR. Validated high-performance liquid chromatography-electrochemical method for determination of glutathione and glutathione disulfide in small tissue samples. Anal Biochem 1997; 247: 63-8.

[103] Giustarini D, le-Donne I, Colombo R, Milzani A, Rossi R. An improved HPLC measurement for GSH and GSSG in human blood. Free Radic Biol Med 2003; 35: 1365-72.

[104] Pendyala L, Creaven PJ, Perez R, Zdanowicz JR, Raghavan D. Intracellular glutathione and cytotoxicity of platinum complexes. Cancer Chemother Pharmacol 1995; 36: 271-8.

[105] El-Akawi Z, Bu-Hadid M, Perez R, Glavy J, Zdanowicz J, Creaven PJ et al. Altered glutathione metabolism in oxaliplatin resistant ovarian carcinoma cells. Cancer Lett 1996; 105: 5-14.

[106] Hector S, Nava ME, Clark K, Murphy M, Pendyala L. Characterization of a clonal isolate of an oxaliplatin resistant ovarian carcinoma cell line A2780/C10. Cancer Lett 2007; 245: 195-204.

[107] Boubakari, Bracht K, Neumann C, Grunert R, Bednarski PJ. No correlation between GSH levels in human cancer cell lines and the cell growth inhibitory activities of platinum diamine complexes. Arch Pharm 2004; 337: 668-71.

[108] Johnson SW, Laub PB, Beesley JS, Ozols RF, Hamilton TC. Increased platinum-DNA damage tolerance is associated with cisplatin resistance and cross-resistance to various chemotherapeutic agents in unrelated human ovarian cancer cell lines. Cancer Res 1997; 57: 850-6.

REFERENCES

[109] Franco R, Cidlowski JA. Apoptosis and glutathione: beyond an antioxidant. Cell Death Differ 2009; 16: 1303-14.

[110] Higgins LG, Hayes JD. The cap'n'collar transcription factor Nrf2 mediates both intrinsic resistance to environmental stressors and an adaptive response elicited by chemopreventive agents that determines susceptibility to electrophilic xenobiotics. Chem Biol Interact 2011; 192: 37-45.

[111] Pallardo FV, Markovic J, Garcia JL, Vina J. Role of nuclear glutathione as a key regulator of cell proliferation. Mol Aspects Med 2009; 30: 77-85.

[112] Wang XJ, Sun Z, Villeneuve NF, Zhang S, Zhao F, Li Y et al. Nrf2 enhances resistance of cancer cells to chemotherapeutic drugs, the dark side of Nrf2. Carcinogenesis 2008; 29: 1235-43.

[113] Pendyala L, Perez R, Weinstein A, Zdanowicz J, Creaven PJ. Effect of glutathione depletion on the cytotoxicity of cisplatin and iproplatin in a human melanoma cell line. Cancer Chemother Pharmacol 1997; 40: 38-44.

[114] Benedetti BT, Peterson EJ, Kabolizadeh P, Martinez A, Kipping R, Farrell NP. Effects of noncovalent platinum drug-protein interactions on drug efficacy: use of fluorescent conjugates as probes for drug metabolism. Mol Pharm 2011; 8: 940-8.

[115] Lai GM, Ozols RF, Young RC, Hamilton TC. Effect of glutathione on DNA repair in cisplatin-resistant human ovarian cancer cell lines. J Natl Cancer Inst 1989; 81: 535-9.

[116] Burns RB, Burton RW, Albon SP, Embree L. Liquid chromatography-mass spectrometry for the detection of platinum antineoplastic complexes. J Pharm Biomed Anal 1996; 14: 367-72.

[117] Poon GK, Mistry P, Lewis S. Electrospray ionization mass spectrometry of platinum anticancer agents. Biol Mass Spectrom 1991; 20: 687-92.

[118] Cui M, Mester Z. Electrospray ionization mass spectrometry coupled to liquid chromatography for detection of cisplatin and its hydrated complexes. Rapid Commun Mass Spectrom 2003; 17: 1517-27.

[119] Liu Q, Wei H, Lin J, Zhu L, Guo Z. Novel polynuclear platinum adducts detected during the reactions of [Pt(Met-S,N)Cl$_2$] with gamma-glutathione and L-cysteine. J Inorg Biochem 2004; 98: 702-12.

[120] Will J, Wolters DA, Sheldrick WS. Characterisation of cisplatin binding sites in human serum proteins using hyphenated multidimensional liquid chromatography and ESI tandem mass spectrometry. Chem Med Chem 2008; 3: 1696-707.

[121] Gerk PM, Vore M. Regulation of expression of the multidrug resistance-associated protein 2 (MRP2) and its role in drug disposition. J Pharmacol Exp Ther 2002; 302: 407-15.

[122] Noordhuis P, Laan AC, van de BK, Losekoot N, Kathmann I, Peters GJ. Oxaliplatin activity in selected and unselected human ovarian and colorectal cancer cell lines. Biochem Pharmacol 2008; 76: 53-61.

[123] Sui H, Zhou S, Wang Y, Liu X, Zhou L, Yin P et al. COX-2 contributes to P-glycoprotein-mediated multidrug resistance via phosphorylation of c-Jun at Ser63/73 in colorectal cancer. Carcinogenesis 2011; 32: 667-75.

[124] Xu Y, Jiang Z, Yin P, Li Q, Liu J. Role for Class I histone deacetylases in multidrug resistance. Exp Cell Res 2012; 318: 177-86.

[125] Gourdier I, Crabbe L, Andreau K, Pau B, Kroemer G. Oxaliplatin-induced mitochondrial apoptotic response of colon carcinoma cells does not require nuclear DNA. Oncogene 2004; 23: 7449-57.

[126] Mandic A, Hansson J, Linder S, Shoshan MC. Cisplatin induces endoplasmic reticulum stress and nucleus-independent apoptotic signaling. J Biol Chem 2003; 278: 9100-6.

[127] Vollrath V, Wielandt AM, Iruretagoyena M, Chianale J. Role of Nrf2 in the regulation of the Mrp2 (ABCC2) gene. Biochem J 2006; 395: 599-609.

[128] Calvert P, Yao KS, Hamilton TC, O'Dwyer PJ. Clinical studies of reversal of drug resistance based on glutathione. Chem Biol Interact 1998; 111-112: 213-24.

[129] ClinicalTrials.gov. Available at: www.clinicaltrials.gov. Last retrieved on April 3, 2012.

[130] Gandhi L, Harding MW, Neubauer M, Langer CJ, Moore M, Ross HJ et al. A phase II study of the safety and efficacy of the multidrug resistance inhibitor VX-710 combined with doxorubicin and vincristine in patients with recurrent small cell lung cancer. Cancer 2007; 109: 924-32.

[131] Seiden MV, Swenerton KD, Matulonis U, Campos S, Rose P, Batist G et al. A phase II study of the MDR inhibitor biricodar (INCEL, VX-710) and paclitaxel in women with advanced ovarian cancer refractory to paclitaxel therapy. Gynecol Oncol 2002; 86: 302-10.

[132] Carlson RW, O'Neill AM, Goldstein LJ, Sikic BI, Abramson N, Stewart JA et al. A pilot phase II trial of valspodar modulation of multidrug resistance to paclitaxel in the treatment of metastatic carcinoma of the breast (E1195): a trial of the Eastern Cooperative Oncology Group. Cancer Invest 2006; 24: 677-81.

[133] Baekelandt M, Lehne G, Trope CG, Szanto I, Pfeiffer P, Gustavsson B et al. Phase I/II trial of the multidrug-resistance modulator valspodar combined with cisplatin and doxorubicin in refractory ovarian cancer. J Clin Oncol 2001; 19: 2983-93.

[134] Fracasso PM, Brady MF, Moore DH, Walker JL, Rose PG, Letvak L et al. Phase II study of paclitaxel and valspodar (PSC 833) in refractory ovarian carcinoma: a gynecologic oncology group study. J Clin Oncol 2001; 19: 2975-82.

REFERENCES

[135] Friedenberg WR, Rue M, Blood EA, Dalton WS, Shustik C, Larson RA et al. Phase III study of PSC-833 (valspodar) in combination with vincristine, doxorubicin, and dexamethasone (valspodar/VAD) versus VAD alone in patients with recurring or refractory multiple myeloma (E1A95): a trial of the Eastern Cooperative Oncology Group. Cancer 2006; 106: 830-8.

[136] Lhommé C, Joly F, Walker JL, Lissoni AA, Nicoletto MO, Manikhas GM et al. Phase III study of valspodar (PSC 833) combined with paclitaxel and carboplatin compared with paclitaxel and carboplatin alone in patients with stage IV or suboptimally debulked stage III epithelial ovarian cancer or primary peritoneal cancer. J Clin Oncol 2008; 26: 2674-82.

[137] Saeki T, Nomizu T, Toi M, Ito Y, Noguchi S, Kobayashi T et al. Dofequidar fumarate (MS-209) in combination with cyclophosphamide, doxorubicin, and fluorouracil for patients with advanced or recurrent breast cancer. J Clin Oncol 2007; 25: 411-7.

[138] Pusztai L, Wagner P, Ibrahim N, Rivera E, Theriault R, Booser D et al. Phase II study of tariquidar, a selective P-glycoprotein inhibitor, in patients with chemotherapy-resistant, advanced breast carcinoma. Cancer 2005; 104: 682-91.

[139] Rudin CM, Hann CL, Garon EB, Ribeiro de OM, Bonomi PD, Camidge DR et al. Phase II study of single-agent navitoclax (ABT-263) and biomarker correlates in patients with relapsed small cell lung cancer. Clin Cancer Res 2012; 18: 3163-9.

[140] Zhao Z, Tepperman K, Dorsey JG, Elder RC. Determination of cisplatin and some possible metabolites by ion-pairing chromatography with inductively coupled plasma mass spectrometric detection. J Chromatogr 1993; 615: 83-9.

9 APPENDIX

APPENDIX A

Cytotoxicity

Sensitivity of HCT-8 and HCT-8ox (A) and A2780 and A2780cis (B) cells towards cisplatin and oxaliplatin expressed as pEC_{50} investigated using an MTT-based cytotoxicity assay (results of single testing days, n = 3-11).

A		pEC_{50}		B		pEC_{50}	
		Cisplatin	Oxaliplatin			Cisplatin	Oxaliplatin
HCT-8		5.13	5.43	A2780		5.57	6.08
		5.07	5.66			5.36	5.56
		4.94	5.61			5.56	6.45
			5.87			5.63	
			5.63			5.58	
			5.22			5.63	
			5.51			5.94	
			5.75			5.76	
			5.44			6.03	
			5.29			6.01	
			5.73			5.60	
HCT-8ox		4.52	4.25	A2780cis		4.80	5.53
		4.57	4.44			4.91	5.16
		4.81	4.60			4.89	5.61
			4.51			4.87	
			4.36			5.20	
			4.55				
			4.52				
			4.19				
			4.21				
			4.56				

APPENDIX B

GSH in platinum resistance

B1 GSH assay validation

Within-day accuracy and precision of six runs (SD = standard deviation, RSD = relative standard deviation, RE = relative error).

	GSH content [µM]		
	3	**12**	**18**
Run 1	3.18	11.77	18.78
Run 2	3.17	13.52	19.92
Run 3	3.08	11.52	16.57
Run 4	3.01	12.80	16.60
Run 5	3.43	13.04	19.36
Run 6	2.89	13.80	20.19
Mean	3.13	12.74	18.57
SD	0.18	0.92	1.61
RSD [%]	5.87	7.24	8.68
RE [%]	+4.22	+6.18	+3.17

Between-day accuracy and precision comparing the results of five different days (SD = standard deviation, RSD = relative standard deviation, RE = relative error).

	GSH content [µM]		
	3	**12**	**18**
Day 1	3.08	12.67	18.27
Day 2	2.93	10.92	15.95
Day 3	3.01	11.93	18.18
Day 4	3.18	11.77	18.78
Day 5	3.03	12.30	18.21
Mean	3.05	11.92	17.88
SD	0.09	0.66	1.11
RSD [%]	3.03	5.52	6.18
RE [%]	+1.53	-0.68	-0.68

Recovery of a low, medium and high GSH content tested (n = 3).

GSH content [µM]	Recovery [%]			Mean [%] (SD)
0.5	57.4	54.2	32.3	48.0 (13.6)
3.3	48.5	43.7	35.8	42.7 (6.4)
7.5	53.0	46.9	38.2	46.0 (7.4)

Linearity of the fluorescence signal of the GSH-NDA adduct after isolation and lysis of different numbers of cells (r = correlation coefficient, df = degrees of freedom (= number of x-values − 2); n = 2-3).

A2780				
	Slope	**Intercept**	**df**	**r**
	2.181	+0.408	2	0.9683
	2.534	-0.340	2	0.9995
	1.291	-1.173	2	0.9135

A2780cis				
	Slope	**Intercept**	**df**	**r**
	2.916	-0.220	2	0.9993
	2.332	-1.036	2	0.9920

HCT-8				
	Slope	**Intercept**	**df**	**r**
	5.103	0.000	1	0.9999
	5.230	-0.065	1	0.9989

HCT-8ox				
	Slope	**Intercept**	**df**	**r**
	14.52	-0.326	1	0.9992
	16.20	-0393	1	0.9981

Calibration curves from five testing days (SD = standard deviation, RSD = relative standard deviation, RE = relative error).

	Concentration [µM]						
	1	**2**	**5**	**10**	**15**	**20**	**r**
Day 1	1.00	1.97	5.02	10.41	14.83	19.54	0.9998
Day 2	0.95	2.19	5.13	10.82	13.45	19.10	0.9976
Day 3	1.00	1.98	5.28	10.20	14.38	19.60	0.9995
Day 4	1.01	1.97	4.85	10.11	15.11	20.31	0.9998
Day 5	1.01	1.97	5.07	10.20	14.75	19.87	0.9998
Mean	0.99	2.02	5.07	10.35	14.50	19.68	0.9993
SD	0.03	0.10	0.16	0.29	0.64	0.45	0.001
RSD [%]	2.53	4.83	3.10	2.76	4.44	2.27	
RE [%]	-0.60	+0.80	+1.40	+3.48	-3.31	-1.58	

Comparison of unweighted and weighted calibration of the calibration curves of five testing days (RSS = residual sum of squares, r = correlation coefficient).

Weighting	Unweighted		1/x		$1/x^2$	
	RSS	r	RSS	r	RSS	r
Day 1	0.293	0.9998	0.089	0.9998	0.012	0.9998
Day 2	2.230	0.9977	0.128	0.9981	0.145	0.9976
Day 3	0.329	0.9997	0.137	0.9997	0.026	0.9995
Day 4	0.036	0.9999	0.025	0.9999	0.008	0.9998
Day 5	0.093	0.9999	0.031	0.9999	0.006	0.9999
Mean	0.596	0.9994	0.082	0.9995	0.039	0.9993
Sum	2.981	-	0.411	-	0.196	-

B2 Cellular GSH content

Cellular GSH content related to the protein content [µM/g] in untreated cells; results from three independent experiments (n = 3).

Cell line	HCT-8	HCT-8ox	A2780	A2780cis
	30.9	45.6	18.0	45.5
	68.2	55.7	23.6	58.8
	54.8	52.4	18.8	54.6
Mean	51.3	51.3	21.2	53.0
SD	18.9	5.1	3.4	6.8

Cellular GSH content related to the protein content relative to baseline value (0 h = 100%) [%] upon incubation with 100 nM oxaliplatin (HCT-8, HCT-8ox) or 100 nM cisplatin (A2780, A2780cis) (mean (SD), n = 3).

Time	HCT-8		HCT-8ox		A2780		A2780cis	
[h]	+oxaliplatin	control	+oxaliplatin	control	+cisplatin	control	+cisplatin	control
4	101.2	95.6	111.2	90.4	128.5	112.8	110.1	99.6
	(29.8)	(44.6)	(15.6)	(19.2)	(30.2)	(13.5)	(12.7)	(16.0)
8	111.1	91.0	91.7	87.0	123.6	110.0	98.4	92.9
	(20.2)	(22.8)	(18.0)	(32.1)	(36.7)	(35.2)	(11.0)	(3.1)
12	100.5	98.8	98.4	94.5	132.7	105.3	88.3	99.2
	(9.3)	(28.6)	(39.5)	(38.1)	(30.1)	(4.1)	(5.9)	(15.1)
24	75.0	75.8	80.5	95.4	100.6	98.9	79.0	86.1
	(41.3)	(42.2)	(15.0)	(31.2)	(46,4)	(34.9)	(11.0)	(4.8)

Results of two-way ANOVA analysis of influence of time and cisplatin or oxaliplatin treatment on cellular GSH content.

Variable	HCT-8 % of total variation	p value	HCT-8ox % of total variation	p value
Oxaliplatin [100nM]	1.07	0.6159	0.44	0.7527
Time [h]	14.45	0.4942	5.99	0.8442
Interaction	2.23	0.9673	9.80	0.8118
	A2780 % of total variation	p value	A2780cis % of total variation	p value
Cisplatin [100nM]	5.03	0.2705	0.03	0.9162
Time [h]	12.91	0.5254	41.36	0.0104
Interaction	3.70	0.9146	11.55	0.3308

B3 GSH depletion

Impact of GSH depletion (50 μM BSO) on oxaliplatin cytotoxicity expressed as pEC_{50} determined by the MTT assay (n = 4-5).

	HCT-8 +BSO	control	HCT-8ox +BSO	control
	5.877	5.80	4.30	4.10
	5.883	5.71	4.43	4.47
	5.956	5.78	4.51	4.17
	5.232	5.00	4.53	4.58
	-	-	4.57	4.51
Mean	5.74	5.57	4.47	4.37
SEM	0.17	0.19	0.05	0.10

Cellular platinum accumulation related to protein content [ng/μg] after 2 h incubation with 100 μM oxaliplatin with or without 12 h preincubation with 100 μM BSO, results from five independent experiments.

	HCT-8 +BSO	control	HCT-8ox +BSO	control
	0.40	0.42	0.16	0,20
	0.56	0.60	0.44	0.26
	0.31	0.31	0.24	0.26
	0.32	0.32	0.22	0.28
	0.39	0.48	0.24	0.28
Mean	0.40	0.43	0.25	0.26
SD	0.10	0.12	0.03	0.11

APPENDIX C

C1 Experiments identifying platinum-GSH adducts described in literature

Author	Experimental setting	Analytical method	Adducts
Appleton et al. [90]	Cisplatin diaqua complex (0.42 mM) + GSH (0.34 mM)	^{15}N NMR	Adduct
Bernareggi et al. [91]	Cisplatin (3.33 mM) + GSH (3.33 mM) in buffer 37 °C, 1 h	LC-MS	Two adducts
Berners-Price and Kuchel [92]	Cisplatin (50 mM) + GSH (150 mM) in buffer,23 °C, 7 h	Diverse NMR	Macromolecular polymer with a 1:2 Pt:GSH stoichiometry, adducts
Dedon and Borch [93]	Cisplatin (3mM) + GSH (6 to 2 mM), 37 °C, several days of incubation, in H_2O und 0.9% NaCl	^{1}H NMR	Macromolecular adduct with a 1:2 Pt:GSH stoichiometry and one adduct
Goto et al. [37]	Cisplatin (1.67 mM) + GSH (3.33 mM) in PBS, 24 °C, 48 h; HCT-8 and A2780 cells incubated with 3 μM cisplatin	HPLC, AAS	One adduct, also detected in cells
Heudi et al. [94]	Cisplatin (0.9 mM) + GSH (0.9 mM), 37 °C, 24h	LC-ESI-MS	Eleven different adducts, only two of those left after 24 h
Ishikawa and Ali-Osman [35]	Cisplatin (1.67 mM) + GSH (3.33 mM) in PBS, 37 °C, 48 h; leukemia cells incubated with 20 μM cisplatin	HPLC, MALDI, ^{1}H NMR	One adduct, also detected in cells
Odenheimer et al. [95]	Cisplatin (0.33 mM) + GSH (0,67 mM) in 0.9% NaCl, 37 °C, 4-5 days	IR	One adduct
Peklak-Scott et al. [41]	Cisplatin (1 mM) + GSH (2 mM) 25 °C, up to 60 min	HPLC, ESI-MS	Two adducts
Townsend et al. [96]	Cisplatin (3.33 mM) + GSH (3.3 mM) in buffer, 37 °C	LC-MS	Two adducts

Author	Experimental setting	Analytical method	Adducts
Zhao et al. [140]	Cisplatin (0.1 mM) + GSH (2 mM) in saline solution, 37 °C, 4 h	LC-ICP-MS	Two adducts, no structure suggested
Luo et al. [97]	Oxaliplatin (50 μM) in heparinized rat blood	HPLC	Suggestion of two adducts
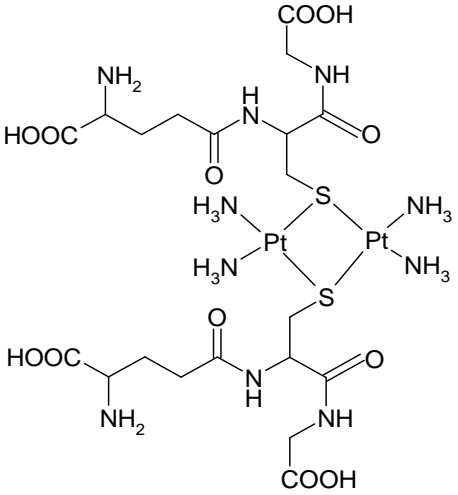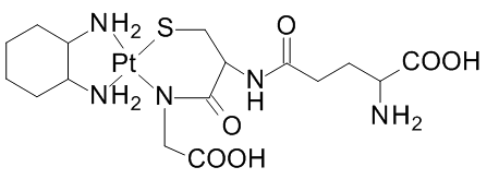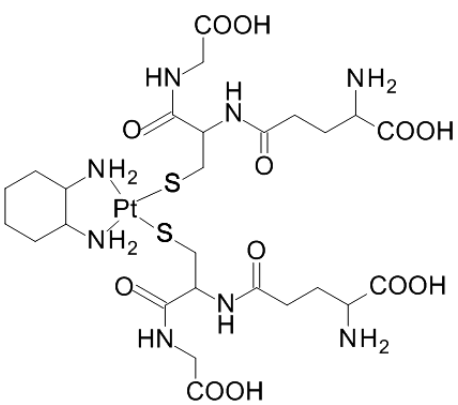
AAS: Atomic absorption spectroscopy, HPLC: high-performance liquid chromatography, ICP: inductively coupled plasma, IR: infrared spectrometry, LC: liquid chromatography, MALDI: matrix-assisted laser desorption/ionization, MS: mass spectrometry, NMR: nuclear magnetic resonance.

C2 Chemical structure of cisplatin- and oxaliplatin-GSH adducts described in literature

	Chemical structure	Molar mass	Literature
1		570.9 g/mol	Bernareggi et al., 1995 [91] Townsend et al., 2003 [96] Peklak-Scott et al., 2008 [41]
2		534.5 g/mol	Berners-Price and Kuchel, 1990 [92]
3		807.6 g/mol	Dedon and Borch, 1987 [93] Odenheimer, 1982 [95] →*trans* Ishikawa and Ali-Osman, 1993 [35] →*cis*

	Chemical structure	Molar mass	Literature
4		843.6 g/mol	Berners-Price and Kuchel, 1990 [92] (macromolecular polymer)
5		835.5 g/mol	Appleton et al., 1998 [90], Bernareggi et al., 1995 [91], Peklak-Scott et al., 2008 [41]
6		835.5 g/mol	Townsend et al., 2003 [96] Heudi et al., 2001 [94]
7		798.64 g/mol	Heudi et al., 2001 [94]

	Chemical structure	Molar mass	Literature
8		1070.9 g/mol	Appleton et al., 1998 [90]
9		614 g/mol	Luo et al., 1999 [97]
10		1037 g/mol	Luo et al., 1999 [97]

C3 Isotope pattern for adduct 1 created *in silico* using an isotope distribution calculator

Isotope distribution calculator available at www.sisweb.com/mstools/isotope.htm.
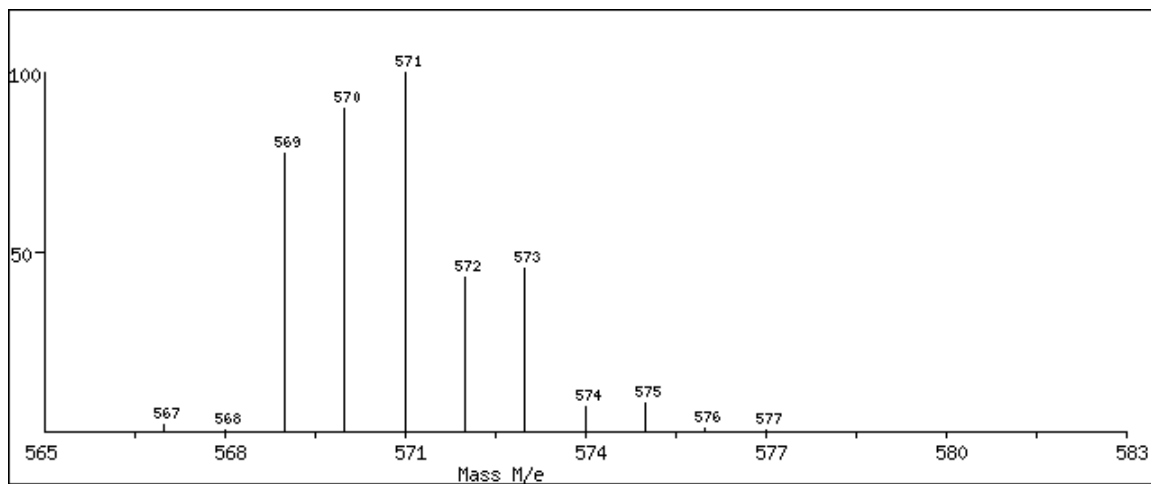
APPENDIX D

MRP2 in platinum resistance

D1 MRP2 expression

Expression of MRP2 normalized to β-actin in untreated cells and after treatment with 10 μM oxaliplatin for 12 h (mean ± SD, n = 2-6).

Cell line	Mean	SD	n
HCT-8	1.06	0.57	5
HCT-8 + oxaliplatin	1.91	0.70	3
HCT-8ox	0.97	0.32	6
HCT-8ox+ oxaliplatin	1.12	0.40	3
A2780	n. d.	-	2
A2780cis	0.26	0.32	3

n. d.: not detected

D2 Effects of MRP modulators on platinum accumulation and DNA platination

Cellular platinum accumulation related to protein content [ng/μg] after 2 h incubation with different concentrations of Gü83 and 100 μM oxaliplatin in HCT-8 cells (results of individual testing days, n = 1-5).

log [Gü83]	HCT-8					Mean	SD
-7	0.38	0.32	0.39	0.34	-	0.36	0.03
-5	0.26	0.46	-	-	-	0.36	0.14
-4.7	0.27	0.35	-	-	-	0.30	0.05
-4.4	0.50	0.25	0.47	0.78	0.53	0.51	0.19
-4	0.91	0.65	0.82	0.69	-	0.77	0.12
-3.7	2.00	1.62	-	-	-	1.81	0.27

Cellular platinum accumulation related to protein content [ng/μg] after 2 h incubation with different concentrations of Gü83 and 100 μM oxaliplatin in HCT-8ox cells (results of individual testing days, n = 1-5).

log [Gü83]	HCT-8ox					Mean	SD
-7	0.16	0.20	0.12	0.20	-	0.17	0.04
-5	0.10	-	-	-	-	-	-
-4.7	0.09	-	-	-	-	-	-
-4.4	0.18	0.08	0.42	0.52	-	0.30	0.20
-4	0.59	1.01	0.95		-	0.85	0.23
-3.7	1.22	-	-	-	-	-	-

Cellular platinum accumulation related to protein content [ng/µg] after incubation with DMSO or 100 µM Gü83 in DMSO and 100 µM oxaliplatin (mean (SD), n = 3).

Time [h]	HCT-8		HCT-8ox	
	+Gü83	control	+Gü83	control
0.5	0.13 (0.03)	0.10 (0.04)	0.04 (0.01)	0.09 (0.06)
1	0.21 (0.07)	0.15 (0.03)	0.07 (0.02)	0.09 (0.01)
2	0.54 (0.07)	0.34 (0.22)	0.17 (0.05)	0.25 (0.06)
3	1.11 (0.13)	0.48 (0.05)	0.25 (0.20)	0.70 (0.06)

Results of two-way ANOVA analysis of influence of time and Gü83 on platinum accumulation.

Variable	HCT-8		HCT-8ox	
	% of total variation	p value	% of total variation	p value
Gü83 [100µM]	14.91	0.0002	15.78	< 0.0001
Time [h]	64.54	< 0.0001	65.90	< 0.0001
Interaction	17.26	0.0013	15.23	0.0011

Cellular platinum accumulation related to protein content [ng/µg] after 2 h incubation with 100 µM Gü83 and 100 µM cisplatin (results of individual testing days, n = 4-5).

	HCT-8		HCT-8ox	
	+Gü83	control	+Gü83	control
	1.56	2.33	1.49	2.21
	1.58	2.01	1.64	1.03
	1.10	1.77	0.61	1.02
	1.13	2.63	1.22	2.11
	1.33	-	0.90	1.42
Mean	1.34	2.18	1.17	1.56
SD	0.23	0.38	0.42	0.57

Cellular platinum accumulation related to protein content [ng/µg] after 2 h incubation with 100 µM Gü83 and 100 µM cisplatin (mean ± SD, n = 3).

	A2780		A2780cis	
	+Gü83	control	+Gü83	control
	1.27	1.71	0.92	0.82
	1.87	1.89	0.75	0.56
	1.12	1.73	0.78	0.68
Mean	1.42	1.78	0.81	0.69
SD	0.39	0.09	0.09	0.13

Platinum efflux illustrated as platinum content related to protein content [ng/µg] after 2 h incubation with 100 µM oxaliplatin without or with 100 µM Gü83 over time after replacing cell culture medium (mean (SD), n = 3).

Time with platinum free medium [min]	HCT-8		HCT-8ox	
	+Gü83	control	+Gü83	control
0	0.76 (0.06)	0.83 (0.01)	0.18 (0.04)	0.15 (0.04)
2	0.59 (0.02)	0.48 (0.01)	0.11 (0.03)	0.11 (0.05)
5	0.55 (0.01)	0.49 (0.12)	0.12 (0.04)	0.12 (0.02)
10	0.50 (0.01)	0.47 (0.05)	0.13 (0.08)	0.16 (0.06)
60	0.40 (0.10)	0.44 (0.15)	0.12 (0.06)	0.10 (0.05)

Results of two-way ANOVA analysis of influence of time and Gü83 on platinum efflux.

Variable	HCT-8		HCT-8ox	
	% of total variation	p value	% of total variation	p value
Gü83 [100µM]	0.32	0.6402	0.27	0.8668
Time [h]	65.71	< 0.0001	23.53	0.1446
Interaction	5.27	0.4712	3.87	0.7694

DNA platination [platinum atoms/106 nucleotides] (A) and platinum accumulation [ng/µg] (B) after 3 h incubation with 200 µM Gü83 and 100 µM oxaliplatin (results of individual testing days, n = 3).

A

	HCT-8		HCT-8ox	
	+Gü83	control	+Gü83	control
	67.4	19.8	69.7	16.6
	52.1	22.4	24.1	17.0
	97.4	22.8	49.4	8.7
Mean	72.3	20.7	47.7	14.1
SD	23..0	3.3	22.8	4.7

B

	HCT-8		HCT-8ox	
	+Gü83	control	+Gü83	control
	5.36	0.64	3.20	0.47
	5.30	0.85	1.41	0.63
	6.86	0.35	4.42	0.35
Mean	5.84	0.61	3.01	0.48
SD	0.88	0.25	1.51	0.14

Cellular platinum accumulation related to protein content [ng/µg] after 2 h incubation with 200 µM indometacin and 100 µM oxaliplatin (results of individual testing days, n = 3).

	HCT-8		HCT-8ox	
	+indometacin	control	+indometacin	control
	0.68	0.42	0.56	0.15
	0.43	0.29	0.40	0.13
	0.88	0.45	0.83	0.22
Mean	0.66	0.39	0.60	0.17
SD	0.23	0.09	0.22	0.05

Cellular platinum accumulation related to protein content [ng/µg] after 2 h incubation with 100 µM ciclosporin and 100 µM oxaliplatin (results of individual testing days, n = 3).

	HCT-8		HCT-8ox	
	+ciclosporin	control	+ciclosporin	control
	1.31	0.94	0.75	0.59
	1.41	0.98	0.43	0.61
	1.31	0.94	0.75	0.59
Mean	1.34	0.95	0.64	0.60
SD	0.06	0.02	0.18	0.02

D3 Comparative potency of MRP modulators

pIC_{50} of the MRP modulators derived from calcein efflux experiments (results of individual testing days, n = 3).

	pIC_{50}	
	HCT-8	HCT-8ox
Gü83	4.75	5.05
	5.88	4.39
	5.02	4.82
Indometacin	4.35	4.01
	3.60	4.26
	3.09	3.72
Ciclosporin	5.24	5.50
	6.11	6.03
	5.99	5.72

D4 Effect of Gü83 on oxaliplatin cytotoxicity

pEC_{50} of oxaliplatin with or without coincubation with 100 μM Gü83 (results of individual testing days, n = 4).

	HCT-8		HCT-8ox	
	+Gü83	control	+Gü83	control
	5.42	5.45	5.20	4.15
	5.49	5.59	4.66	4.88
	5.41	5.54	5.51	4.72
	5.08	5.21	4.13	4.63
Mean	5.35	5.45	4.62	4.84
SEM	0.09	0.08	0.22	0.11